The investigation of microbial denitrification processes for the removal of nitrate from water using bio-electrochemical methods and carbon nano-materials.

Alharbi, Njud Saleh F

Swansea University
Prifysgol Abertawe

The Investigation of Microbial Denitrification Processes for the Removal of Nitrate from Water Using Bio-Electrochemical Methods and Carbon Nano-Materials

NJUD SALEH F. ALHARBI

A thesis submitted to the University of Swansea
in fulfilment of the requirements for the degree of Doctor of Philosophy
Biochemical Engineering, School of Engineering

2012

Abstract

With ever increasing regulation of the quality of drinking water and wastewater treatment, there is a need to develop methods to remove nitrogenous compounds from water. These processes are mediated by a variety of micro-organisms that can oxidise ammonia to nitrate, and then reduced to gaseous nitrogen by another set of organisms. This two stage process involves the relatively slow oxidation of ammonia to nitrate followed a relatively fast reduction of nitrate to nitrogen. Nitrate reduction normally requires anaerobic environments and the addition of organic matter to provide reducing power (electrons) for nitrate reduction. In practical situations the nitrate reduction can be problematic in those precise quantities of organic matter to ensure that the process occurs while not leaving residual organic matter.

The aim of this study was to investigate microbial denitrification using electrochemical sources to replace organic matter as a redactant. The work also involved developing a system that could be optimised for nitrate removal in applied situations such as water processing in fish farming or drinking water, where high nitrate levels represent a potential health problem. Consequently, the study examined a range of developments for the removal of nitrate from water based on the development of electrochemical bio-transformation systems for nitrate removal. This also offers considerable scope for the potential application of these systems in broader bio-nanotechnology based processes (particularly in bioremediation).

The first stage of the study was to investigate the complex interactions between medium parameters and their effects on the bacterial growth rates. The results proved that acetate is a good carbon source for bacterial growth, and therefore it was used as an organic substrate for the biological process. High nitrate removal rate of almost 87% was successfully achieved by using a microbial fuel cell (MFC) enriched with soil inocula with the cathodes cells fed with nitrate and the anode fed with acetate. The maximum power density obtained was 1.26 mW/m^2 at a current density of 10.23 mA/m^2. The effects of acetate, nitrate and external resistance on current generation and denitrification activity were investigated, and the results demonstrated that nitrate removal was greatly dependent on the magnitude of current production within the MFC. Increase of acetate (anode) and nitrate (cathode) concentrations improved the process, while increasing external resistance reduced the activity. Furthermore, for a clear understanding of the nitrate reduction process, the analysis of the associated bacteria was performed through biochemical tests and examination of morphological characteristics. A diversity of nitrate reducing bacteria was observed; however a few were able to deliver complete denitrification. Pure cultures in MFC were examined and the voltage output achieved was about 36% of that obtained by mixed cultures. The nitrate removal gained was 56.2%, and this is almost 31% lower than that obtained by the mixed bacterial experiment.

In an attempt to improve the MFC, modifications to the electrochemical properties of the electrode were investigated through the use of a cyclic voltammetry using carbon nanomaterials to coat the graphite felts electrodes. Among all the nanomaterials used in this study, graphitised carbon nanofibres (GCNFs) was selected for further investigation as it offered the best electrochemical performance and was thought to provide the largest active surface area. The performance of the MFC system coupled with the GCNFs modified electrodes was evaluated and significant improvements were observed. The highest voltage output achieved was about 41 mV with over 95% nitrate removal.

The work is discussed in the context of improved MFC performance, potential analytic applications and further innovations using a bio-nanotechnology approach to analyse cell-electrode interactions.

Acknowledgments

First and foremost I thank and praise Allah Subhana Wa Tallah who granted me health and knowledge to complete this work. This research project would not have been possible without the support of many people. I wish to express my gratitude to my resourceful supervisor, Dr Lovitt, for his abundant help and invaluable support and guidance throughout my research. I would also like to present all respect, gratitude and appreciation to my parents for their continued prayers, love and support throughout my entire life, and my husband for his care, love and understanding. This research project has been supported by the Government of the Kingdom of Saudi Arabia; their support is fully appreciated.

Table of Contents

List of Figures

List of Tables

List of Abbreviations

ADP.....	Adenosine DiPhosphate
ATP.....	Adenosine TriPhosphate
BES.....	Bio-Electrochemical Systems
BOD.....	Biological Oxygen Demand
BUG.....	Benthic Unattached Generator
CE.....	Coulombic Efficiency
CE.....	Counter Electrode
CEM.....	Cation Exchange Membrane
CoA.....	Coenzyme A
COD.....	Chemical Oxygen Demand
CNF.....	Carbon NanoFibre
GCNFs.....	Graphitised Carbon NanoFibres
CNT.....	Carbon NanoTube
CV.....	Cyclic Voltammetry
CVD.....	Chemical Vapour Deposition
cyt a.....	cytochrome a
cyt a_3.....	cytochrome a_3
cyt b.....	cytochrome b
cyt c.....	cytochrome c
cyt c_1.....	cytochrome c_1
DET.....	Direct Electron Transfer
DMF.....	N,N.DiMethylFormamide

DMRB.....	Dissimilatory Metal-Reducing Bacteria
DMSO.....	DiMethyl SulfOxide
DNA.....	DeoxyriboNucleic Acid
DNB.....	DeNitrifying Bacteria
DNRA.....	Dissimilatory Nitrate Reduction to Ammonium
EIS.....	Electrochemical Impedance Spectroscopy
emf.....	electromotive force
EPA.....	Environmental Protection Agency
ETC.....	Electron Transport Chain
Euk-NR.....	Eukaryotic assimilatory Nitrate Reductase
FAD.....	Flavin Adenine Dinucleotide
$FADH_2$.....	Reduced form of Flavin Adenine Dinucleotide
FMN.....	Flavin MonoNucleotide
FP.....	Final Potential
GAC.....	Granular Activated Carbon
GCB.....	Graphitised Carbon Black
GF.....	Graphite Felt
GFE.....	Graphite Felt Electrode
GGs.....	Graphite Granules
GPa.....	GigaPascal
Gr/PP.....	Graphite rod wrapped with PolyPropylene mesh
GTP.....	Guanosine TriPhosphate
HRT.....	Hydraulic Residence Time
IP.....	Initial Potential

MCL	Maximum Contaminant Level
MET	Mediated Electron Transfer
MF	MicroFiltration
MFC	Microbial Fuel Cell
ML-MFCs	MembraneLess Microbial Fuel Cells
mm	millimetre
MV	Methyl Viologen
MWCNT	Multi-Wall Carbon NanoTube
NAD^+	Nicotine Adenine Dinucleotide
NADH	Reduced form of Nicotine Adenine Dinucleotide
NADP	form of Nicotinamide Adenine Dinucleotide Phosphate
NADPH	Reduced form of Nicotinamide Adenine Dinucleotide Phosphate
Nap	Nitrate reductase periplasmic dissimilatory
Nar	Nitrate reductase membrane-bound dissimilatory
Nas	Nitrate reductase cytoplasmic assimilatory
NHE	Normal Hydrogen Electrode
Nir	Nitrite reductase
Nor	Nitric oxide reductase
Nos	Nitrous oxide reductase
NR	Nitrate Reductase
OCV	Open Cell Voltage
O.D.Units	Optical Density Units
ORP	Oxidation Reduction Potential
PBS	Phosphate Buffer Solution

PEM.....	Proton Exchange Membrane
PMF.....	Proton Motive Force
Pt.....	Platinum
RHE.....	Reversible Hydrogen Electrode
SCE.....	Saturated Calomel Electrode
SEM.....	Scanning Electron Microscopy
SGSA.....	Specific Geometric Surface Area
SHE.....	Standard Hydrogen Electrode
SO.....	Sulphite Oxidase
SP.....	Switching Potential
SR.....	Scan Rate
SRB.....	Sulphate-Reducing Bacteria
SS/SS.....	Stainless Steel rods wrapped with Stainless Steel mesh
SWCNT.....	Single Wall Carbon NanoTube
TCA.....	TriCarboxylic Acid
TCC.....	Total Cathodic Compartment
TEA.....	Terminal Electron Acceptors
TPa.....	TeraPascal
UV.....	UltraViolet
WE.....	Working Electrode
WHO.....	World Health Organisation

Glossary of Symbols

A	Surface area
A_{an}	Anode surface area
A_{cat}	Cathode surface area
A_{corr}	Corrected UV-light absorbance of NO_3^- in the sample
A_{220}	Absorbance reading at 220 nm
A_{275}	Absorbance reading at 275 nm
$Abs_{(s1)}$	Absorbance of the sample
$Abs_{(b11)}$	Absorbance of the blank
b	Amount of moles of electrons produced per mol of substrate
b_1	Gradient of the calibration graph
c_i	Concentration of species *i*
C_E	Coulombic efficiency
C_O	Concentration of oxidised species at the electrode surface
C_P	Total number of electrons calculated by integrating the current over time
C_R	Concentration of reduced species at the electrode surface
C_T	Theoretical number of electrons that can be produced from the substrate
c_O^∞	Concentration of analyte in bulk solution
D	Diffusion coefficient of analyte
E	Potential versus a reference electrode
e^-	Electron
ΔE	Potential difference between electron donor and acceptor
$E^{o'}$	Formal standard potential

E_e	Potential of the working electrode
E_e^o	Standard potential for the redox reaction
E_{cell}	Cell voltage
E_{emf}	Electromotive force
E_{emf}°	Standard cell electromotive force
E_P^C	Shift of peak potential with scan rate
ΔE_p	Difference between the peak potentials
$E_P^{\rightarrow}$	Forward peak potential
$E_P^{\leftarrow}$	Reverse peak potential
F	Faraday's constant
F_d	Dilution factor
ΔG	Metabolic energy
ΔG_r	Gibbs free energy
ΔG_r°	Gibbs free energy under standard conditions
H	Height
I	Current
$I^{\rightarrow}$	Cathodic current density for the forward reaction
$I^{\leftarrow}$	Anodic current density for the back reaction
I_{an}	Current density calculated on the basis of the anode surface area
I_o	Exchange current density
I_P	Peak current density
$I_P^{\rightarrow}$	Forward peak current
$I_P^{\leftarrow}$	Reverse peak current
$k^{\rightarrow}$	Rate constant for the forward reaction

$k^{\leftarrow}$	Rate constant for the back reaction
$k_o^{\rightarrow}$	Standard rate constant for the forward reaction
$k_o^{\leftarrow}$	Standard rate constant for the back reaction
L	Length
$\mathcal{L}$	Fibre length
M	Molecular weight of the substrate
n	Number of electrons
n_α	Number of electrons transferred
O	Oxidised electroactive species involved in the redox reaction at the electrode
OCV^*	OCV implied by extrapolating the linear region of the polarisation curve to the y-axis
P	Power
P_{an}	Power density calculated on the basis of the anode surface area
P_{cat}	Power density calculated on the basis of the cathode surface area
P_{max}	Maximum power
$P_{max,emf}$	Maximum power output
$P_{t,emf}$	Total maximum power
$P_{t,OCV}$	Maximum possible power based on the measured open cell voltage
P_v	Volumetric power
R	Reduced electroactive species involved in the redox reaction at the electrode
r	Fibre radius
R_{ext}	External resistance
R_{int}	Internal resistance
R_g	Universal gas constant
R_{ohmic}	ohmic resistance

S	Concentration of substrate
SA	Outer surface area of a rectangular prism-shape electrode
S_F	Surface area of the fibre
SGSA	Specific geometric surface area
T	Absolute temperature
t	Time from commencement of experiment
v	Reactor volume (or Liquid volume)
V_E	Volume of the GF electrode
V_F	Volume of the fibre
ν_s	Potential sweep rate
$\nu_s^{1/2}$	Square root of the scan rate
W	Width
x	Distance perpendicular to the electrode surface
$x_{NO_2^-}$	Nitrite concentration of the test sample
Π	Reaction quotient derived as the activities of the products divided by those of the reactions
η	Overpotential
η_{ohmic}	Ohmic overpotential
α_A	Transfer coefficients for the anodic reaction
α_C	Transfer coefficients for the cathodic reaction
δ_E	Apparent density of the GFE
δ_F	Density of the fibre

1. INTRODUCTION

1.1. State-of-the-Art and Problem Definitions

Water is very important for life and has become one of the environmental problems in many parts of the world. These problems are due to the excessive use of nitrogen compounds in agriculture and discharge of human and animal waste that contains nitrogen, and this contaminates water sources. Overall, nitrogen takes many forms in water, such as ammonia (NH_3/NH_4^+), nitrite (NO_2^-) and nitrate (NO_3^-).

These forms of nitrogen can have serious consequences when released into water and wastewater. Nitrate is one of these nitrogen forms and is not toxic at the levels usually attained in water sources. However, a key problem occurs with the reduction of nitrate to nitrite, which is more toxic and can affect many organisms health, including humans. Consumption of drinking water containing high nitrate levels can cause methemoglobinemia and gastric cancer due to endogenous formation of genotoxic N-nitroso compounds by bacteria in the gastrointestinal tract (van Maanen *et al.* 1996). Nitrate is colourless, odourless and tasteless, and therefore it is detectable in water only by chemical testing. Two main groups of treatment processes, physico-chemical and biological treatment methods, can be used for nitrate removal. Physico-chemical (abiotic) methods have been shown to fail to treat nitrate and resulted in some bi-product problems. For instance, with reverse osmosis the end product is concentrated waste brine that becomes difficult to dispose of. In contrast, biological methods can provide an efficient treatment of nitrate, and novel techniques are proposed (Clauwaert *et al.* 2009, Clauwaert *et al.* 2007a, Logan *et al.* 2006, Sakakibara and Nakayama 2001). Biological methods are easier to operate and

maintain and are consequently cheaper. Often the end products are harmless and easily disposed of.

In order to protect consumers from the adverse impacts of high nitrate intake, standards were established to regulate the nitrate concentrations in drinking water. The maximum contaminant level (MCL) for nitrate in drinking water was set as 50 mg NO_3^-/L by the US, Canada and the world health organisation (WHO) (Sayre 1988). However, a limited MCL of 10 mg $NO_3^- - N/L$ was established by the US Environmental Protection Agency (EPA) and WHO (Cast and Flora 1998). Improvements in removal of nitrogen components, especially nitrate, from water and wastewater have been achieved by many researchers (Ghafari *et al.* 2009, Sakakibara and Nakayama 2001). A biological nitrate removal using microbial fuel cells (MFCs) has attracted great attention due to its ability to directly generate electricity, while accomplishing water and wastewater treatment. In addition, anaerobic biocathodes can offer the advantages of having a microbial fuel cell (MFC) system with both anaerobic anode and cathode chambers. This helps minimise the risk of oxygen leaking in the anode chamber, thus increasing the efficiency of its reaction, and also helps reduce the cost of the catalyst used.

1.2. Research Objectives

The objectives of the study were

i. To develop a system capable of nitrate reduction in clean water using a simple electrochemical setup.
ii. To develop suitable methods for the measurement and operation of an electrochemical reduction system.

iii. To demonstrate the activity and utility of the electrochemical system.

iv. To isolate and characterise the microbes present in such enrichment systems.

v. To characterise the biochemistry of the electrode-cell interactions.

vi. To improve the electrochemical activities of graphite felt electrodes using carbon nanomaterials due to their excellent electrical conductivity, nanometer size, and good chemical stability.

vii. To demonstrate the improvements achieved in such nitrate reducing systems through the use of nanomaterial modified electrodes.

1.3. Original Contributions

The author has:

1. Studied the isolation and characterisation of nitrate reducing bacteria.
2. Designed, investigated and examined two cultivation media with different carbon sources, sodium formate and sodium acetate, in order to optimise the bacterial growth rate. Medium optimisation was achieved by individually evaluating the effect of chemical components on the bacterial growth rate.
3. Proposed a bio-electrochemical denitrification reaction through the use of 100% MFCs enriched only with soil inocula. The performance of such a system was examined and evaluated under closed and open circuit conditions. Moreover, the effects of acetate/nitrate on the denitrification activity were investigated. Current generation and nitrate reduction as a function of external resistance were also studied.
4. Analysed the characterisation of bacteria from electrodes that carry out biological mediated nitrate reduction. Bacterial analysis was performed through biochemical tests and morphological characteristics.

5. Studied the characterisation on the nanoscale of the electrodes and the nature of the interaction of the associated microbes.
6. Investigated the electrochemical properties of the electrode through the use of a cyclic voltammetry technique.
7. Modified the electrode surfaces using carbon nanomaterials in order to improve its redox behaviours.
8. Proposed a microbial fuel cell system utilising the modified electrodes, and demonstrated the improvements achieved due to the enhanced reaction kinetics and mass transfer.

1.4. Thesis Outline

Chapter 2 gives a general overview of bio-electrochemical nitrate reduction systems. The chapter outlines the merits of and problems affecting microbial fuel cell systems and previous advances made. Bacterial metabolism and their interaction at the electrode surface are also given. Furthermore, denitrification in natural ecosystems and the corresponding enzymes and bacteria are addressed. In addition, an overview is given to both carbon nanomaterials and electrochemical theory.

Chapter 3 outlines the isolation and characterisation of denitrifying bacteria and culture conditions. The chapter investigates the optimisation of the growth medium by studying the complex interactions between medium parameters and their impacts on the bacterial growth.

A mediatorless H-shaped MFC system with bacteria both in the anode and cathode chambers is presented in Chapter 4. The design and setup of such a system and the associated enrichment and operation are discussed. Moreover, denitrification

activities at different acetate and nitrate concentrations and various external resistances are examined.

Chapter 5 analyses the microbial communities on the electrodes and discusses the roles of nitrate reducing bacteria in the electrode communities.

Electrochemical characterisation and conductivity modification of graphite felt electrodes are studied in Chapter 6. The electrochemical properties are investigated through cyclic voltammetry methods, and the conductivity modification is achieved by using carbon nanomaterials. Furthermore, an MFC system employing electrodes modified with carbon nanomaterials is investigated, and its performance is evaluated.

A summary of the contributions of the present study and the thesis conclusions are given in Chapter 7. Proposals towards further research are drawn in Chapter 8.

2. LITERATURE REVIEW

2.1. Denitrification in Natural Ecosystems

2.1.1. Nitrogen Cycle

Nitrogen atoms move in a constant circle from the air into the bodies of plants and animals through the soil, and eventually back to the air. This process defines the nitrogen cycle (N-cycle), see Fig. 2.1. Nitrogen is a fundamental element for life due to its critical role in forming the two essential biological macromolecules: proteins and nucleic acids. Although, nitrogen is the most abundant gas in the atmosphere (79% of the atmosphere), it is limited as a nutrient in aquatic and agricultural land environments (Bitton 1994). Nitrogen exists in the biosphere in several oxidation degrees, from N^{5+} to N^{3-}, producing many species that constitute the biogeochemical cycle of nitrogen.

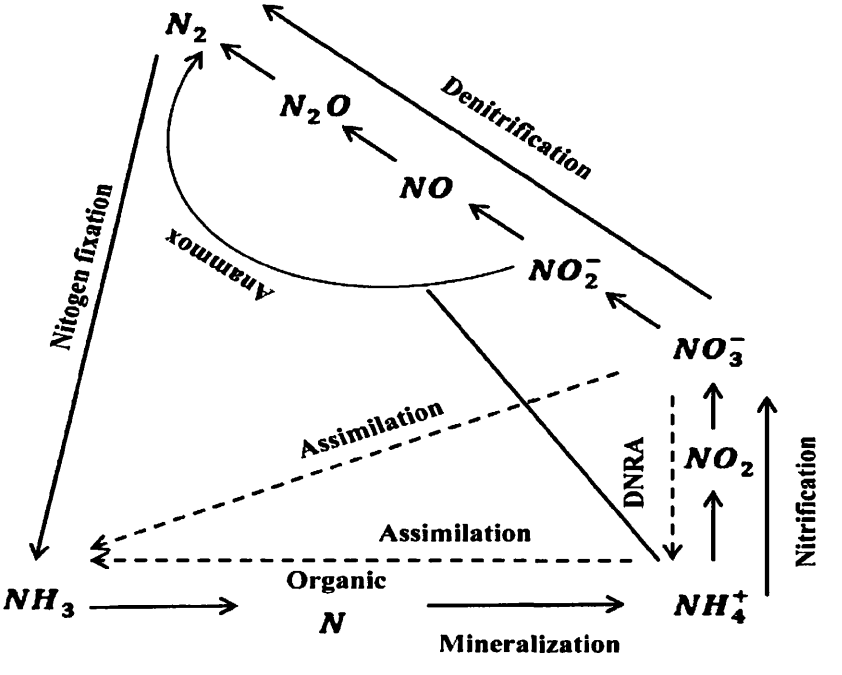

Figure 2-1: Diagram of the nitrogen cycle, adapted from (Bitton 1994) .

Microorganisms play an important role in the nitrogen cycle, including nitrogen fixation, nitrogen assimilation, nitrogen mineralization (ammonification), nitrification and denitrification (Bitton 1994).

2.1.1.1. Nitrogen Fixation

Most organisms cannot use nitrogen in its basic form (as nitrogen gas N_2), and therefore N_2 needs to be first converted to ammona NH_3 to be available to make proteins, deoxyribonucleic acid (DNA) and other biologically important compounds. The process of conversion N_2 to NH_3 is called nitrogen fixation. This process requires a large amount of energy to break the nitrogen atoms' bond attributed to the stability of the nitrogen molecule as a result of the strength observed in the triple bond between the nitrogen atoms. A few species of bacteria and cyanobacteria are able to carry out nitrogen fixation since they have the enzyme nitrogenase, which helps reducing triple-bonded molecules (Bitton 1994). The chemical reaction of nitrogen fixation can be expressed as

$$N_2 + 8H^+ + 8e^- \rightarrow 2NH_3 + H_2. \quad (2.1)$$

2.1.1.2. Nitrogen Assimilation

Microorganisms take up and assimilate ammonia (NH_3) produced by the nitrogen fixation process to incorporate it into proteins and other organic nitrogen compounds.

2.1.1.3. Nitrogen Mineralization (Ammonification)

Ammonification is a transformation process of organic nitrogenous compounds to inorganic forms (Bitton 1994). When an organism excretes waste or dies, various

bacteria and fungi decompose its tissues, which contain organic nitrogen, and then release inorganic nitrogen back into the ecosystem as ammonium ions NH_4^+. The later then becomes available for uptake by plants and other microorganisms for growth.

2.1.1.4. Nitrification

Nitrification is defined as the conversion of ammonium to nitrate through microbial action. The nitrification process occurs in an aerobic condition and is carried out exclusively by prokaryotes in two main categories. The first approach is the conversion of ammonia to nitrite, which is known as ammonium oxidation, and the organisms involved are called ammonia oxidisers. It was believed that all ammonia oxidation is carried out by only a few types of bacteria in the genera *Nitrosomonas*, *Nitrosospira*, *Nitrosococcus* and *Nitrosolobus* (Reynolds and Richards 1996). However, it was discovered that an archaeon can also oxidize ammonia (Konneke *et al.* 2005). The ammonium oxidation is carried out as follows:

$$NH_3 + O_2 + 2e^- \rightarrow NH_2OH + H_2O, \tag{2.2}$$

$$NH_2OH + H_2O \rightarrow NO_2^- + 5H^+ + 4e^-. \tag{2.3}$$

The second step of nitrification, where nitrite is converted to nitrate, is called nitrite oxidation. This step is carried out by a group of bacteria known as nitrite oxidising bacteria, e.g., *Nitrobacter* (Reynolds and Richards 1996). The reaction of this step (nitrite oxidation) is written as:

$$NO_2^- + \frac{1}{2}O_2 \rightarrow NO_3^-. \tag{2.4}$$

Although microbes that perform nitrification produce acid, they are fragile and acid-sensitive. Nitrification is a nuisance to the agricultural industry due to the

rapid conversion of ammonia to nitrate under optimal conditions (Burrell *et al.* 1998).

2.1.1.5. Denitrification

Denitrification is the biological reduction of nitrate (NO_3^-) and nitrite (NO_2^-) to nitrous oxide (N_2O) or nitrogen gas (N_2), resulting in energy conservation and growth yield (Mahne and Tiedje 1995). The redox reaction of the denitrification process is expressed as:

$$2NO_3^- + 10e^- + 12H^+ \rightarrow N_2 + 6H_2O. \quad (2.5)$$

The denitrification rate decreases with the increase of oxygen levels and with the decrease of pH values (Cavigelli and Robertson 2000). Denitrification is a series of anaerobic respiration processes, each coupled to adenosine triphosphate (ATP) generation and can support the growth of organisms (Koike and Hattori 1975). These sequential processes, defined as the denitrification pathway, are carried out as follows (Sedlak 1991):

$$NO_3^- \xrightarrow{Nitrate\ reductase\ (NR)} NO_2^- \xrightarrow{Nitrite\ reductase\ (Nir)} NO \xrightarrow{Nitric\ oxide\ reductase\ (Nor)} N_2O \xrightarrow{Nitrus\ oxide\ reductase\ (Nos)} N_2, \quad (2.6)$$

where NO is nitric oxide. The redox reaction of the denitrification pathway is accomplished in four enzymatic steps:

$$NO_3^- + 2e^- + 2H^+ \rightarrow NO_2^- + H_2O, \quad (2.7)$$

$$NO_2^- + e^- + 2H^+ \rightarrow NO + H_2O, \quad (2.8)$$

$$2NO + 2e^- + 2H^+ \rightarrow N_2O + H_2O, \quad (2.9)$$

$$N_2O + 2e^- + 2H^+ \rightarrow N_2 + H_2O. \quad (2.10)$$

There are general requirements (Philippot *et al.* 2007) for the biological denitrification pathway, such as:

i. The presence of bacteria that possess the metabolic capacity.
ii. The availability of suitable electron donors such as organic carbon compounds.
iii. Anaerobic condition or limited oxygen levels.
iv. The presence of nitrogen-oxides as terminal electron acceptors.

2.1.1.5.1. The Denitrification Pathway

The denitrification pathway consists of four different steps, where each requires a specific enzyme. Several enzymes are involved in the denitrification pathway, though individual denitrifying bacteria can either catalyse every step of this denitrification pathway or participate only in particular stages (Paul and Clark 1996). These corresponding enzymes are synthesised when conditions become advantageous for denitrification (Knowles 1982). Synthesis of denitrifying enzymes occurs under anaerobic conditions (Hochstein and Tomlinson 1988). However, denitrification can also occur in the presence of oxygen (Hochstein *et al.* 1984, Hooijmans *et al.* 1990, Lloyd *et al.* 1987, Robertson and Kuenen 1984). Although enzyme induction, in some cases, may even require low concentrations of oxygen (Aida *et al.* 1986, Körner and Zumft 1989), significant enzyme levels can be present as a result of anaerobiosis even in the absence of nitrate or other nitrogenous oxides (Frunzke and Zumft 1986, Koike and Hattori 1975). The associated enzymes include nitrate reductase (NR), nitrite reductase (Nir), nitric oxide reductase (Nor) and nitrous oxide reductase (Nos).

A. Nitrate reductase

Nitrate reductases catalyse the reduction of NO_3^- to NO_2^- as indicated in Eq. (2.6). Nitrate reduction is typically performed for three purposes:

i. Nitrate assimilation where nitrate is utilised as a nitrogen source for growth.

ii. Nitrate respiration where nitrate is used as a terminal electron acceptor for metabolic energy generation.

iii. Nitrate dissimilation where the energy excess generated by the cell metabolism is dissipated to maintain redox balance.

However, nitrate reductase enzymes are involved in two different nitrate metabolic pathways in microorganisms, as shown in Fig. 2.2. The two main nitrate-metabolising pathways are assimilatory and dissimilatory nitrate reductions (Robertson and Kuenen 1992). Furthermore, nitrate reductases which catalyse the two-electron reduction of nitrate to nitrite, according to equation (2.7), are often classified into four types with respect to different criteria, such as: cell localisation, protein structure and molecular properties of the catalytic centre, metabolic routes and sources. These four types include eukaryotic assimilatory nitrate reductase (Euk-NR) (Campbell 1999, Campbell 2001) and three different prokaryotic nitrate reductases: cytoplasmic assimilatory (Nas), membrane-bound dissimilatory (respiratory) (Nar) and periplasmic dissimilatory (Nap) nitrate reductases (Moreno-Vivián *et al.* 1999, Richardson 2000, Richardson* *et al.* 2001, Stolz and Basu 2002). All nitrate reductases (either eukaryotic or prokaryotic) are mononuclear molybdenum-containing enzymes that, according to Hille's classification (Hille 1996), belong to the dimethyl sulfoxide (DMSO) reductase family, with the exception of eukaryotic nitrate reductase, which belongs to the sulphite oxidase (SO) family. This study focuses only on the prokaryotic nitrate reductases.

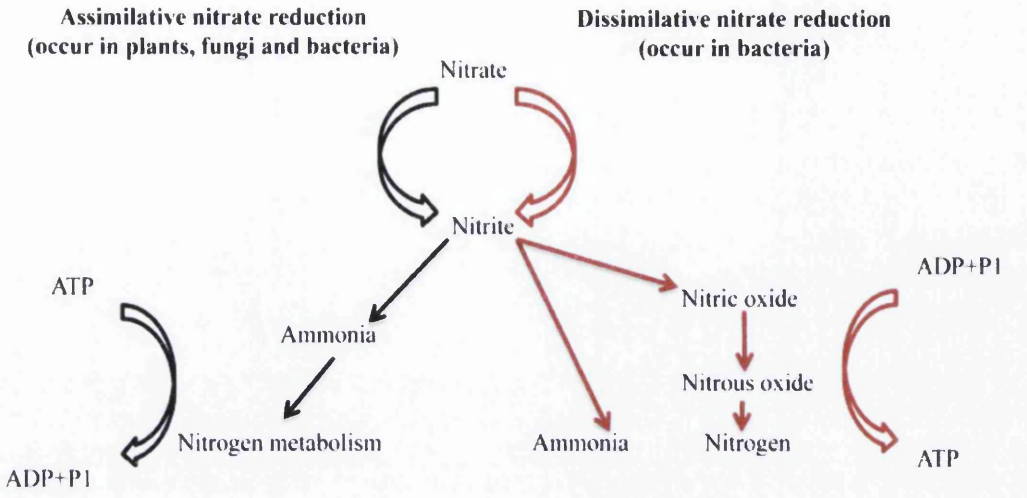

Figure 2-2: Nitrate reducing metabolic pathways

A1. Assimilatory cytoplasmic nitrate reductase (Nas)

The assimilatory nitrate reductase reduces nitrate to ammonium ions that are used by cells as a major nitrogen source for biosynthetic purposes. The assimilatory nitrate reductases may occur under aerobic or anaerobic conditions and require energy (Rowe *et al.* 1994). They occur in all plants, in most fungi, and in many bacteria. The nitrate reduction strictly takes place in the cytoplasm due to the cytoplasmic localisation of the enzyme, and therefore, it has to be transferred into the cell through specific transporters. The nitrate anion is reduced at the catalytic site in Nas releasing nitrite. The latter is exported to the periplasm and reduced immediately to ammonium in a six-electron reaction, catalysed by Nir. The resultant ammonium is then transferred to the cytoplasm to incorporate with biomolecules. Based on the cofactor structure, the bacterial assimilatory nitrate reductases are classified into two categories: ferredoxin- or flavodoxin-dependent Nas and NADH-dependent Nas. It has been shown that the ferredoxin-Nas can be found in *Azotobacter chroococcum*,

Clostridium perfringens and *Ectothiorhodospira shaposhnikovii* (Guerrero *et al.* 1981), whereas the flavodoxin-Nas is present in *Azotobacter vinelandii* (Gangeswaran and Eady 1996). On the other hand, the NADH-Nas proteins can be found in *Klebsiella pneumonia* (Lin *et al.* 1994) and in *Rhodobacter capsulatus* (Blasco *et al.* 1997).

A2. Dissimilatory (respiratory) membrane-bound nitrate reductase (Nar)

Membrane-bound nitrate reductases involved in the denitrification and anaerobic nitrate respiration where nitrate and nitrite act as terminal electron acceptors instead of molecular oxygen and are reduced to nitrous oxides, or further up to gaseous molecular nitrogen (Knowles 1982). The respiratory nitrate reduction is combined with the generation of the electrochemical proton gradient across the membrane (Boogerd *et al.* 1983), and is also coupled with the ATP generation (Carlson *et al.* 1982). The respiratory nitrate reductases are expressed in cells only under anoxic conditions in the presence of nitrate. They are inducible enzymes and their induction does not depend on degree of reduction of the carbon source available to the cell (Boogerd *et al.* 1983). They are also trans-membrane, highly hydrophobic enzymes with high degree of similarity in different bacterial strains (Hochstein and Lang 1991). In addition to nitrate, chlorate and bromate can be used as substrates of the Nar (Morpeth and Boxer 1985). Furthermore, the Nar can be competitively inhibited by azides (Carlson *et al.* 1982) or cystein (Yamaoka *et al.* 1994). Nar enzymes can be found in some bacteria and yeasts. They have been purified from several denitrifying and nitrate-respiring bacteria (Zumft 1997). They have also been found in *Thermus thermophilus* (Ramírez-Arcos *et al.* 1998), *E. coli* and *Paracoccus*

(Zumft 1997), some *Pseudomonas* species (Galimand *et al.* 1991, Sawers 1991) and *Staphylococcus carnosus* (Fast *et al.* 1997).

A3. Dissimilatory periplasmic nitrate reductase (Nap)

Periplasmic nitrate reductases were first reported for phototrophic and denitrifying bacteria; however they are widely spread among gram-negative bacteria. Although the nitrite generated by Nap can be used as a nitrogen source or as a substrate for anaerobic respiration, the Nap activity seems not to be primarily involved in nitrate assimilation or anaerobic respiration. Furthermore, the Nap enzyme does not have a direct contribution to the generation of a proton electrochemical gradient due to its periplasmic location (González *et al.* 2006, Moura *et al.* 2004). It has been clearly seen that Nap is a dissimilatory enzyme used for redox balancing (Berks *et al.* 1994, Moreno-Vivián and Ferguson 1998, Sears *et al.* 1997). The latter is necessary for optimal bacterial growth under some physiological conditions, particularly during fermentative processes in enteric bacteria, oxidative metabolism of highly reduced carbon substrates in aerobic heterotrophs, or anaerobic photoheterotrophic growth in photosynthetic bacteria. Nap enzymes have been found in *Desulfovibrio desulfuricans* (Dias *et al.* 1999), *Rhodobacter sphaeroides* (Reyes *et al.* 1996), *Paracoccus pantotrophus* (Berks *et al.* 1994) and *Pseudomonas putida* (Carter *et al.* 1995).

B. Nitrite reductase

Nitrite reductase (Nir) catalyses the reduction of nitrite to nitric oxide; thus, it is a key enzyme in denitrification due to the product of a gaseous compound that can be lost to the atmosphere. The Nir enzyme can distinguish denitrifying bacteria from

nitrate respiring bacteria which can convert nitrate to nitrite, but are not able to reduce nitrite to gaseous nitrogen (Priemé *et al.* 2002). It is a membrane-bound as well as a cytoplasmatic enzyme (Shapleigh *et al.* 1987). In denitrifying bacteria, nitrite reductases are classified into two different types, based on their prosthetic groups. The former is a cytochrome cd_1 and the other is a copper enzyme. Both of the nitrite reductase types are present in distinct strains from the genera *Pseudomonas* and *Alcaligenes*. Most of the studied denitrifying strains contain cytochrome cd_1 nitrite reductases. However, the copper nitrite reductases are found in a greater number of genera (Coyne *et al.* 1989).

C. Nitric oxide reductase

Nitric oxide reductase (Nor) is a membrane-bound enzyme (Zumft *et al.* 1987) and is responsible for the reduction of nitric oxide to nitrous oxide. The Nor enzymes are particularly interesting as they catalyse the formation of a double bond between two nitrogen atoms. They have been isolated from a few denitrifying bacteria, such as *Pseudomonas stutzeria* (Kastrau *et al.* 1994), *Paracoccus denitrificans* (Carr and Ferguson 1990), *Halomonas halodenitrificans* (Sakurai *et al.* 2005), *Pseudomonas aeruginosa* (Kumita *et al.* 2004) and *Pseudomonas nautica* (Stolz and Basu 2002).

D. Nitrous oxide reductase

Nitrous oxide reductase (Nos) catalyses the last denitrification step, where nitrous oxide is reduced to dinitrogen. This final step is coupled to ATP generation (Bazylinski and Hollocher 1985, Bryan *et al.* 1985). It has been found that the Nos enzyme is a copper protein (Michalski *et al.* 1986, Snyder and Hollocher 1987) as well as a cytoplasmatic enzyme (Kristjansson and Hollocher 1980). It has been

isolated from different denitrifying bacteria, including *Pseudomonas nautica (Brown et al. 2000a)*, *Paracoccus denitrificans* (Alvarez *et al.* 2000, Brown *et al.* 2000b) and *Paracoccus pantotrophus* and *Pseudomonas Stutzeri* (Rasmussen *et al.* 2000).

2.1.1.5.2. Classification of Denitrifying Bacteria

Microorganisms involved in denitrification are often characterised as either aerobic autotrophic or heterotrophic. These denitrifying bacteria can turn to anaerobic growth if nitrate is used as an electron acceptor (Blackall and Burrell 1999, Ward 1998). However, the ability to denitrify is not only limited to bacteria, as it has been reported that different archaea (Zumft 1997) and fungi (Shoun and Tanimoto 1991, Usuda *et al.* 1995) have the ability to denitrify. This thesis focuses on denitrifying bacteria only. Over 130 denitrifying bacteria species within more than 60 genera have been listed by Philippot *et al.* (2007). These denitrifying bacteria can be found in *Alpha-*, *Beta-*, *Gamma-*, *Epsilon-proteobacteria* and *Bacteroides*, and also among the Gram-positive bacteria *Firmicutes* and *Actinobacteria*.

Denitrifying bacteria are often classified into five different functional groups with respect to their ability to reduce nitrate or nitrite (Drysdale *et al.* 2001). These groups are the incomplete denitrifiers, true denitrifiers, sequential denitrifiers, exclusive nitrite reducers and non-denitrifiers.

A. Incomplete denitrifiers

Incomplete denitrifiers, which are also known nitrate respirers, are able to reduce nitrate to nitrite, but they lack the enzyme that facilitates nitrite reduction. These bacteria require oxygen, however they have the ability to adapt to an oxygen-free

environment, in which nitrate is used as an alternative electron acceptor (Drysdale *et al.* 2001).

B. True denitrifiers

True denitrifiers have nitrate and nitrite reductase enzymes, allowing simultaneous reduction of both nitrate and nitrite, resulting in a complete denitrification (Drysdale *et al.* 2001). This denitrification occurs under anaerobic conditions where these enzymes are induced (Drysdale *et al.* 2001).

C. Sequential denitrifiers

Sequential denitrifiers can facilitate both nitrate and nitrite reduction (similar to the true denitrifiers) with the exception of inhibiting the nitrite reduction in the presence of nitrate. This inhibition in the nitrite reduction can result in nitrite accumulation during nitrate reduction (Drysdale *et al.* 2001).

D. Exclusive nitrite reducers

Exclusive nitrite reducers exhibit non-denitrification characteristics in nitrate media due to the absence of nitrate reductase enzymes. However, they can efficiently reduce nitrite in nitrite media (Drysdale *et al.* 2001).

E. Non-denitrifiers

Non-denitrifiers have no role in the denitrification process, due to the lack of nitrate and nitrite reductase enzymes (Drysdale *et al.* 2001).

2.2. Microbial Fuel Cells (MFCs)

2.2.1. Overview

The conventional fuel cell is an electrochemical device that generates electricity by using the chemical energy from a fuel through a chemical reaction. In contrast, MFCs are bio-electrochemical systems (BESs) that use electrochemically active microorganisms. The microorganisms act as a catalyst for the electrochemical oxidation of the organic material, and the electrode is therefore referred to as a microbial bioanode (Cohen 1931). This oxidation occurs in an anaerobic environment, resulting in producing electrons, protons and CO_2. The protons, which are created at the anode to maintain a charge balance, typically migrate through the solution to the cathode. In contrast, the electrons flow through an external electrical circuit with a load resistance to the cathode, and in turn combine with protons and an oxidant to generate electricity. Typical electrode reactions, which use acetate as an example of a substrate on the anodic compartment, is given as

$$CH_3COO^- + 4H_2O \rightarrow 2HCO_3^- + 9H^+ + 8e^- \quad (2.11)$$

On the cathodic compartment, the reaction can be expressed either as

$$4H^+ + 4e^- + O_2 \rightarrow 2H_2O \quad (2.12)$$

or

$$4H^+ + 4e^- + 2O_2 \rightarrow 2H_2O_2 \quad (2.13)$$

Based on electron transfer mechanisms (the ability of microorganisms to transfer the electron), MFCs are often categorised into two distinct groups: mediator MFCs and mediatorless MFCs. The microbial cells are electrochemically inactive due to the nonconductive cell surface structure. Therefore, mediators are used to facilitate electron transfer from the microbial cells to the anode. Several mediator compounds

are used including dyes and potassium ferricyanide (Emde *et al.* 1989), azure A (Choi *et al.* 2001), metalorganics such as thionine (Kim *et al.* 2000), neutral red (Park and Zeikus 2000). Good mediators should offer the following features, having (Ieropoulos *et al.* 2005a):

i. The ability to easily cross the cell membrane.
ii. The ability to grab electrons from the electron carriers of the electron transport chains.
iii. High electrode reaction rates.
iv. A good solubility in the analyte.
v. Non-biodegradability (not being metabolised by the biocatalyst) and being non-toxic to microbes.
vi. Low cost.

Mediatorless MFCs do not require the aid of a mediator, as the microorganisms used are able to directly transfer electrons to the electrode surface. This requires a physical contact between the microorganisms and the electrode for current production. The contact point can be facilitated by outer membrane-bound cytochromes or putatively conductive pili called nanowires. Mediatorless MFCs use bio-electrochemically active bacteria that can form a biofilm on the anode surface, allowing a direct electron transfer to the anode. The anode acts as a final electron acceptor in the dissimilatory respiratory chain of the microbes on the biofilm. A biofilm that is formed on the cathode surface may also play an important role in electron transfer between the microbes and the electrodes. Mediatorless MFCs are advantageous in wastewater treatment and power generation (Ieropoulos et al. 2005a). A typical two chamber MFC with possible modes of electron transfer is shown in Fig. 2.3. In a

conventional MFC, the cathode is abiotic, due to the use of expensive and sustainable catalysts. Microbial biocathodes have been shown as a greatly promising alternative, as inexpensive and sustainable electrode materials can be used (He and Angenent 2006). Biocathodes, which adopt terminal electron acceptors (TEA), can be classified into two categories: aerobic and anaerobic. The former uses oxygen as a terminal electron acceptor. While the latter uses other compounds, such as nitrate, iron, manganese, selenate, arsenate, urinate, fumarate and carbon dioxide, as terminal electron acceptors (Lefebvre *et al.* 2008).

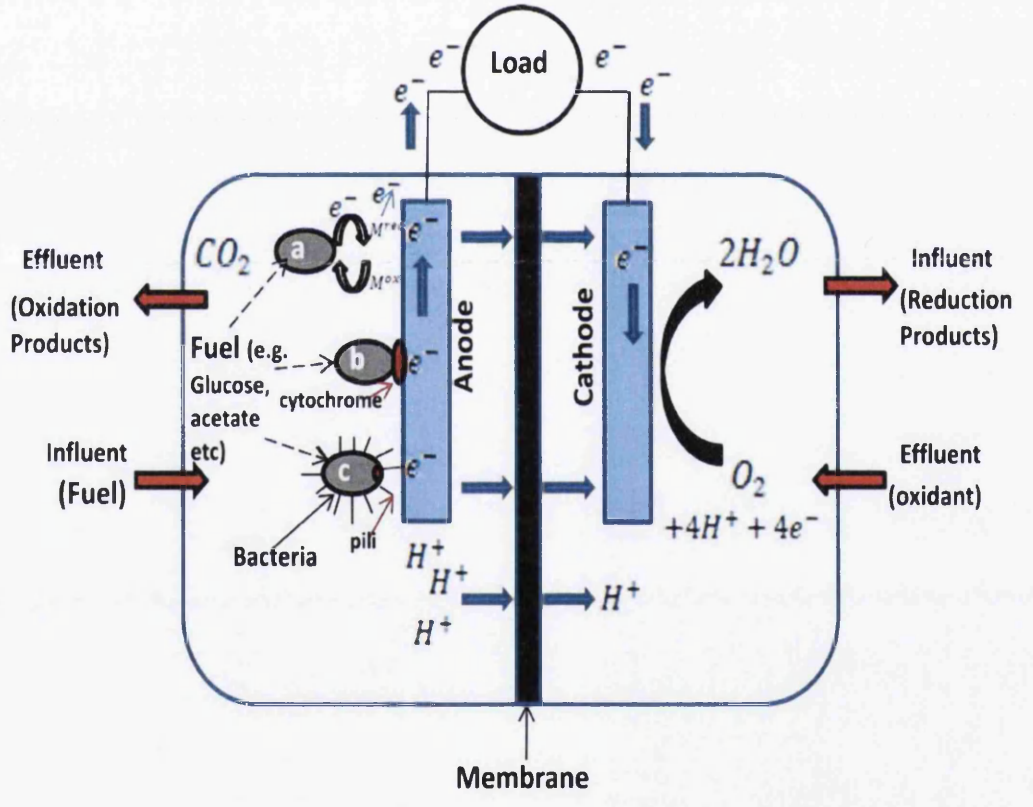

Figure 2-3: Schematic of a conventional two chamber MFC with three possible modes of electron transfer: (a) electron transfer through a mediator, (b) direct electron transfer via outer membrane cytochromes, and, (c) electron transfer through a nanowire.

In the absence of oxygen and when nitrate is used as the electron acceptor, the reduction reaction can be expressed as given in equation (2.5).

The performance of MFCs using glucose/nitrate was assessed under closed and open circuit conditions (Jia *et al.* 2008). MFCs operating with anaerobic bio-cathode and using nitrate as the terminal electron acceptor were presented and shown to be a promising technology for nitrate removal (Lefebvre *et al.* 2008). The mechanism for this system is shown in Fig. 2.4.

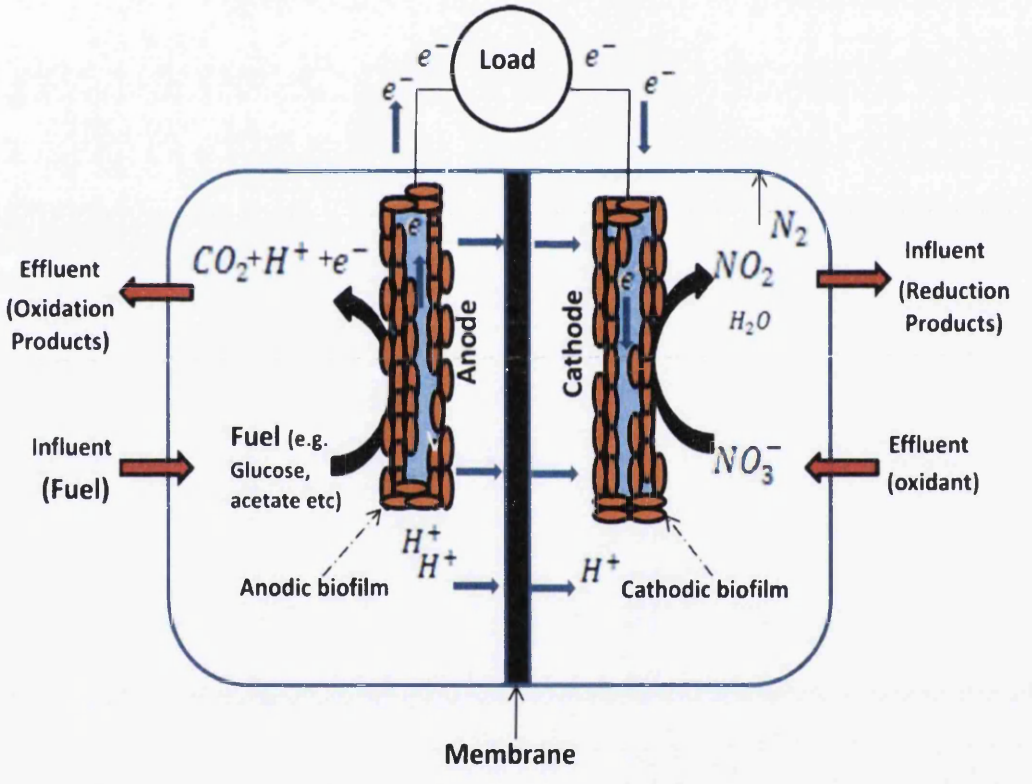

Figure 2-4: Diagram of an MFC's mechanism using nitrate as the terminal electron acceptor.

2.2.2. MFC History and Developments

Many researchers have studied the application of MFCs for biological processes in wastewater treatment. The MFC is a special type of biofuel cell, which can convert

dissolved organic matter into electricity using microorganisms. The evidence of bioelectricity was first experimentally found in the late eighteenth century by Luigi Galvani (Piccolino 1998). He observed an electric response by connecting a frog's legs to a metallic conductor. In 1911, Michael C. Potter built the first MFC where a current flow between two electrodes could emerge in a bacterial culture and in sterile medium (Lewis 1966). In 1931, Cohen revived Potter's idea and demonstrated that a batch of biological fuel cells could produce more than 35V. In the mid-19th century, (Rohrback *et al.* 1962) designed a biological fuel cell for the first time that used Clostridium butyricum as a biological material to generate hydrogen by glucose fermentation. The increased interest in converting organic waste into electrical energy has encouraged research into MFCs. The MFC is a demi-biological system, since only the anode side contains microorganisms, while the cathode is abiotic. This can lead to a major limitation in MFC applications and their economic viability. Therefore, to maximise the power output as well as reduce operating costs there has been an increased interest in replacing abiotic cathodes with biocathodes where living microorganisms can enhance the reduction catalysis (He and Angenent 2006). A biocathode MFC, which used denitrifying bacteria to reduce nitrate to nitrogen gas, was proposed 40 years ago (Lewis 1966), and this concept was recently verified through further experiments. Heterotrophic denitrifiers were applied to compare the denitrification efficiency of two cathode materials in water treatment (Cast and Flora 1998). Stainless steel rods wrapped with stainless steel mesh (SS/SS) and graphite rods wrapped with polypropylene mesh (Gr/PP) were examined in their study. A bio-electrochemical system was employed, consisting of a graphite anode rod surrounding by four cathode rods, switching to continuous flow operation after 5 days of batch operations in order to cultivate a biofilm on the cathode's surface (for

over a month). Initial concentration of 100 mg $NO_3^- - N/l$ was tested, applying 1 mA electric current with a flow rate of 640 ml/d corresponding to a hydraulic residence time (HRT) of 5.5 days. The effect of copper on water denitrification was investigated. During all their experiments, nitrite was produced by denetrification and accumulated in the electrochemical cell. However, complete denitrification was not achieved, and the exact removal rate using each cathode material was not mentioned. It was also found that the denitrifying process would not be possible when a wastewater stream contained heavy metals due to inhibition of biofilm activity caused by depositing heavy metals on the surface of cathodes (Cast and Flora 1998).

Another experiment involved a recycle biofilm-electrode reactor, consisting of a cylindrical graphite cathode placed along the reactor wall and a graphite anode rod at the centre of the reactor (Islam and Suidan 1998). The aim was to obtain a uniform current distribution throughout the reactor. Groundwater treatment was examined utilising a synthetic wastewater that contains 20 mg $NO_3^- - N/l$ and autotrophic denitrifying microorganisms immobilised on the inner surface of cylindrical cathode. Phosphate was first used as a buffer, and then replaced with carbonate to simulate real groundwater. It was demonstrated that nitrate removal increased when the electric current intensity increased to 20 mA. However, a decline in nitrate removal was observed when the electric current intensity exceeded 25 mA due to hydrogen inhibition. The highest nitrate removal efficiency of 98% was achieved at a current of 20 mA using phosphate as a buffer.

Watanabe *et al.* (2001) utilised a cylindrical reactor centred by one carbon rod as the anode, surrounded by 12 carbon cathode rods wrapped with carbon fiber felt. This was employed to study the denitrification of high acidic wastewater from

copper metal pickling using heterotrophic denitrifiers (Watanabe *et al.* 2001). This reactor was continuously operated with synthetic wastewater, adding acetate to support heterotrophic denitrifying bacteria. Nitrate and copper removal at a range of copper concentrations of 1-35 mg/l was investigated. An electrical current intensity range of 15-23 mA and C/N ratio of 0.7-1.2 were examined over different ranges of HRT (5-36 h). The results showed that copper ion removal, denitrification and neutralisation can be simultaneously achieved using a single bio-electrochemical reactor. It was also shown that denitrification was efficient at a copper concentration less than 30 mg/l. In 2001 Sakakibara and Nakayama proposed a multi-electrode reactor where an autotrophic denitrifying biofilm was located on the cathode surface (Sakakibara and Nakayama 2001). Eight cathodes and two anodes in cylindrical shapes made from expanded metal were concentrically placed in that reactor. Polyurethane foam was used on the surface of each cathode to support the denitrifying biofilm. An electrode potential or electric current was individually applied to each part of the multi-electrode in order to achieve uniform cathodic or anodic reactions without the limitation caused by low electrolytic conductance. A long term (over 500 days) continuous experiment was performed to improve treatment of dilute solutions, such as groundwater or surface water containing nitrate of 20 mg $NO_3^- - N/l$. The system provided a large effective surface area, a charge transport mechanism by dissociative electrolytes (HCO_3^- and CO_3^{2-}), and the formation of a low oxidation reduction potential (ORP) zone in the multi-electrode system.

The performance of a combined Bio-Electrochemical System (BES) was studied, which consisted of five porous electrodes acting as multiple cathodes and an inert anode, and microfiltration (MF) membrane (Prosnansky *et al.* 2002). The MF

membrane was used to avoid escaping microorganisms from the BES. Autotrophic denitrification using CO_2 was applied. Cathodes, made of a granular activated carbon (GAC), coupled with stainless steel expanded metals, were connected in series with a platinum anode coated with titanium. Experimental results demonstrated the capability of the multi-cathode BES to operate at high denitrification rates with a low hydraulic retention time of 20 min. An improvement in the denitrification rate of 16.4 mg $NO_3^- - N/h$ was reported. This significant enhancement, due to the large effective surface area and low ORP zone formation in the multi-cathode region, can overcome the slow operation of biological denitrification.

Further, in 2004, Gregory and his group demonstrated that electrodes can serve as electron donors for nitrate reduction to nitrite when an electrode is poised at a negative potential with the presence of *Geobacter metallireducens* or an adapted enrichment culture (Gregory *et al.* 2004). This result was in agreement with that achieved by another group of researchers, who observed biological nitrate reduction through accepting electrons from the cathode electrode in a potentiostat-poised half cell (Park *et al.* 2005). It was shown that nitrate was completely reduced to nitrogen gas, and the reactions occurred without using any organic substrates (electron donors). A maximum nitrate reduction rate of 98% was achieved at an applied current of 200 mA. However, a decline in the nitrate reduction rate was observed when the applied current exceeded 200 mA due to the consumption of electricity for hydrolysis of water and due to the production of hydrogen on the cathode. It was also shown that hydrogen was an undesirable key electron donor for nitrate reduction, and the cathode electrode directly delivered electrons to denitrifying bacteria.

In this regard, an electrolytic cell was employed to perform nitrification in the anode and denitrification in the cathode (Goel and Flora 2005). Biological reactions were promoted using electrical power. The results showed that bacteria in the cathode can use the electrode as a sole electron donor. However, the first development of a biocathode was achieved by (Clauwaert *et al.* 2007a). A tubular MFC was designed with the cathode placed inside the anode. The two chambers were filled with graphite granules and separated by a cation exchange membrane (CEM). They demonstrated that a complete denitrification, where nitrate was completely converted to nitrogen gas, can be performed using microorganisms in the cathode with electrons supplied by microorganisms oxidising acetate in the anode. The highest power output achieved was 4 W/m^3 total cathodic compartment (TCC) with a cell voltage of 0.214 V and a current of 35 A/m^3. Organic removal and bio-electrochemical denitrification were simultaneously achieved through the use of two chamber MFCs (Jia *et al.* 2008). The highest power output gained was 1.7 mW/m^2 at a current density of 15 mA/m^2. A maximum volumetric nitrate removal of 0.084 mg $NO_3^- - N\ cm^{-2}$ and coulombic efficiency of 7% were reported. It was found that the reduction of nitrate in the cathode chamber was relatively dependent on the magnitude of the electricity current. This encouraged the researchers to carry out biological denitrification through a biofilm-cathode, using electrons generated from the anodic bio-reaction in the MFC. The effect of nitrate on the performance of a single chamber air cathode MFC system was investigated by Sukkasem *et al.* (2008). They also examined the denitrification activities at various nitrate concentrations and external resistances. Their design consisted of an anode and cathode both were placed in a plastic cylindrical chamber with an electrode spacing of 2 cm. The anode electrode was made of carbon cloth, and the cathode was prepared by coating

platinum catalyst of 0.5 mg/cm^2 on a carbon cloth. The results showed that the single chamber MFCs could remove more than 85% of nitrate in less than 8 h in the first batch, and in an hour after a 4-month operation. It was, however, observed that the maximum voltage output was affected by the nitrate at low resistance due to low organic carbon availability, it was not affected at higher external resistance. It was also noticed that the coulombic efficiency (CE) was greatly affected by the nitrate due to the competition between the electricity generation and the denitrification processes. In 2008, Lefebvre and coworkers proposed a novel type of two-chambered MFC where the costly catalyst on the cathode surface was replaced by an autoheterophic denitrifying biofilm (Lefebvre *et al.* 2008). Denitrification was performed by microorganisms using electrons supplied by bacteria oxidising domestic wastewater and with acetate as the substrate in the anode chamber. A maximum power density of 9.4 mW/m^2 of anode surface and a maximum volumetric power of 0.19 W/m^3 of anode chamber volume were generated over more than 45 days. It was also demonstrated that over 65% of chemical oxygen demand (COD) and 84% of total nitrogen were removed.

2.2.3. MFC Configurations and Designs

An MFC typically consists of an anodic chamber and a cathodic chamber that are separated by a proton exchange membrane (PEM). However, two basic MFC designs can be used in analysing the different aspects and potential of MFCs. These are single chambered and two chambered MFCs. Two chamber fuel cells consist of two separated chambers, where each has at least one electrode. The reactor should be designed so that the ionic strength is identical in the two chambers. A single chamber fuel cell has one chamber that is an anaerobic environment. The cathode of the

chamber has two faces, one is placed in the anaerobic solution and the other is exposed to the air. Two chamber MFCs are difficult to scale up due to their complex design. Single chamber MFCs offer simpler designs and cost savings, and they eliminate the need for the cathodic chamber by exposing the cathode directly to the air. MFCs can be run in fed-batch or continuous operation mode under open or closed circuits.

Several designs for MFCs with improved performance have emerged (see Fig. 2.5). To the best of my knowledge, the highest power density was achieved through the use of a design with four continuous MFCs side-by-side in which the chambers were separated by the PEM, as shown in Fig. 2.5B (Rabaey *et al.* 2005a). A modification of this design, proposed by Rabaey *et al.* (2005b), including a granular graphite matrix for the anode and close anode-cathode placement, is shown in Fig. 2.5C. This modified MFC design achieved a maximum power density of 49 W/m^3 with coulombic and energy conversion efficiencies of 50.3% and 26% respectively. Fig. 2.5D shows an example of a photobiological fuel cell that utilises the metabolic activity of *Rhodobacter sphaeroides* to generate electricity based on the in situ oxidation of photobiological hydrogen (Rosenbaum *et al.* 2005). It achieved 8.4% energy conversion efficiency and a current density of 28.8 A/m^3. Fig. 2.5A displays an MFC system with a salt bridge and two chambers (bottles) connected using a glass tube. The latter was heated and bent into a U-shape. It was then filled with agar and salt to serve as a CEM and then inserted through the lid of each bottle. The salt bridge MFC, however, produced little power due to the high internal resistance observed (Min *et al.* 2005a).

A single chamber MFC, which represents the simplest configuration where both anode and cathode are placed on either side of a tube, is seen in Fig. 2.5E. The

anode was sealed against a flat plate and the cathode was placed in direct contact with air (Liu and Logan 2004). A widely used and inexpensive design is a two chamber MFC built in a traditional 'H' shape, as shown in Fig. 2.5F. The H-shape design usually consists of two bottles connected by a tube. The tube contains a separator that is usually a CEM, such as Nafion (Logan *et al.* 2005, Min *et al.* 2005a), Ultrex (Rabaey *et al.* 2003) or a plain salt bridge (Min *et al.* 2005a). The key feature in this design is the ability to choose a membrane that allows protons to pass between the chambers. H–shape systems are acceptable for basic parameter studies, such as the examination of power production using new materials or types of microbial communities arising during the degradation of specific compounds.

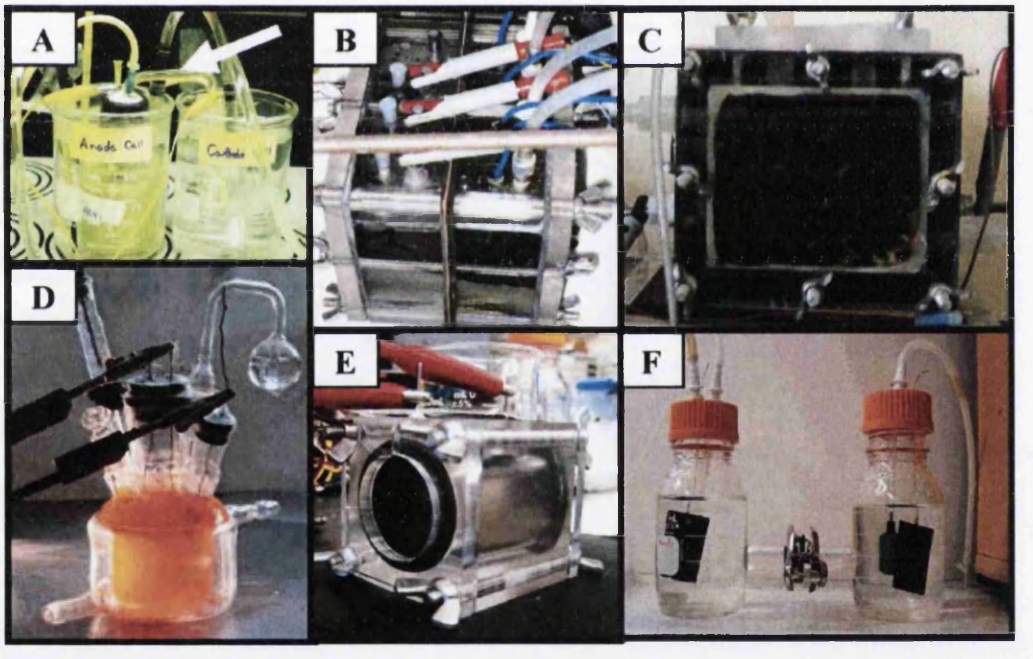

Figure 2-5: Types of MFCs used in studies: (A) two chamber system with a salt bridge (shown by arrow) (Min *et al.* 2005a). (B) four batch-type MFCs where the chambers are separated by the PEM (Rabaey *et al.* 2005a). (C) similar to B but with a continuous flow-through anode of granular graphite matrix and close anode-cathode placement (Rabaey *et al.* 2005b). (D) photoheterotrophic MFC (Rosenbaum *et al.* 2005). (E) single chamber MFC with air cathode (Liu and Logan 2004). (F) two chamber H-shape system (Logan *et al.* 2005).

The power density produced by these systems is typically limited due to high internal resistance and due to electrode-based losses. The power generation is also affected by the surface area of the cathode relative to that of the anode (Oh *et al.* 2004) and the surface area of the membrane (Oh and Logan 2006).

In order to increase the power density as well as offer the possibility of a continuous flow through the anode chamber, several changes have been introduced to the previously described systems (which were operated in batch mode). A tubular single chamber continuous MFC, which uses granular graphite matrix as the anode and a ferricyanide solution in the cathode chamber, was proposed by Rabaey *et al.* (2005c), and is shown in Fig. 2.6A. Two substrates: glucose and acetate were used. The power density achieved using acetate was higher than that obtained when glucose was used. An up-flow MFC is an alternative design that used a cathode chamber located on the top of the anode chamber, with the fluid flowing continuously through porous anodes towards a membrane separating the two chambers (He *et al.* 2005). The design, shown in Fig. 2.6B, was able to continuously generate electricity with a maximum power density of 170 mW/m^2 over a five month period of feeding with a sucrose solution as the electron donor. Fig. 2.6C shows a flat plate design that contains a single channel separated into two halves forming the anode and cathode chambers (Min and Logan 2004). The maximum power density obtained for domestic wastewater was 2.8 times that obtained in Liu *et al.* (2004) under continuous flow conditions using a single chamber MFC (see Fig. 2.6D). The single chamber MFC consisted of a single cylindrical chamber containing eight graphite rods (anode) placed in a concentric arrangement about a single air cathode. In addition, it was shown that stacking several MFCs in series or parallel can increase the overall system voltage (Aelterman *et al.* 2006), see Fig 2.6E.

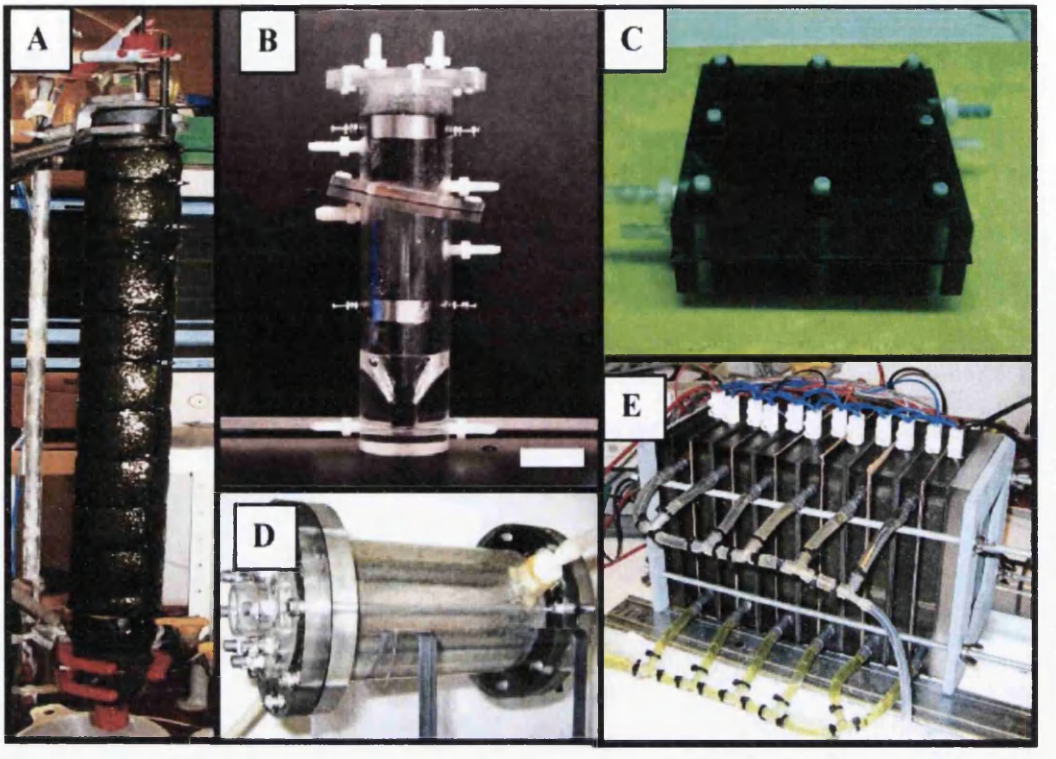

Figure 2-6: MFCs used for continuous operation: (A) upflow, tubular type MFC with inner graphite bed anode and outer cathode (Rabaey *et al.* 2005c); (B) upflow, tubular type MFC with anode below and cathode above, the membrane is inclined (He *et al.* 2005); (C) flat plate design where a channel is cut in the blocks so that liquid can flow in a serpentine pattern across the electrode (Min and Logan 2004); (D) single-chamber system with an inner concentric air cathode surrounded by a chamber containing graphite rods as anode (Liu *et al.* 2004); (E) stacked MFC, in which 6 separate MFCs are joined in one reactor block (Aelterman *et al.* 2006).

2.2.4. Microbiology

2.2.4.1. Bacterial Metabolism

Metabolism refers to the sum of all chemical reactions carried out in a living organism (Chapelle and Francis 2001). Since chemical reactions either release or require energy, metabolism can be viewed as the means of balancing energy. Accordingly, metabolism is often categorised into two classes of chemical reactions: catabolic and anabolic reactions. Catabolic reactions release energy through the

breakdown of complex organic compounds into simpler ones. The reverse process is carried out in anabolic reactions in which energy is used to build complex organic molecules from simpler ones. Catabolic reactions are generally hydrolytic reactions (which make use of water to break chemical bonds), and these are exergonic reactions (which produce more energy than that consumed). In contrast, anabolic reactions release water and consume more energy than that produced, and these are therefore dehydrolytic and endergonic reactions.

The metabolism functions in the cell, including energy extraction from certain compounds, storing and then using the energy to grow and maintain necessary functions, must follow two basic laws of thermodynamics. The first states that energy can neither be created nor destroyed (Halliday *et al.* 2003). For bacteria, this thermodynamic law indicates that the amount of energy made possible from organic compounds is the amount available for use only. The second thermodynamic law states that in closed, irreversible systems, entropy will always increase (Halliday *et al.* 2003). This reflects that the energy available in a system can be made up of usable energy and unavailable energy. The unavailable energy leads to increase the entropy of a system and losses such as through heat. The usable energy which is released during a reaction is called the Gibbs free energy (ΔG_r). ΔG_r has a negative value for an energy-releasing reaction, while it is positive if the reaction is energy-consuming.

2.2.4.2. Energy Production

Examination of energy production in microorganisms needs to take account of two general aspects: the concept of oxidation-reduction and the mechanism of ATP (Adenosine TriPhosphate) generation.

2.2.4.2.1. Oxidation-Reduction Reactions

Oxidation refers to the process of electron removal from an atom or molecule, while gaining one or more electrons is called reduction. However, it has to be noted that oxidation and reduction reactions are always coupled, and their combination is called oxidation-reduction reaction or a redox reaction. In many cellular oxidations, electrons and protons (hydrogen ions, H^+) are always removed at the same time. This equates to the removal of hydrogen atoms, since each hydrogen atom is made up of one proton and one electron. As most biological oxidation reactions involve the loss of hydrogen atoms, they are denoted as dehydrogenation reaction. Enzymes that help in removing hydrogen atoms from organic compounds are called dehydrogenases. These enzymes often have electron-storing intermediate compounds as their coenzymes. One of these coenzymes is called nicotine adenine dinucleotide (NAD^+). The loss of hydrogen atoms allows a reduction in the NAD^+, forming a reduced coenzyme, NADH. This is due to the NAD^+ accepting two electrons and one proton from each of the two hydrogen atoms removed from the substrate. One proton (H^+) is left over from each single reduction, and this is then released to the surrounding medium. This reaction can be written as

$$NAD^+ + 2H^+ + 2e^- \rightarrow NADH + H^+ \qquad (2.14)$$

The reduced coenzyme, NADH, has more energy than NAD^+, and this energy can be used to generate ATP in later reactions (Pommerville 2010). It has to be noted that cells use biological oxidation-reduction reactions in catabolism to extract energy from nutrient molecules through the degradation of the highly reduced compounds to highly oxidised compounds.

2.2.4.2.2. The Mechanisms of ATP Generation

Living cells use certain compounds to temporarily store energy to be used in coupling catabolic and anabolic reactions. These energy-storing compounds include ATP, guanosine triphosphate (GTP) and acetyl-coenzyme A. ATP, which is the most important energy-storing compound, stores energy obtained from catabolic reactions, and releases that energy later in deriving anabolic reactions and performing other cellular work (Pommerville 2010). A molecule of ATP contains adenine, ribose and three phosphate groups. An adenosine diphosphate (ADP) compound can be formed when ATP loses one of its phosphate groups located at the end of the molecule. This results in an energy that can help deriving anabolic reactions. Representing a phosphate group as *p,* this reaction can be expressed as:

$$ATP \rightarrow ADP + p + energy \tag{2.15}$$

ADP can be converted back to ATP through the process of phosphorylation using the energy derived from catabolic reactions to combine ADP and a phosphate group, p to resynthesise ATP as follows:

$$ADP + p + energy \rightarrow ATP \tag{2.16}$$

In order to generate ATP from ADP, organisms use three phosphorylation mechanisms: substrate-level phosphorylation, oxidative phosphorylation and photophosphorylation.

A. Substrate-level phosphorylation

In substrate-level phosphorylation, ATP is usually generated through a direct transfer of a high-energy phosphate from a substrate to ADP. The phosphate generally achieved its energy during an earlier reaction of substrate oxidation.

B. Oxidative phosphorylation

In oxidative phosphorylation, electrons are transferred from organic compounds to one group of electron carriers. The electrons are then passed to oxygen molecules or other oxidised inorganic and organic molecules through a sequence of electron carriers called an electron transport chain (ETC). The transfer of electrons between adjacent electron carriers results in releasing energy which helps generating ATP from ADP through a process called chemiosmosis. This process is carried out in the plasma membrane of prokaryotes and in the inner mitochondrial membrane of eukaryotes. The ETC process, including chemiosmosis, is discussed in Section 2.2.4.3.

C. Photophosphorylation

Photophosphorylation involves an electron transport chain and occurs only in photosynthetic cells, which consists of light-trapping pigments such as chlorophylls. It starts with converting light energy into the chemical energy of ATP and NADPH (the reduced form of nicotinamide adenine dinucleotide phosphate (NADP)). The resultant chemical energy is then used to synthesise organic molecules.

2.2.4.3. Metabolic Pathways of Energy Production

A metabolic pathway is a sequence of enzymatically catalysed chemical reactions that occur in a cell. It helps organisms to release energy from organic molecules and store it in a chemical form. Carbohydrates (mainly glucose) are the main source of cellular energy in most microorganisms. However, they can also catabolise various lipids and proteins in order to produce energy. Energy production in microorganisms can be generally carried out in two processes: cellular respiration and fermentation.

Fermentation is the carbohydrate enzymatic degradation in which the final electron acceptor is an organic molecule. In the fermentation process, ATP is generated through the substrate-level phosphorylation, where oxygen is not required. Cellular respiration is a process of ATP-generation where molecules are oxidised and the final electron acceptor is an inorganic molecule. It uses oxygen as a final electron acceptor if the organism is aerobic, while the final electron acceptor is an inorganic molecule other than oxygen in an anaerobic respiration. Typically, carbohydrate respiration occurs in three stages: glycolysis, the Krebs cycle and the electron transport chain (ETC). Both cellular respiration and fermentation have a similar start for glycolysis, but they follow different subsequent pathways. The fermentation process neither involves the Krebs cycle nor ETC. Therefore, fermentation relies only on glycolysis to generate ATP, which is lower than that produced through respiration. The three stages (glycolysis, the Krebs cycle and ETC) involved in carbohydrate catabolism are considered next.

A. Glycolysis

Glycolysis is typically the first stage of carbohydrate catabolism, and is defined as the breakdown of glucose into two molecules of pyruvic acid (Nester 2007). Oxygen is not required in the glycolysis, and an ATP is produced through the substrate-level phosphorylation by reducing the NAD^+ to NADH. Many bacteria use other pathways, in addition to using glycolysis, for carbohydrate oxidation. The most common alternatives pathways are the pentose phosphate and the Entner-Doudoroff pathways. The former simultaneously operates with glycolysis, and offers the means of breaking down five-carbon sugar (pentose) as well as glucose. A key feature of this pathway is that it produces important intermediate pentoses that are used in the

synthesis of nucleic acids, glucose from carbon dioxide in photosynthesis and certain amino acids. Bacteria, which use the pentose phosphate pathway, include *Bacillus subtilis*, *E. coli*, *Leuconostoc mesenteroides* and *Enterococcus faecalis*. Furthermore, bacteria that have the enzymes for the Entner-Doudoroff pathway are able to metabolise glucose without using either glycolysis or the pentose phosphate pathway. These bacteria are gram-negative bacteria, including *Rhizobium*, *Pseudomonas* and *Agrobacterium*. It has to be noted that gram-positive bacteria do not use the Entner-Doudoroff pathway.

B. The Krebs cycle

The Krebs cycle, which is also known as the citric acid cycle, is a series of biochemical reactions that help release of a large amount of potential chemical energy stored in acetyl coenzyme-A (acetyl Co-A). This cycle also makes use of a series of oxidations and reductions to transfer that potential energy, in the form of electrons, to electron carrier coenzymes (mainly NAD^+). Since pyruvic acid, the product of glycolysis, cannot directly enter the Krebs cycle, it must lose one molecule of CO_2 through a process called decarboxylation. The pyruvic acid then becomes a two-carbon compound called an acetyl group, which attaches to coenzyme A through a high-energy bond to form acetyl Co-A. The oxidation of acetyl Co-A leads to reducing the coenzymes NAD^+ and flavin adenine dinucleotide (FAD). The coenzyme FAD requires two complete hydrogen atoms (two electrons and two protons) to reduce to $FADH_2$, in contrast to the reduction of NAD^+ where two electrons and one proton are needed. Some ATP is also produced in the Krebs cycle.

C. Electron transport chain (ETC)

The ETC consists of a sequence of carrier molecules that have the capability of oxidation and reduction. Electrons pass along the chain in a gradual and stepwise fashion so that energy is released in manageable quantities that help to drive the chemiosmotic generation of ATP. The final oxidation is irreversible. In the ETC, there are three classes of carrier molecules including flavoproteins, cytochromes and ubiquinones (coenzyme Q).

Flavoproteins, which contain flavin, are coenzymes that are derived from riboflavin (vitamin B_2), and are able to perform alternative oxidations and reductions. One important flavoprotein coenzyme is flavin mononucleotide (FMN). Cytochromes, which are proteins with an iron-containing group (heme), are able to alternately exist as a reduced form (Fe^{2+}) and an oxidised form (Fe^{3+}).

The cytochromes involved in the ETCs include cytochrome b (cyt b), cytochrome c (cyt c), cytochrome c_1 (cyt c_1), cytochrome a (cyt a) and cytochrome a_3 (cyt a_3).

Ubiquinones, symbolised as Q, are small nonprotein carriers. FMN and Q carriers can accept and release protons as well as electrons, whereas cytochromes transfer electrons only. The ETCs are somewhat diverse in that the particular carriers utilised by a bacterium and the order of their functions may differ from those of other bacteria and eukaryotic mitochondrial systems. Several types of ETCs may even exist in a single bacterium. However, they have the same function, which is releasing energy due to the transfer of electrons from higher- to lower-energy compounds.

In prokaryotic cells, when energetic electrons flow down the ETCs some of the chain carriers pump (i.e., actively transfer) protons across the plasma membrane from the cytoplasmic side. These carrier molecules are known as proton pumps. The

phospholipid plasma membrane is normally impermeable to protons, thus forming one-directional pumping of protons, which results in a proton gradient (a difference in the proton concentrations on the two sides of the plasma membrane). In addition to this proton gradient, an electrical charge gradient is also established due to the excess protons on one membrane side, so that side is positively charged compared to the other side. This can result in a potential energy called the proton motive force (PMF). The protons concentrated on the side of the membrane can only diffuse across the membrane through special protein channels containing an enzyme known as ATP synthase. This proton flow releases energy that is then used by the enzyme to generate ATP from ADP and a phosphate group. The mechanism of ATP generation using the ETC is called chemiosmotic.

2.2.5. Electron Transfer Mechanisms in MFCs

In microbial fuel cells (MFCs), bacteria act as a catalyst in transferring electrons from the substrate to the electrode (anode). Attachment of bacteria forming a biofilm on the anode surface is essential for an efficient biological electron transfer. Bacterial biofilms are extremely complex bacterial ecosystems that consist of bacteria attached to a surface and which are embedded in a matrix of proteins, DNA and polysaccharides and a high water content (>90%). They can increase the phenotypic changes in colony morphology and can also enhance access to nutrients and closer proximity between cells, which facilitates mutualistic or synergistic associations and protection (Costerton *et al.* 1995). Electrode associated biofilms can form conductive networks that are capable of long-range electron transfer, though the exact mechanisms are still unknown (Franks *et al.* 2010). The electron transfer mechanism is metabolically active, but is limited due to proton accumulation (Franks *et al.*

2010). In addition, the attached bacteria oxidise the substrate as part of the metabolism process, resulting in electron transfers extracellularly to the electrode. These bacteria have the capability of extracellular electron transfer, and are therefore called exoelectrogens (Logan *et al.* 2008). It has to be noted that some bacteria do not have the ability to accomplish this extracellular electron transfer and instead use soluble compounds that diffuse through the cell membrane to receive electrons. Exoelectrogens are primarily categorised into several functional groups, based on the anaerobic respiration types (Logan 2009).

The first functional group is dissimilatory metal-reducing bacteria (DMRB) such as *Geobacter* (Bond and Lovley 2003), *Shewanella* (Kim *et al.* 2002), *Geopsychrobacter* (Holmes *et al.* 2004a) and *Geothrix* (Bond and Lovley 2005). The second group is sulphate-reducing bacteria (SRB) including *Desulfuromonas* (Bond *et al.* 2002) and *Desulfobulbus* (Holmes *et al.* 2004b). The third is nitrate-reducing bacteria (denitrifying bacteria (DNB)) such as *Pseudomonas* (Rabaey *et al.* 2004) and *Ochrobactrum* (Zuo *et al.* 2008). Furthermore, fermentative bacteria, including *Clostridium* (Park *et al.* 2001) and *Escherichia coli* (Zhang *et al.* 2006), are able to produce electricity through anaerobic respiration pathways. It was also found that purple nonsulfur bacteria, including nonphotosynthetic *Rhodoferax ferrireducens* and photosynthetic *Rhodopseudomonas palustris* DX-1, can produce electricity via anaerobic respiration pathways in an MFC (Chaudhuri and Lovley 2003, Xing *et al.* 2008).

Electron transfer in MFCs is accomplished in either direct or indirect (mediated) ways. Electron transfer mechanisms in bioanode MFCs have been widely investigated by many researchers (Chang *et al.* 2006, Karube *et al.* 1977, Lovley 2006a, Newman and Kolter 2000, Park and Zeikus 2003). However, limited

investigations have been carried out in the electron transfer mechanisms in biocathode MFCs (Cao *et al.* 2009, Lovley 2008, Rabaey *et al.* 2008). Both direct and mediated electron transfer are discussed next.

2.2.5.1. Direct Electron Transfer (DET)

DET takes place through physical contact of the bacterial cell membrane with the fuel cell anode or by making use of conductive bacterial appendages (nanowires). The direct electron transfer requires that the bacteria have membrane bound electron transport protein relays, such as c-type cytochromes, to facilitate the transfer of the electrons from the inside of the bacterial cell to its outside. However, only bacteria in the first monolayer at the anode surface are allowed to transfer electrons (Lovley 2006a). It has been found that some bacteria including *Geobacter* (Holmes *et al.* 2004a, Lovley 2006a), *Shewanella* (Chang *et al.* 2006, Kim *et al.* 1999) and *Rhodoferax* (Chaudhuri and Lovley 2003) have the c-type cytochromes that are involved in direct electron transfer. It has also been demonstrated that some strains of bacteria, including *Shewanella* and *Geobacter*, possess nanowires that are able to carry electrons from the bacterial cell to the anode surface (Gorby *et al.* 2006, Reguera *et al.* 2005). These nanowires allow for multiple layers of bacteria attached to the anode surface to transfer electrons to the anode (Logan 2008). Nanowires are connected to the membrane bound cytochromes where the electron can be transferred to the outside of the cell.

Very few of the bacteria are able to feed on complex substrates, such as glucose, beyond their ability to accomplish direct electron transfer. Only *Rhodoferax ferrireducens* (Chaudhuri and Lovley 2003) has been reported to use glucose. Other bacteria strains, including *Shewanella* and *Geobacter*, are not able to utilise complex

substrates and instead rely on low-molecular organic acids and alcohols provided by fermenting bacteria (Lovley 2006b).

2.2.5.2. Mediated Electron Transfer (MET)

MET mechanisms have been shown as effective in connecting the microbial metabolism to a fuel cell anode. They can be classified with respect to the nature of the mediating redox species to three categories: electron transport by artificial mediators, electron transport by reduced product and electron transport through the microorganism's own mediator.

2.2.4.2.3. Electron Transport by Artificial Mediators

Electron transport via artificial mediators, sometimes known as electron shuttles, is typically able to cross cell membranes and accept electrons from one or more electron carriers within the cell. They enter the cell in an oxidised state and exit the cell in a reduced form carrying electrons to the electrode surface (Lovley 2006b). Accordingly, they become oxidised again in the anodic chamber and thus are reutilised. Mediators are important in MFCs using bacteria incapable of effectively transferring electrons derived from central metabolism to the outside of the cell. These bacteria include *Escherichia coli*, *Pseudomonas*, *Proteus* and *Bacillus* species (Davis and Higson 2007). However, it was demonstrated that *Escherichia coli* K12 can produce power in MFCs without using an exogenous (artificial) redox mediator, and its power increased six times through repeated cycles in a low current MFC (Zhang *et al.* 2006). Researchers also indicated that *Escherichia coli* strain can

produce a hydroquinone derivative, which is able to transfer electrons to an electrode surface even when the cells are not in direct contact (Qiao *et al.* 2008).

2.2.4.2.4. Electron Transport by Reduced Product

Two basic anaerobic metabolic pathways: anaerobic respiration and fermentation can lead to the production of reduced metabolites suited to MFCs. Microbial fermentation results in the formation of energy rich reduced products that provide electrons due to their abiotic oxidisation at the anode surface (Reddy *et al.* 2010). These reduced products, including hydrogen, alcohols or ammonia (Lovley 2006b, Lovley and Phillips 1989), react very slowly with electrodes, which results in an inefficient production of electricity. The composition of anodes can be modified to increase their reactivity with some metabolic end products, however these electrodes may foul with oxidation products (Aston and Turner 1984).

Direct electricity production using fermentation products was first investigated by Karube and co-workers (Karube *et al.* 1977, Suzuki *et al.* 1983). In their study, immobilised hydrogen producing cultures were used as biocatalysts, and platinum was utilised as an electrocatalyst for hydrogen oxidation. Anaerobic respiration is an alternative pathway suitable for MFCs, but a few examples were reported of the beneficial use of anaerobic respiration for MFC operation. Sulphate reduction is one of the common bacterial anaerobic respiratory paths (Madigan *et al.* 1997). Additionally, sulphide oxidation represents an important mechanism for electron transfer, especially in MFCs using wastewater (Rabaey *et al.* 2006) and Benthic fuel cells (Reimers *et al.* 2000).

2.2.4.2.5. Electron Transport through a Microorganism's Own Mediator

Some microorganisms are able to produce their own mediators via secondary metabolic pathways, hence establishing extracellular electron transfer (Hernandez and Newman 2001, Newman 2001, Newman and Kolter 2000). These secondary metabolites include bacterial phenazines such as pyocyanine and 2-amino-3-carboxy-1,4-naphtho-quinone (ACNQ) (Hernandez and Newman 2001). Such a mechanism was first proposed in Park and Zeikus (2003) to facilitate electron transfer to Fe^{3+} in *Shewanella oneidensis*. Other microorganisms, including *Geothrix ferementans* (Newman and Kolter 2000) and *Pseudomonas* species (Nevin and Lovley 2002) can also produce electron shuttles. It has been proved that pyocyanine and phenazine-1-carboxamide, produced by *Pseudomonas aeruginosa*, can be involved in electron transfer to an MFC anode (Rabaey *et al.* 2005a). Furthermore, it has been reported that a quinine-type redox shuttle, produced by *Shewanella* species such as *Shewanella oneidensis* (Newman and Kolter 2000), can support a long distance electron transfer to an external solid electron acceptor (MFC electrodes or a metal oxide like iron (III) oxide). It has also been suggested that *Shewanella* can use overlapping transfer mechanisms (Lies *et al.* 2005), which include direct electron transfer through c-type cytochromes (Chang *et al.* 2006) and nanowires (Gorby *et al.* 2006). However, biosynthesising an electron shuttle is energetically expensive and may induce additional biological losses.

2.2.6. MFC Operational Factors

The operation of MFCs is influenced by several factors: microbial type and activity, substrate used for oxidation, proton exchange material, internal resistance of MFC component, ionic strength, pH, and temperature. Furthermore, the MFC performance

can be improved through a proper design of the MFC reactor and the selection of appropriate materials. Operational factors that affect the MFC are considered next.

2.2.6.1. Electrodes

In MFCs, electrodes can be made of any conductive material and catalysts can be incorporated into the electrode to enhance power output. The electrodes are often composed of graphite, carbon paper, or carbon cloth. The performance of MFCs can be improved by using better performing electrode materials. The combination of Mn(IV)-graphite anodes and Fe^{+3} –graphite cathodes can achieve a four times higher current level than that generated by plain graphite electrodes (Park and Zeikus 2000, Park and Zeikus 2003). A wide variety of carbon-based material, including carbon paper, carbon cloth, carbon felt, and graphite granules(GGs) has been examined as an electrode in MFC (Liu *et al.* 2005a, Min *et al.* 2005a, Rabaey et al. 2005c, You *et al.* 2008).

Based on the potential of the electrode, microorganisms can use electrodes as either an electron donor or an electron acceptor. Applying an additional voltage with the potentiostat can reduce the cathode potential, which gives microorganisms (e.g., *Geobacters*) an option to accept electrons from the cathode under anaerobic condition. A potentiostat is an electronic device that controls the voltage difference between the working and reference electrodes, which are both contained in an electrochemical cell. This control can be implemented by injecting current into the cell through an auxiliary electrode. The potentiostat measures the current flow between the working and auxiliary electrodes. The controlled variable in a potentiostat is the cell potential and the measured variable is the cell current. The working electrode is the electrode where the potential is controlled and where the

current is measured. The auxiliary electrode is a conductor that completes the cell circuit. The reference electrode is used in measuring the working electrode potential. The reference electrode is designed to produce the same potential no matter in what solution it is placed.

Geobacter sp. can make an electrical connection with graphite electrodes and can accept electrons from an electrode when the electrode is poised at a negative potential (Gregory *et al.* 2004). A similar system showed that nitrate was completely reduced to nitrogen gas by using the microorganisms consuming electrons from the cathode (Park *et al.* 2005).

2.2.6.2. Proton/Cation Exchange Membrane

A proton (cation) exchange membrane (PEM/ CEM) can be used to separate the cathode and anode liquids into two different chambers, or just act as a barrier that keeps materials, except protons, from reaching the cathode (i.e., it only allows protons to pass through) (Logan and Regan 2006). Nafion is the most popular PEM that is used in MFCs due to its highly selective permeability for protons, but it is costly. It was shown that using a PEM with a surface area smaller than that associated with the electrodes can limit the output power due to an increase in the internal resistance (Oh and Logan 2006). Furthermore, the PEM has a drawback of creating a pH gradient (Zhao *et al.* 2006). This in turn may lead to a decrease in microbial activity at the anode, as well as a drop in the reduction performance at the cathode. In Min *et al.* (2005a), a salt bridge was used instead of a PEM, resulting in a significant drop in power output, attributed to the higher internal resistance of the salt bridge system. In addition, the cation-specific membrane is the major cost in MFC construction. It may allow transport of cations rather than protons. These cations are

produced through the dissociation of the inorganic chemical, which is used in MFCs to support microbial metabolism. Membraneless microbial fuel cells (ML-MFCs) could improve the economic feasibility and avoid the transportation of cations to the cathode.

The most important steps in electricity generation are proton transfers and cathode reactions, which affect the feasibility of MFC applications (Gregory *et al.* 2004, Oh *et al.* 2004). The proton transfer can be affected by the ionic strength of the fuel and electrolyte, the resistance of proton exchange membrane, and the MFC design (Oh *et al.* 2004, Park *et al.* 2005). In a membraneless MFC, the proton transfer process can be improved by using an anodic electrolyte with a high salt concentration, whereas an anodic electrolyte with a low salt concentration can be used to enhance an MFC with a membrane.

2.2.6.3. Substrates

Concentration, type and feed rates of a substrate greatly affect an MFC's performance, including its power density and coulombic efficiency (CE). MFCs have been operated using a wide variety of substrates: glucose, acetate, cystein and protein (Heilmann and Logan 2006, Liu *et al.* 2005a, Logan *et al.* 2005). It has been found that acetate is most preferential for electricity generation with the highest CE (Chae *et al.* 2009), while the glucose-fed-MFC generates the lowest CE, due to the fermentable nature of glucose. This implies its consumption by diverse competing metabolisms, such as fermentation and methanogenesis that cannot produce electricity. Complex substrates such as domestic wastewater can also be used (Cheng *et al.* 2006a). Laboratory substrates including acetate, glucose, or lactate, are

commonly used. Moreover, the substrates affect not only the MFC's performance, but also the composition of the bacterial community in the anode's biofilm.

2.2.6.4. Microorganisms

The size of the bacterial community (as a biocatalyst) is one of the most critical factors that helps improve an MFC's performance. A biocatalyst's quantity can be enhanced by increasing the number of metabolically viable cells, contributing to electron transfer on a given surface. An acetate-enriched MFC demonstrated the highest number of viable cells at 69% (Chae *et al.* 2009). Other substrates such as glucose-, propionate-, and butyrate-enriched MFCs presented 63%, 60%, 53% of viable cells, respectively (Chae *et al.* 2009). MFCs that make use of mixed bacterial cultures offer several advantages over MFCs driven by pure cultures. They provide higher resistance to process disturbances, higher substrate consumption rates, lower substrate specificity, and higher power output. However, MFCs cannot operate at extremely low temperatures due to slow microbial reactions when temperatures decrease.

2.2.6.5. pH

The complete reduction of nitrate (NO_3^-) to nitrogen gas (N_2) involving four consecutive steps was given in equation (2.6). This produces a strong base. The release of alkalinity occurs when nitrite (NO_2^-) is reduced to nitric oxide (NO) (Lee and Rittmann 2003). In a working MFC, the pH level can be adjusted through the use of a buffer and can be monitored by using a pH meter. In a denitrification system, a pH range between 7 and 8 has been identified as the optimal pH (Knowles 1982,

Kurt *et al.* 1987). It has been successfully demonstrated that a bio-cathode denitrification rate can be significantly increased by continuous neutralisation of the bulk pH in the cathode (Clauwaert *et al.* 2009).

2.2.6.6. Ionic Strength

An MFC's performance can be improved by increasing its ionic strength by adding NaCl to the system. This is due to the fact that NaCl can enhance the conductivity of both the analyte and the catholyte. NaCl can also increase proton availability to the cathode (Jang *et al.* 2004, Liu *et al.* 2005a).

2.2.7. MFC Performance

The ideal performance of an MFC relies on the electrochemical reactions taking place between the organic substrate at a low potential, such as glucose, and the final electron acceptor with a high potential, like oxygen (Rabaey and Verstraete 2005). However, its ideal cell voltage is changeable due to the fact that the electrons are transferred from the organic substrate to the anode through a complex microbial respiratory chain. The latter varies from microorganism to microorganism, and even for the same microorganism when using different growth conditions. The cell voltage can be determined by being based on an anodic reaction between the anode and the final bacterial outer-membrane cytochrome or the reduced redox potential of the mediator, if employed. In mediator-less MFCs, the anodic potential can be defined by the ratio of the final cytochrome of the chain in its reduced and oxidised states. Meanwhile, in mediator MFCs, the anodic potential is the ratio between the reduced and oxidised redox potentials of the mediator.

Electricity in an MFC can be generated only when the overall reaction is thermodynamically favourable. The reaction can be characterised as Gibbs free energy (ΔG_r) which is a measure of the maximum work derived from the reaction (Bard *et al.* 1985, Newman 1973). The Gibbs free energy for specific conditions, is expressed as

$$\Delta G_r = \Delta G_r^\circ + RT\ln(\Pi), \tag{2.17}$$

where ΔG_r° (J) is the Gibbs free energy under standard conditions, usually defined as 298.15 K, 1 bar pressure and 1 M concentration for all species, where R is the universal gas constant, which equals 8.31447 J $mol^{-1}K^{-1}$, T (K) as the absolute temperature, and Π (unitless) is the reaction quotient derived as the activities of the products divided by those of the reactions.

The theoretical cell voltage or electromotive force (emf), E_{emf}(v), is a key MFC performance characteristic. It is defined as the potential difference between the cathode and anode, and can be calculated as (Logan *et al.* 2006)

$$E_{emf} = -\frac{\Delta G_r}{nF}, \tag{2.18}$$

where n is the number of electrons per reaction mol, and F is Faraday's constant (9.64853×10^4 c/mol). By evaluation the reaction at standard conditions where $\Pi = 1$, the equation (2.18) can be rewritten as

$$E_{emf}^\circ = -\frac{\Delta G_r^\circ}{nF}, \tag{2.19}$$

where E_{emf}° is the standard cell electromotive force.

Therefore, the overall reaction, in terms of the potentials, can be expressed as

$$E_{emf} = E_{emf}^\circ - \frac{RT}{nF}\ln(\Pi). \tag{2.20}$$

For a favourable reaction, this equation (2.20) produces a positive emf value for the reaction. This value is the upper limit for the cell voltage where the actual potential derived from the MFC will be lower due to various potential losses.

2.2.8. Key Performance Characteristics

2.2.8.1. Power Generation

The performance of an MFC can be evaluated in terms of current, power density and the rate of fuel oxidation. Though the current is difficult to measure, however it can be calculated from Ohm's law as

$$I = \frac{E_{cell}}{R_{ext}}, \tag{2.21}$$

where E_{cell} is the cell voltage and can be measured across a fixed external resistance, R_{ext}. Power is a common approach for researchers to report voltage data, (Logan *et al.* 2006) and is usually calculated as

$$P = \frac{E_{cell}^2}{R_{ext}}. \tag{2.22}$$

In order to compare power output of different systems, power is often normalised to certain characteristics of the reactor. The selection of the parameters, used for normalisation, depends on the application of the MFC. Since the biological reaction occurs in the anode, the power output is usually normalised to the projected anode surface area (Park and Zeikus 2003, Rabaey *et al.* 2004). Therefore, the power density ($P_{an}, W/m^2$) is calculated on the basis of the anode surface area (A_{an}, m^2) as

$$P_{an} = \frac{E_{cell}^2}{A_{an}\ R_{ext}}. \tag{2.23}$$

In a similar fashion, the current density ($I_{an}, Amp/m^2$) is calculated on the basis of the anode surface area (A_{an}, m^2) as

$$I_{an} = \frac{E_{cell}}{A_{an}\ R_{ext}}. \tag{2.24}$$

The anode consists of materials that can be difficult to express in terms of surface area (Rabaey *et al.* 2005c). As an alternative, the cathode area (A_{cat}) can be used to obtain a power density (P_{cat}). However, the cathode reaction may limit overall power generation (Cheng *et al.* 2006b, Liu and Logan 2004). In order to consider the size and cost of reactions, the power is normalised to volume of the reactor as

$$P_v = \frac{E_{cell}^2}{v\ R_{ext}}, \tag{2.25}$$

where P_v is the volumetric power (W/m^3) (Bullen *et al.* 2006), and v is the reactor volume(m^3).

Internal resistance (R_{int}) of the MFC reactor may affect its power output. This can explain why some MFCs produce only a few milliwatts per reactor volume, while others achieve hundreds of watts. Therefore, the MFC can be viewed to have current through two resistors serially connected, with one being the external resistance, R_{ext} and the other is the internal resistance, R_{int}. The total maximum power can then be theoretically expressed as (Logan 2008)

$$P_{t,emf} = \frac{E_{emf}^2}{(R_{int}+R_{ext})}. \tag{2.26}$$

Equation (2.26) indicates that the power is directly proportional to the square of the maximum potential, E_{emf}. However, it has to be observed that this maximum power cannot be achieved since the actual potential derived from the MFC will be lower due to various potential losses. The maximum possible power based on the measured open cell voltage (OCV) can be calculated as (Logan 2008)

$$P_{t,OCV} = \frac{OCV^2}{(R_{int}+R_{ext})}. \quad (2.27)$$

The maximum power output that can be produced by the system for a calculated cell electromotive force can be given as (Logan 2008)

$$P_{max,emf} = \left(\frac{E_{emf}^2}{(R_{int}+R_{ext})}\right)\left(\frac{R_{ext}}{(R_{int}+R_{ext})}\right) = \frac{E_{emf}^2 R_{ext}}{(R_{int}+R_{ext})^2}. \quad (2.28)$$

Since the OCV is a more useful measure of maximum power, its associated maximum power is given as

$$P_{max} = \frac{OCV^2 R_{ext}}{(R_{int}+R_{ext})^2}. \quad (2.29)$$

Given that $R_{int} = R_{ext}$, the maximum power, P_{max} can be written as

$$P_{max} = \frac{OCV^2}{4R_{int}}. \quad (2.30)$$

Thus, the power maximises as the internal resistance, R_{int}, minimises. Therefore, the fundamental objective in MFC construction is to minimise the internal resistance.

2.2.8.2. Coulombic and Energy Efficiency

The coulombic efficiency (CE) is a common measure of an MFC's performance. The CE can be defined as the ratio of the number of electrons recovered as current to the total number of electrons that were in the starting substrate (organic matter). Therefore, the CE can be expressed as (Gregory *et al.* 2004, Jia *et al.* 2008)

$$C_E = \frac{C_P}{C_T} \times 100, \quad (2.31)$$

where C_P is the total number of electrons calculated by integrating the current over time, and then converting to electrons using the conversion of $1\ ampere = coulomb/second$, $1\ coulomb = 6.25 \times 10^{18}\ electrons/second$ and $1\ mol =$

$6.25 \times 10^{23}\ electrons.$ C_T is the theoretical number of electrons that can be produced from the substrate and can be calculated as

$$C_T = \frac{FbSv}{M}, \tag{2.32}$$

where F is the Faraday's constant ($9.64853 \times 10^4\ c/mol$) , b is the amount of moles of electrons produced per mole of substrate, S is the concentration of substrate, v is the liquid volume and M is the molecular weight of the substrate.

2.2.8.3. Polarization and Power Density Curve

A polarization curve can help in evaluating an MFC's performance by characterising current as a function of voltage. Prior to obtaining a polarization curve, it is recommended to fully perform an open cell voltage (OCV) by conducting the MFC in the open circuit mode (under a condition of infinite resistance where no current is passing through) for several hours (Logan 2008). The OCV is the maximum voltage that can be produced by an MFC within the limitations imposed by the bacterial enzymes and the cathode potential. The latter can be established with oxygen reduction. Once the OCV is performed, the MFC is connected to a resistor box, varying the external resistance, and recording the voltage when pseudo steady state conditions have been established. This may take several minutes or more, depending on the system and the external resistance. Longer times may change the community structure that affects the stability conditions. However, the system will not equilibrate if the time is too short. Therefore, times at each resistance need to be carefully set and only experience with a particular system can help identify the response time characteristics of a particular MFC. This method, where the polarization curve is obtained based on varying the resistance of the MFC circuit

over a single batch reactor cycle at its maximum potential (Liu and Logan 2004), is known as "single cycle". Polarization curves can also be obtained over multiple batch cycles where a different fixed resistance is used for each complete cycle, and this is called the "multiple cycle" (Heilmann and Logan 2006). A comparison of the single and multiple cycle methods was made by Heilmann and Logan (2006), and it was shown that the single cycle method produced a slightly lower power density than that obtained with the multiple cycle method. It was also suggested that acclimatising the MFC reactor over a long period of time to different external resistances could change the maximum power density achieved. The impact of the resistor selected for the acclimatisation procedure on the maximum power density and on the composition of the microbial community developing in the system warrants further investigations.

2.2.8.4. Internal Resistance Measurements

The internal resistance in an MFC can be evaluated through a number of different approaches. These include polarization slope, power density peak, electrochemical impedance spectroscopy (EIS) using a Nyquist plot and current interrupt approaches. The first two methods are simple and can provide a quick estimation for the internal resistance. The latter two methods are preferable, but require the use of a potentiostat.

The polarization slope method can simply evaluate the internal resistance by calculating the slope of a plot of current versus the measured voltage, i.e., a polarization curve. The slope has to be calculated over the region of interest of the polarization curve where a direct linear relationship between the voltage produced

and the current is observed (see Fig. 4.1). This linear relationship between potential and current can be expressed as (Logan 2008)

$$E_{emf} = OCV^* - IR_{int}, \tag{2.33}$$

where R_{int} is the internal resistance and the product IR_{int} indicates the sum of all internal resistance losses in the MFC. The OCV^* is the OCV implied by extrapolating the linear region of the polarization curve to the y-axis (see Fig. 4.1). This linear relationship between voltage and current is a defining characteristic of MFCs due to a relatively high internal resistance. Therefore, the internal resistance of the cell can be easily identified by making use of the linear response in the MFCs. Furthermore, the internal resistance can be identified as similar to the external resistance that yields the maximum power output through the power density peak method. For simplicity, these two methods (polarization slope and power density peak) are used in this study.

Electrochemical impedance spectroscopy (EIS) has been shown as a preferable method to identify the internal resistance compared to the above two methods (polarization slope and power density peak). This is due to its ability to measure the dynamic response of the system. However, a potentiostat with EIS software is required to obtain the data. EIS relies on imposing a sinusoidal signal with a small amplitude on the applied potential of a working electrode. The dynamic response of the system can be measured through the variation of the sinusoidal signal frequency over a wide range (typically 10^{-4} to 10^{6} Hz) and plotting the measured electrode impedance (Logan *et al.* 2006). Electrode impedance measurements can easily be achieved at the OCV. Additional information of this method can be found in Bard and Faulkner (2001).

Current interrupt is an alternative preferred approach for identifying the internal resistance, and it also requires the use of a potentiostat. In addition, a very fast recording of the potential (μs scale) is needed after current interruption to achieve an accurate potential determination (Larminie and Dicks 2000).

2.2.9. MFC Limitations

The open circuit voltage (OCV) is the cell voltage that can be measured, under a no-load condition (no current generation), using a high impedance voltmeter or potentiometer. Theoretically, the OCV should approach the cell emf. However, the practical OCV is considerably less than the cell emf due to a number of losses. These losses are the internal resistance (R_{int}) of the MFC, which is made up of overpotentials and Ohmic losses. The overpotentials are often referred to as irreversible losses, and can be categorised into three main types: activation losses, bacterial metabolic losses and mass transfer losses.

2.2.9.1. Activation Losses

Activation losses occur due to the energy required to transfer the electrons, from or to a compound reacting at the electrode surface, in an oxidation/ reduction reaction. Activation overpotentials dominate at a low current density. The current density is typically expressed per total electrode surface. On the other hand, activation loss is minimal when the rate of an electrochemical reaction, at an electrode surface, is controlled by slow reaction kinetics. Both anode and cathode compartments are subject to activation losses.

At the anode side, activation loss is an energy barrier for those microbes that do not readily release electrons to the anode, and this can be overcome by adding mediators. However, in mediator-less MFC, activation loss is lower due to conducting pili and their producing redox mediators themselves. Furthermore, the reaction kinetics, in the cathode, is limited due to the impediment of converting the oxidant into reduced form, caused by an activation energy barrier. When current is derived from a fuel cell, a portion of the cathode potential is then lost to combat this activation barrier. Activation losses can be reduced by improving the electrode catalysis, increasing the surface area of the electrode, increasing the operating temperature and establishing an enriched biofilm on the electrode (Logan *et al.* 2006).

2.2.9.2. Bacterial Metabolic Losses

Metabolic energy is the energy gained by transferring electrons from a reduced substrate at low potential, such as glucose, to an electron acceptor with a high potential, such as oxygen. This energy can be calculated as (Rabaey and Verstraete 2005)

$$\Delta G = -n \times F \times \Delta E, \tag{2.34}$$

where ΔE is the potential difference between electron donor and acceptor.

In a MFC, the energy gain for the bacteria can be determined based on the difference between the potential of the anode electrode, which is the final electron acceptor, and the redox potential of the substrate. The metabolic energy gain for the bacteria exhibits an increase with the increase in the difference between the anode potential and the redox potential of the substrate. However, the attainable MFC voltage decreases accordingly. Therefore, the anode potential should be kept as low (negative) as possible in order to maximise the MFC voltage. However, this may

cause inhibition to the electron transport and fermentation of the substrate may provide greater energy for the microorganisms.

2.2.9.3. Mass Transfer Losses

Concentration losses occur mainly at high current density due to insufficient mass transfer through diffusion and convection of substrate or removal of products. Inefficient mass transfer results in product accumulation or reactant depletion. The latter affects the Nernstian cell voltage and the reaction rates, resulting in a performance loss. This loss is the voltage needed to drive the mass transfer process at both anode and cathode compartments. Mass transfer limitations, due to oxidant transfer at the cathode, are typically more restricted than those at the anode compartment. Furthermore, mass transfer at the cathode surface is typically dominated by diffusion, whereas mass transfer in bulk catholytes is dominated by convection. Mass transfer losses can be reduced by maintaining high bulk concentrations and an even distribution of oxidant across the cathode compartment (Rismani-Yazdi *et al.* 2008). Clauwaert *et al.* (2007a) employed an MFC with a microbial consortium that contained denitrifiers in the anaerobic cathode compartment and reduced nitrate as the final electrode acceptor. In addition, mass transfer limitations can be minimised through the optimisation of MFC operating conditions, electrode materials and cathode compartment geometry (Logan *et al.* 2006, Rismani-Yazdi *et al.* 2008).

2.2.9.4. Ohmic Losses

Ohmic losses can be categorised into two types, electrolyte ohmic losses and electrode ohmic losses. The first refers to the voltage losses due to the ion transfer through the electrolyte, whereas the latter refers to the voltage losses caused by transferring electrons through the electrodes. The ohmic voltage loss can be determined based on the resistivity of the conductors used (electrodes, current collectors, wires, membranes and electrolyte). The ohmic overpotential (η_{ohmic}), therefore, represents the voltage lost in order to accomplish charge transfer (i.e. electrons and protons). This loss generally follows ohm's law, and can be expressed as (Rismani-Yazdi *et al.* 2008)

$$\eta_{ohmic} = iR_{ohmic}, \tag{2.35}$$

where i is the current (A) and R_{ohmic} is the ohmic resistance (Ω) of the MFC.

Ohmic losses can be reduced by minimising the electrode space, using membrane with a low resistivity and increasing solution conductivity to the maximum tolerated by the bacteria (Logan *et al.* 2006).

2.2.10. Applications

MFC system can be used for various purposes such as, bacterial activity monitoring, electricity generation in local area, biosensor and wastewater treatment processes (Du *et al.* 2007, Kim *et al.* 2004).

2.2.10.1. Electricity Generation

MFCs make use of the catalytic reaction of microorganisms to convert the chemical energy stored in the chemical compounds into electrical energy. Since chemical

energy from the oxidisation of fuel molecules is directly converted into electricity, much higher conversion efficiency (> 70%) can be theoretically achieved. It has been reported that *Rhodoferax ferrireducens* can generate an almost 80% electricity (Chaudhuri and Lovley 2003). Much more electricity of up to 89% can also be generated using a mixed bacterial culture fed with glucose as carbon source (Rabaey *et al.* 2003). Furthermore, high Coulombic efficiency of 97% can be achieved through the oxidation of fermentation product formate at platinum black modified electrodes (Rosenbaum *et al.* 2006). However, the power generated by MFC is very low due to the limited rate of electrons abstraction (DeLong and Chandler 2002, Tender *et al.* 2002). This problem can be solved by storing electricity in rechargeable devices and then distributing the stored electricity to end-users (Ieropoulos *et al.* 2003). MFCs are suitable for power electrochemical sensors and small telemetry systems that require minimal power for data transmission to receivers in remote locations (Shantaram *et al.* 2005). Realistic robots such as EcoBot-II would probably use MFCs as a power supply to perform some behaviours including sensing, motion, computing and communication (Ieropoulos *et al.* 2005b). The MFCs, equipped with the robot EcoBot-II, were enriched with bacteria from sewage sludge and were employed oxygen from air by exposing the cathode to air. Different substrate can be utilised including sugar, fruit, dead insects, grass and weed. Furthermore, MFCs can be used as an in situ power source for electronic devices in remote areas including the ocean and the bottom of deep-water, due to the difficulty of changing traditional batteries (Logan and Regan 2006, Lovley 2006a). Sediment MFC is a good example which is well known as benthic unattached generator (BUG), where the anode is buried in anaerobic marine sediments that is connected to a cathode suspended in the overlying aerobic water. Electricity was produced by the organic matter in the

sediments. However, the energy produced is low due to the low concentration of organic matter and high internal resistance (Logan and Regan 2006). It is believed that a miniature MFC can be implanted in a human body to power implementable medical device with the nutrients supplied by the human body (Chiao *et al.* 2002). The MFC technology is favourable for sustainable long-term power applications.

2.2.10.2. Biohydrogen

An MFC can be easily modified to produce hydrogen rather than electricity, and its modified form is referred to as bio-catalysed electrolysis (Rozendal *et al.* 2007, Rozendal *et al.* 2006). However, hydrogen generated from protons and electrons that are produced through microbial metabolism is thermodynamically unfavourable (Rozendal *et al.* 2006). This is attributed to that most of the substrate is converted to by-products such as acetate and butyrate instead of hydrogen due to thermodynamical limitations. This thermodynamic barrier can be suppressed through the use of an external potential, in which protons and electrons produced by the anodic reaction migrate and combined at the cathode forming hydrogen under anaerobic conditions. The potential for the oxidation of 1M acetate at the anode is -0.28, while the potential for the reduction of protons to hydrogen at the cathode is -0.42 V (normal hydrogen electrode (NHE)). This can confirm that hydrogen can theoretically be generated at the cathode by applying a voltage just greater than 0.14 V (Rozendal *et al.* 2006), which is substantially lower than that required to produce hydrogen from the direct electrolysis of water (1.23 V at pH 7). The rest of energy needed can be provided from the oxidation of substrate in the anode chamber. Modified MFCs can potentially produce a yield of 4-5 mol H_2/ mol glucose higher than the typical 4 mol H_2/ mol glucose achieved in conventional fermentation (Liu *et*

al. 2005b). Furthermore, hydrogen can be accumulated and stored for later contribution to the overall hydrogen demand in a hydrogen economy (Holzman 2005), hence overcoming the inherent low power feature of the MFCs.

2.2.10.3. Wastewater Treatment and Cathodic Denitrification

MFCs were first considered to be used for wastewater treatment in 1991 (Habermann and Pommer 1991). Municipal wastewater contains a multitude of organic compounds, such as acetate, propionate and butyrate that can fuel MFCs and in turn can be thoroughly broken down to CO_2 and H_2O. MFCs can reduce the sludge disposal cost in wastewater by as much as 50% of the electricity usage, and yield 50-90% less solids to be exposed of (Holzman 2005). Furthermore, MFCs (with certain microbes) are able to eliminate sulphides as needed in wastewater treatment (Rabaey *et al.* 2006). The single-chambered MFC with a continuous flow and a membrane-less MFC are the most attractive MFCs for treating wastewater due to scale-up concerns (He *et al.* 2005, Jang *et al.* 2004, Moon *et al.* 2005). Sanitary wastes, corn stover, food processing wastewater and swine wastewater are rich in organic matters, and therefore they are good biomass sources for MFCs (Liu *et al.* 2004, Min *et al.* 2005b, Oh and Logan 2005, Suzuki *et al.* 1978, Zuo *et al.* 2006).

MFCs can also be used for nutrient removal, where bio-cathode MFCs can be effectively used to reduce nitrate to nitrite (Gregory *et al.* 2004) or to nitrogen gas (Clauwaert *et al.* 2007a). It was reported that a bacterial culture enriched in *Geobacter* species could reduce nitrate to nitrite by using the cathode as the terminal electron donor (Gregory *et al.* 2004). Clauwaert and co-workers (Clauwaert *et al.* 2007b) demonstrated the possibility of complete biological denitrification using a bio-cathode MFC fed with acetate. They were able to achieve simultaneous organic

removal, power production and full denitrification without relying on H_2-formation or external power.

2.2.10.4. Biosensor

The use of MFCs as biosensors for pollutant analysis and in situ process monitoring is one of the most common applications of MFCs. This is due to the instant and reliability of the current response during the degradation of electron donors. It has been demonstrated that MFCs utilising *Shewanella* as biocatalyst are an affective sensor for quantifying the biological oxygen demand (BOD) due to the proportional correlation between the Coulombic yield of MFCs and the wastewater strength within a quite large range (Chang *et al.* 2005, Chang *et al.* 2004, Kim *et al.* 2003). An accurate measure of the BOD value of a liquid stream can be achieved by calculating its Coulombic yield. A good linear relationship between Coulombic yield and the wastewater strength has been seen in a wide range of BOD concentrations (Chang *et al.* 2004, Kim *et al.* 2003). However, a high BOD concentration calls for longer response time since the calculation of Coulombic yield can be done only after the complete depletion of BOD. The employment of a dilution mechanism can reduce the response time required. So many efforts have been made to improve the dynamic responses in MFCs based sensors (Moon *et al.* 2004). MFC-type of BOD sensors offers a number of advantages over other types of BOD sensors. The advantages include excellent operational stability, good reproducibility and accuracy. Furthermore, MFC-type of BOD sensor constructed with the microorganisms enriched with MFC can continuously operate for over 5 years without the need for serious maintenance (Kim *et al.* 2003).

2.3. Carbon Nanotubes and Nanofibres

2.3.1. Overview

Carbon is one of the abundant elements in the universe. It is a non-metallic and tetravalent chemical element with atomic number 6. Carbon can be found in many stable forms known as allotropes due to its high stability. Until 1985, Diamond and graphite were only pure crystalline carbon allotropes. In 1985, group of researchers discovered a new carbon allotrope, C_{60}, known as Buckminsterfullerene. The molecule of C_{60} is also named buckyball as it has a shape of soccer ball. Other carbon molecules such as C_{70}, C_{76}, C_{78}, and C_{82} have also been found, and all are named fullerenes (Wong and Akinwande 2011). The discovery of fullerenes was followed by the discovery of carbon nanotubes (CNTs) by Sumio Iijima in 1991 (Iijima 1991). The discovery of CNTs has encouraged the rapid growth of the nanotechnology field and also the rapid increase of nanotechnology-based products (Ventra *et al.* 2004, Wong and Akinwande 2011). An extensive research into their physical and chemical properties has since been carried out (Guzmán *et al.* 2009, Rivas *et al.* 2007, Valentini *et al.* 2004). CNTs have been shown as good nano-structured materials for different applications in a wide range of technological fields including chemistry, biology, medicine, electronics, materials, and engineering. They can be described as sp^2 carbon atoms that are arranged in graphitic sheets seamlessly wrapped into cylinders and capped by fullerene-like hemisphere. Their unique C-C covalent bonding and seamless hexagonal network make them the strongest and the most flexible molecular material. CNTs have diameters in a typical range of 1-50 nm and lengths of few μm, and they may consist of one or more concentric graphitic cylinders.

2.3.2. Classifications of Carbon Nanotubes

CNTs can be classified into three common types including single wall carbon nanotubes (SWCNTs), multi-wall carbon nanotubes (MWCNTs) and carbon nanofibres (CNFs) (Kang *et al.* 2006). A combination of these three types of CNT raw materials can develop intelligent materials. A single wall carbon nanotube contains of a single graphitic layer with a diameter ranging from 0.4 nm to 2 nm and a length longer than 0.2 μm. SWCNTs are usually found in bundles that are composed of tens to hundreds of parallel tubes contacting each other. Multi-wall carbon nanotubes consist of several layers of graphitic cylinders (typically between 2 and 30) that are concentrically nested like the rings of a tree trunk. They have a diameter that ranges from 10 nm to 50 nm and a length ranging from 1 μm to 50 μm. Carbon nanofibres differ from nanotubes by the orientation of the graphene planes. CNFs show a wide range of orientations of the graphitic layers with respect to the fibre axis in contrast to that shown in the CNTs where the graphitic layers are parallel to the tube axis. CNFs can be illustrated as stacked graphitic disc or cones. They can be found as hollow tubes with an outer diameter that ranges from 50 nm to 100 nm.

2.3.3. Characteristics of Carbon Nanotubes

2.3.3.1. Properties of Carbon Nanotubes

Carbon nanotubes have extraordinary mechanical properties due to the strength of the sp^2 C-C bonds coupled with the stability of their geometric structure (de Heer and Martel 2000). Nanotubes are the stiffest materials with highest Young's modulus of 1 TPa and tensile strength of 50 GPa or above (Meyyappan 2005, Ventra *et al.* 2004).

The Young modulus is one of the most important features that describe an elastic material stiffness and its measure can be used to characterise material. The tensile strength is the force required to break a single nanotube. Furthermore, CNTs have either electrical conductivity or semiconductivity in addition to high thermal conductivity in the direction of the nanotube axis (Krishnan *et al.* 1998, Yu *et al.* 2000). The electrical properties of a nanotube usually differ from those of the fluid. This is due to the fact that a nanotube in an electrolyte will attract ions of opposite electrical polarity, which forms an electrical double layer. Temperature and magnetic fields can affect nanotubes resistance. It has been shown that an individual tube can conduct electrons without scattering and with coherence length of few microns (Tans *et al.* 1998). In addition, a carbon nanotube can continuously produce power due to the ionic flow over its surface. The power production relies on the ionic fluid and flow velocity (Král and Shapiro 2001), and therefore it is promising for medical applications and flow sensing. Although, most electrochemical studies were carried out with SWCNTs due to their unique molecular structures, MWCNTs are potentially more attractive electrode materials. MWCNTs have larger diameters and better electrical conductivity than those of SWCNTs.

2.3.3.2. Synthesis of Carbon Nanotubes

Carbon nanotube was initially synthesised by an arc-plasma evaporation method. However, currently a number of methods, including chemical vapour deposition (CVD) and laser vaporisation, can be used for its preparation. The arc-plasma evaporation method uses two opposing graphite electrodes separated in an apparatus with a gap of 2 mm, and arcs one hundred Amps of electricity across this thin gap under an inert gas atmosphere (e.g. Helium), thus vaporising the graphitic ends in hot

plasma. Almost 30% of the carbon soot produced contains nanotubes that have a length less than 50 microns and a random shape. The volume of the produced nanotubes can be significantly increased through the use of catalytic agents (Collins and Avouris 2000). An alternative method that can be used in the production of nanotubes is chemical vapour deposition (CVD). This technique is simple and can produce longer- length nanotubes compared to the other methods. Such a technique that uses approximately 600° C to slowly heat a carbon substrate and adds carbon rich gases, such as methane, inside the chamber when the temperature is at its optimum level. The use of a catalyst can sufficiently help converting most of the gaseous carbon to nanotubes. The main drawback of CVD is the production of primarily multi-walled nanotubes with lower tensile strength compared to those produced by arc-plasma evaporation or laser vaporisation (Yakobson and Smalley 1997). Laser vaporisation is the most promising method for synthesising SWCNTs, but it is the most expensive one. It relies on focusing a laser onto a graphite specimen in order to produce plasma. Nanotubes are then condensed from the plasma at about 1200° C through the use of a metallic catalyst such as cobalt, nickel or iron. The resultant products are extremely uniform, where approximately 70% of SWCNTs with a length of almost 0.1 mm can be produced (Yakobson and Smalley 1997).

2.4. Electrochemical Theory

2.4.1. Electroanalysis

The interaction between electricity and chemistry, which is known as electroanalysis or electrochemistry, aims for measuring electrical quantities including current, potential and charge and their relationship to chemical parameters. The fundamental

objective of the electrochemistry is to study the charge transfer processes at the electrode/solution interface, either in equilibrium at the interface or under total or partial kinetic control. Electrochemical methods have the ability to assay trace concentrations of an electro-active analyte and to provide information on the physical and chemical properties (Unwin 2007). Electrochemical measurements are often categorised into four types: conductimetry, potentiometry, amperometry and voltammetry. Conductimetry helps measuring the solution resistance through the concentration of charges obtained. Potentiometry measures an equilibrium potential of an indicator electrode based on a reference electrode through the use of high impedance voltmeter at zero current. Amperometry is used to measure the magnitude of current according to the concentration of ions reacted when a fixed potential is applied to the electrodes. Voltammetry indicates a current response as a function of applied potential. Voltammetry is considered in this thesis and is discussed in detail next.

2.4.2. Fundamental of Voltammetry

Voltammetry was facilitated by the discovery of polarography in 1922 by a Czech chemist, Jaroslav Heryrovsky (Kounaves 1997, Settle 1997). Such an active technique involves the application of potential to an electrode and monitoring the current response through the electrochemical cell over a period of time. The applied potential induces a change in the concentration of the electro-active element at the electrode surface through electrochemical oxidation or reduction. This technique (voltammetry) can either be used for organic or inorganic substances. These substances include studies of adsorption processes on surfaces, electron transfer and

reaction mechanisms, kinetics of electron transfer processes and transport of species in solution.

2.4.2.1. Electrochemical Cells

The voltammetric technique is performed in an electrochemical cell with three electrodes: the working electrode, reference electrode and auxiliary electrode. The working electrode represents the most important one in the electrochemical cell as the electrochemical reaction occurs at its surface and its potential is controlled based on a reference electrode, which has no current passing through it. A variety of solid materials such as lead, platinum, gold and glassy carbon can be used as working electrodes. An instrument called a potentiostat can allow the current to pass through the electrochemical cell between the working electrode and auxiliary (or counter) electrode. The potentiostat applies a regulated voltage between two electrodes immersed in solution and measures the current that passes in or out of the working electrode. The auxiliary electrode aims to supply current to the working electrode, and its size should be larger than that of working electrode. The most common materials that can be used as counter electrodes are platinum or silver wire electrodes. Furthermore, the reference electrode maintains a fixed potential regardless of the current density. The most common reference electrodes used are Standard Hydrogen Electrode (SHE), Normal Hydrogen Electrode (NHE), Reversible Hydrogen Electrode (RHE), Saturated Calomel Electrode (SCE) and Silver/Silver Chloride electrode (Ag/AgCl).

2.4.2.2. Electrode Reactions: Electron Transfer and Mass Transfer

Electrode reactions involve the transfer of electrons to or from a surface of an electrode. Different types of electrode reactions, including simple electron transfer, metal deposition, gas evolution, corrosion, oxide film formation and electron transfer with coupled chemistry, are used for analytical purposes (see Fig. 2.7). Considering two species, O and R which are completely stable and soluble in the electrolysis medium, a simple electrode reaction in the electrochemical cell can be described as (Pletcher and Group 2001):

$$O + ne^- \rightleftharpoons R, \tag{2.36}$$

where O and R are the oxidised and reduced electroactive species respectively.

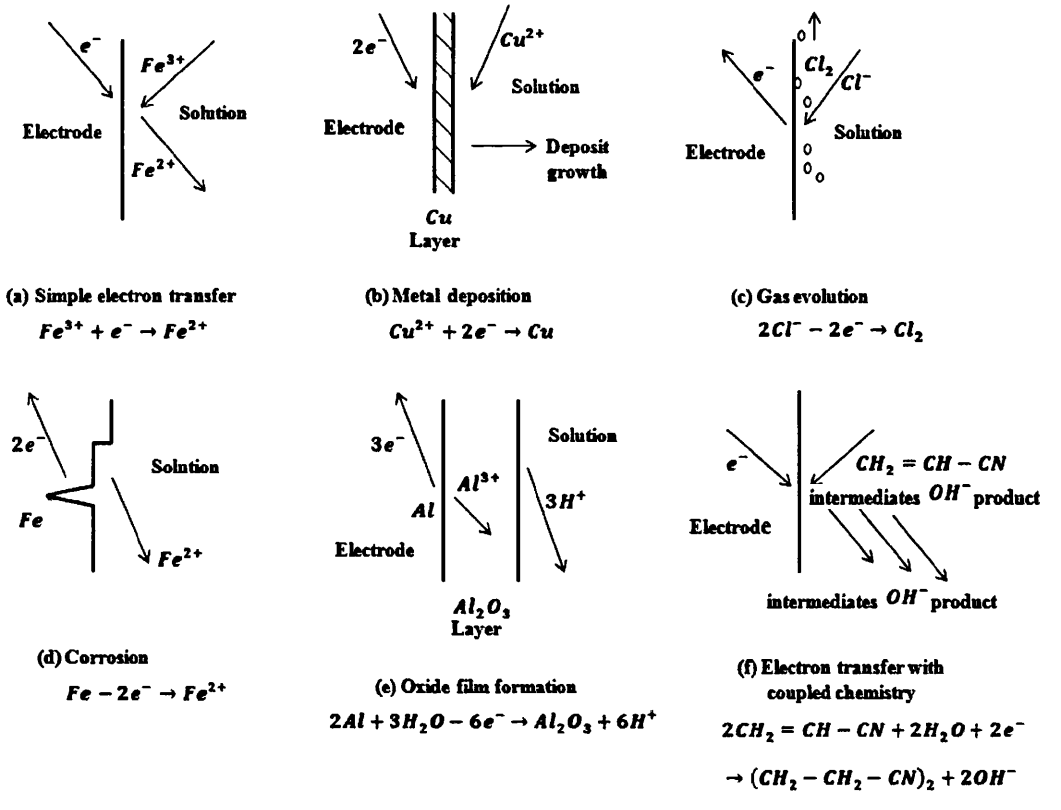

Figure 2-7: Schematic view of some types of electrode reactions (Pletcher and Group 2001).

In order to maintain a current, the electrode reaction involves a sequence of basic steps as follows:

1. Supply reactant to the electrode surface: $O_{bulk} \xrightarrow{mass\ transport} O_{electrode}$
2. Electron transfer reaction at the surface: $O_{electrode} \xrightarrow{electron\ transfer} R_{electrode}$
3. Remove the product formed at the electrode surface: $R_{electrode} \xrightarrow{mass\ transport} R_{bulk}$

2.4.2.2.1. Electron Transfer

In a chemical process, both the thermodynamics and kinetics of the electron transfer process need to be necessarily considered. The potential of the working electrode can reach a steady state value representing the state equilibrium in the cell if no current is passing through the electrolytic cell. Based on the laws of thermodynamics, the potential of the working electrode, E_e, is given by the Nernst equation (Pletcher and Group 2001):

$$E_e = E_e^o + \frac{RT}{nF} ln\left(\frac{C_O}{C_R}\right), \tag{2.37}$$

where E_e^o is the standard potential for the redox reaction, C_O and C_R are the concentrations of oxidised and reduced species respectively at the electrode surface. The Nernst equation (2.37) indicates the relationship between the potential of an electrode and the concentrations of the two species (O and R) involved in the redox reaction at the electrode.

A dynamic equilibrium is established at the surface of the working electrode when no current is passing through the cell and the overall chemical does not change. This

implies that the reduction of O and the oxidation of R are both occurring at equal rate as (Pletcher and Group 2001):

$$-I^{\rightarrow} = I^{\leftarrow} = I_o, \tag{2.38}$$

where I_o is the exchange current density, $-I^{\rightarrow}$ is the cathodic current density for the forward reaction (the negative sign indicates that the cathodic current is negative) and $I^{\leftarrow}$ is the anodic current density for the back reaction.

If the potential of the working electrode is made more negative compared to the equilibrium potential determined by the bulk concentrations of O and R, equilibrium can only be re-performed if the concentrations of O and R are set to the new values required by the Nernst equation at the applied potential. A current is then required to flow through the electrode/solution interface. In fact, it is necessary to decrease the ratio of C_O/C_R, and this can be satisfied through the conversion of O to R by passing a cathodic current. In contrast, an anodic current should be observed if the potential of the working electrode is made more positive than E_e. At any potential, the magnitude of the current that flows through the cell also depends on the kinetics electron transfer, and the measured current density is given by Pletcher and Group (2001) as

$$I = -I^{\rightarrow} + I^{\leftarrow}. \tag{2.39}$$

The partial current densities ($I^{\rightarrow}$ and $I^{\leftarrow}$) rely on a rate constant and the concentration of the electroactive species at the electrode surface where electron transfer occurs and are expressed as (Pletcher and Group 2001)

$$I^{\rightarrow} = -nFk^{\rightarrow}C_O \quad \text{and} \quad I^{\leftarrow} = -nFk^{\leftarrow}C_R. \tag{2.40}$$

The rate constants ($k^{\rightarrow}$ and $k^{\leftarrow}$) change with the applied electrode potential (i.e., the potential difference at the electrode surface during electron transfer) as follows (Pletcher and Group 2001)

$$k^{\rightarrow} = k_o^{\rightarrow}\exp\left(-\frac{\alpha_C nF}{RT}E\right) \quad \text{and} \quad k^{\leftarrow} = k_o^{\leftarrow}\exp\left(\frac{\alpha_A nF}{RT}E\right), \tag{2.41}$$

where $k_o^{\rightarrow}$ and $k_o^{\leftarrow}$ are the standard rate constants, E is the potential versus a reference electrode, α_A and α_C are the transfer coefficients for the anodic and cathodic reactions respectively. For a simple electron transfer reaction $\alpha_A + \alpha_C = 1$.

After some manipulation of equations (2.39)-(2.41), defining the overpotential as the deviation of the potential from the equilibrium value, i.e.,

$$\eta = E - E_e, \tag{2.42}$$

and noting the definition of the exchange current density, $I_o = -I^{\rightarrow} = I^{\leftarrow}$ at $\eta = 0$, the Butler-Volume equation can be written as (Pletcher and Group 2001)

$$I = I_o\left[exp\left(\frac{\alpha_A nF}{RT}\eta\right) - exp\left(-\frac{\alpha_C nF}{RT}\eta\right)\right]. \tag{2.43}$$

The Butler-Volume equation is a simple mathematical relationship between current and overpotential.

2.4.2.2.2. Reversible and Irreversible Reactions

A reversible chemical reaction is a reaction proceeding in both directions (forward and backward) simultaneously, in which the products decompose back into the reactants as they are being produced (Waage and Gulberg 1986). During the cyclic voltammetry of a reversible reaction, the reduction of the reactants and the oxidation of the products are performed sequentially in a reversible scan direction. The peak current density for such a reaction is governed by Randles-Sevcik equation (Pletcher and Group 2001)

$$I_P = (2.69 \times 10^5)n^{3/2}c_O^{\infty}D^{1/2}\nu^{1/2}, \tag{2.44}$$

where I_P is the peak current density in Acm^{-2}, n is the number of electrons passed per molecule of analyte oxidised or reduced, c_O^{∞} is the concentration of analyte in

bulk solution in mol cm^{-3} , D is the diffusion coefficient of the analyte in cm^2s^{-1} and ν is the potential sweep rate in Vs^{-1}. The concentration gradients at the electrode surface, and hence currents, increase as the sweep rate increases, though the time scale of the reaction decreases accordingly. Eventually, equilibrium is not established at the electrode surface and kinetic effects appear due to the increase in the sweep rate (Wang 2006). Equation (2.44) also shows that the peak current density is proportional to the concentration of the electroactive species, the square root of the sweep rate and diffusion coefficient (Pletcher and Group 2001). For a simple reversible reaction, the ratio between the reverse and forward peak currents, $I_P^{\leftarrow}/I_P^{\rightarrow}$ is unity. The reverse and forward peak currents ($I_P^{\leftarrow}$ and $I_P^{\rightarrow}$) and their associated potentials (i.e., potentials at which the peak currents observed), $E_P^{\leftarrow}$ and $E_P^{\rightarrow}$, are key parameters for the cyclic voltammetry. The number of electrons transferred can be determined in proportion to the difference between the peak potentials as follows

$$\Delta E_p = E_P^{\leftarrow} - E_P^{\rightarrow}. \tag{2.45}$$

The anodic and cathodic peak potentials ($E_P^{\leftarrow}$ and $E_P^{\rightarrow}$) are independent of sweep rate (scan rate). The electron transfer rate of a reversible reaction is considerably higher than that of mass transport resulting in maintaining the Nernstian equilibrium at the electrode surface (Pletcher and Group 2001).

In contrast to the reversible reaction, the electron transfer in an irreversible chemical reaction is sluggish in nature as the peaks are lower and widely separated. Also, unlike the reversible reaction where the cathodic potential ($E_P^{\rightarrow}$) is independent of the scan rate, $E_P^{\rightarrow}$ for an irreversible reaction varies with the scan rate. The increase in the scan rate increases the rate of mass transport so as it reaches the electron transfer rate, hence increasing the separation between the peak potentials. The shift of the peak potential with the scan rate can be expressed as (Pletcher and Group 2001)

$$E_P^C = K - \left(\frac{2.3\,RT}{2\alpha_C n_\alpha F}\right) log(v), \tag{2.46}$$

where

$$K = E_e^o - \frac{RT}{\alpha_C n_\alpha F}\left(0.78 - \frac{2.3}{2} log\left(\frac{\alpha_C n_\alpha FD}{k^{O2} RT}\right)\right), \tag{2.47}$$

where α_C is the transfer coefficient and n_α is the number of electrons transferred. The cyclic voltammogram gets wider as the value $(\alpha_C n_\alpha)$ decreases due to the slow electron transfer (Wang 2006). The peak current for an irreversible reaction is calculated by (Pletcher and Group 2001)

$$I_P = -(2.99 \times 10^5) n(\alpha_C n_\alpha)^{1/2} c_O^\infty D_O^{1/2} v^{1/2}. \tag{2.48}$$

A quasi-reversible reaction is a quite common phenomenon in which a reaction that is reversible at low scan rates becoming irreversible at higher scan rates. This is due to the inability to maintain the Nernstian equilibrium at the electrode surface as a result of an insufficient relative rate of electron transfer with respect to that of mass transport.

2.4.2.2.3. Mass Transport

Mass transport describes the movement of material from one location to another in a solution. Three modes of mass transport are available in an electrochemical system: migration, convection and diffusion (Pletcher and Group 2001).

A. Migration

Migration is the movement of charged species by the force of a potential gradient (electric field). The passage of ions through the solution between the electrodes can help balancing the current of electrons through the external circuit.

B. Convection

Convection is the movement of a species due to stirring or by creating a flow in the solution using rotating or vibrating electrodes (mechanical forces).

C. Diffusion

Diffusion is the movement of a species (for example, O) in a solution under the influence of a chemical concentration gradient. It occurs due to the chemical changes at the electrode surface. An electrode reaction converts chemical material to product (O → R) forming a boundary layer (up to 0.1 mm thick) near the electrode surface based on the concentrations of O and R. The concentration of the reactant (O) is lower at the electrode surface than in the bulk, and therefore O will diffuse towards the electrode. The opposite operation is observed for R so that it will diffuse away from the electrode. In unstirred solution and in the presence of a base electrolyte, the movement of electroactive species is limited to diffusion as the effect of migration and convection can be suppressed (Pletcher and Group 2001). Diffusion can be given by Fick's first law, which states that the flux of material across a given plane is proportional to the concentration gradient across the plane, as (Pletcher and Group 2001)

$$Flux = -D_i \frac{dc_i}{dx}, \tag{2.49}$$

where c_i is the concentration of species i, x is the distance perpendicular to the electrode surface and D_i is the diffusion coefficient that has a typical value of 10^{-5} cm^2s^{-1}. In contrast to Fick's first law, which does not consider changing the concentrations with time, the second law describes the changes in concentration with time due to diffusion as (Pletcher and Group 2001)

$$\frac{\partial c_i}{\partial t} = D_i \frac{\partial^2 c_i}{\partial x^2}. \tag{2.50}$$

where t is the time.

2.5. Summary

This chapter has provided a literature review of the main issues associated with the bio-electrochemical nitrate reduction systems. Special attention was given to the limitations associated with microbial fuel cell systems (activation, bacterial metabolic, mass transfer and ohmic losses) and the methods that have been proposed to minimise their effects. This chapter has also focused on bacterial metabolism and their interaction at the electrode surface. In addition, the chapter has addressed denitrification in natural ecosystems and their associated enzymes and bacteria. An overview of both carbon nanomaterials and electrochemical theory was also given.

3. ISOLATION OF DENITRIFYING BACTERIA AND CULTURE CONDITIONS

3.1. Introduction

The selection of an appropriate medium is essential for isolation and cultivation of denitrifying bacteria. So far no single medium has proved to be suitable for all denitrifying bacteria, due to their wide phylogenetic distribution. This chapter aims to design a good cultivation medium that promotes high rates of denitrification. Two media, each with a different carbon source (sodium formate or sodium acetate), were designed, investigated and examined in order to optimise bacterial growth rates. Optimisation was evaluated in two directions: (i) through studying the effect of each medium's components within a selected range of concentrations, and, (ii) measuring component concentrations based on balanced chemical equations. Growth rates were expressed in terms of the reciprocal of their generation time in hours. The efficiency of denitrifying bacteria was investigated using growth yields as an index. The results show that the use of acetate as a carbon source for enhancing the denitrification rate can achieve much higher growth rates compared to those obtained using formate. These results are strongly congruent with that reported in Gerber *et al.* (1986), where compounds including acetate, propionate, butyrate and lactate produced higher denitrification rates than methanol or glucose. This is due to the fact that acetate has two carbon atoms that can easily be converted into acetyl Co-A by bacterial cells (Onnis-Hayden and Gu 2008). This acetyl Co-A is a key compound of the tricarboxylic acid (TCA)/glyoxylate cycle for central metabolism (White 1995). This cycle is the metabolic pathway for utilising an organic substrate as energy and carbon sources in most microorganisms. In contrast, energy is lost during single carbon atom

compound assimilations such as formate, methanol or glucose (Minkevich 1985). Kinetic rates of denitrification with various carbon sources have been extensively studied, and the results are summarised in Onnis-Hayden and Gu (2008).

3.2. Materials and Methods

3.2.1. Enrichment and Isolation

The isolation of specific groups of bacteria, such as denitrifiers, requires knowledge of the interactions of large numbers of medium components and their growth conditions. Many bacteria can be grown in laboratory culture media that are designed to provide all essential nutrients in a solution for bacterial growth. Denitrifying bacteria can gain the energy required for metabolism and growth from the oxidation of organic carbon, sulphide minerals or reduced iron and manganese (Rivett *et al.* 2008). Their metabolic requirements for nitrogen can be achieved through the availability of NH_4^+ or organic nitrogen N in the environment, or from the direct assimilation of nitrate. They also need carbon, phosphorus, sulphur and micro-nutrients (including B, Cu, Fe, Mn, Mo, Zn and Co) for efficient metabolism (Rivett *et al.* 2008). A variety of microorganisms found in soil can denitrify. In order to isolate a certain type of organism from a natural source, selective technique and environment were performed. It has been shown that wetland is a hot spot for denitrification (Reddy and D'Angelo 1994). It has also been found that the highest number of culturable denitrifiers in forest soil was found in autumn, winter and early spring (Mergel *et al.* 2001). This result may originate from the differences in temperature and soil moisture content during these seasons. The total microbial activity is low during hot and dry periods as the soil is dry. Therefore, in this study

denitrifying bacteria were extracted from wet soil collected in autumn. A soil sample was taken from the area around Swansea University. A previous study (Luo *et al.* 1998) has shown that a sharp decrease in the denitrification rates by approximately 10- to 100-fold can be observed for a depth interval of between 0 to 10 cm and 30 cm. Therefore, the sample was collected from 3 cm below the surface of the soil using a clean spatula and bag. The soil sample was then delivered to the laboratory within 5 minutes. Microbial enrichment was started by inoculating 10 grams of soil to 1 L liquid medium that contained several components at different concentrations. Two types of media, which are shown in Table 3.1 and Table 3.2, were examined in this study. The media were buffered to *pH* 7 with 1 M *NaOH* and were incubated at room temperature for 3 days. Foams were produced on the top of the incubated culture media. It has to be observed that culturing was implemented under oxic conditions and the sub-culture was repeated twice. A sample was taken, and colourless liquid preparation was made. The sample was then checked under optical microscopy for morphology (Olympus CHA 842721, Microscopy).

Denitrifying bacteria are usually facultative anaerobes, capable of anaerobic nitrate and aerobic oxygen respiration. In order to achieve an oxygen-free environment the previous experimental process was repeated in the presence of nitrogen gaseous flow. This was accomplished by adding 30 ml liquid medium into each 50 ml serum vial that was sparged with gaseous nitrogen for almost 2 minutes. The serum vials were then sealed with butyle rubber stoppers and alumina seals. Serum vials were incubated at a 25° C for 2 days.

TABLE 3-1: Components and their concentrations for the basal sodium formate medium

1	Sodium Formate ($H-COONa$)	0.5 %
2	Sodium Nitrate ($NaNO_3$)	0.5 %
3	Potassium Dihydrogen Orthophosphate (KH_2PO_4)	0.25 %
4	Ammonium Sulphate ($(NH_4)_2SO_4$)	0.1 %
5	Yeast Extract	0.05 %
6	Water (H_2O)	1 L

TABLE 3-2: Components and their concentrations for the basal sodium acetate medium

1	Sodium Acetate ($CH_3 \cdot COONa \cdot 3H_2O$)	0.5 %
2	Sodium Nitrate ($NaNO_3$)	0.5 %
3	Potassium Dihydrogen Orthophosphate (KH_2PO_4)	0.25 %
4	Ammonium Sulphate ($(NH_4)_2SO_4$)	0.1 %
5	Yeast Extract	0.05 %
6	Water (H_2O)	1 L

3.2.2. Purity of Cultures

Denitrifying species can be found in more than 50 bacterial genera (Zumft 1997), and these can be gram-positive or gram-negative. In order to detect and isolate a certain kind of organism, as well as minimising interference due to other organisms, the sub-culture previously described was repeated using an anoxic technique with sterilised media. The sterilisation was enabled by autoclaving sealed serum vials for

15 minutes at a temperature of 121° C. An Inoculum of 10% was inserted in each serum vial using a sterilised syringe. Media were then incubated at 25° C for 2 days. The sub-culture was repeated 3 times. To obtain single colonies and to investigate the bacteria, a solid agar medium was prepared by adding 20% agar to 1 L of the liquid medium. Solid agar medium was carried out as follows:

i. Powdered components, shown in Table 3.1 and Table 3.2, were weighed into an electronic balance (Voyager OHAUS, V12140), and then added to flasks each containing 1 L of distilled water.
ii. The flasks with a magnetic stir bar inside were placed on a magnetic rotary mixer to mix and dissolve all components.
iii. The flasks with media were autoclaved for 15 minutes at 121° C.
iv. Media were then poured into petri dishes under sterilized conditions.
v. The plates were kept at room temperature to solidify.

A sample was taken from each previous liquid culture medium and streaked on fresh agar plates under sterilised conditions. Cultures were incubated at 25° C for 2 days. Streaking on solid agar plates was repeated 2 times. A colony was carefully taken from each plate and was streaked on a fresh agar plate under sterilized conditions. A sample was taken from each culture and stained by using a simple stain. Each sample was checked under optical microscopy for morphology, purity and cell damage. Colonies with a different morphology were transferred to Durham nitrate broth tubes and incubated for 2 days. Colonies that produced gas were presumed to be denitrifiers. This presumption was proved through nitrate reduction test, and the results showed that the bacteria isolated can reduce nitrate to nitrite. This process is described in detail in Section 5.2.2.1.

A variety of techniques and equipment is used for anaerobic studies. In this study, an oxoid anaerobic jar system was used to produce an oxygen-free environment to cultivate anaerobic bacteria on plating agar media. This technique was performed by immediately placing streaked plates in an upright position inside the anaerobic jar and closing the lid. This jar was connected to a vacuum pump to remove the air and to flush out residual oxygen with nitrogen gas. The anaerobic jar was evacuated at least three times and refilled each time with nitrogen gas. The jar was incubated at a temperature of 25° C for 48 hours. This experimental process was repeated three times to achieve a good microbial isolation. Purity of culture was controlled using a simple stain technique under optical microscopy. In addition, a gram stain was used to identify the type of bacteria, and the results showed bacteria that were gram negative.

3.2.3. Bacterial Preservation

A cryopreservation method was used in order to preserve the bacteria by cooling and storing them at a sub-zero temperature. It has to be noted that, at such temperatures, biological activity, including biochemical reactions that may lead to cell death, is effectively stopped. Cultures that are cryopreserved should be healthy and maintained in log phase growth before freezing. The bacteria were initially inoculated into 50 ml serum vials containing medium under sterilised conditions. Serum vials were sparged with gaseous nitrogen for 2 minutes and were autoclaved for 15 minutes at a temperature of 121° C prior to inoculating them. Bacterial cultures were incubated for 48 hours to reach the log phase. Bacterial inocula and 25% glycerol solution were mixed in equal amounts in 2.5 ml tubes under strictly

sterilised conditions. The 25% glycerol solution was used as a cryoprotectant agent. Tubes were then frozen at -70° C for further use.

3.2.4. Optimisation of the Growth Medium

To achieve higher biomass yield of denitrifying bacteria, an optimisation of the growth medium was performed. Optimisation was evaluated by testing the effect of each medium component within a selective range of concentrations. Medium component concentrations were measured, based on equations of chemical reactions as shown in Appendix A, and were also used to assess the growth medium optimisation. Two media, sodium formate and sodium acetate, were evaluated in this study. A liquid medium of 250 ml was prepared. The concentrations of medium components (shown in Table 3.1 and Table 3.2) were fabricated in proportion to 250 ml water. The medium was buffered to *pH* 7 with 1M *NaOH.* A liquid medium of 15 ml was placed into a 25 ml pressure tube. The pressure tubes were sparged with gaseous nitrogen for an almost 2 minutes to obtain complete anaerobic conditions. The pressure tubes were then sealed with butyl rubber stoppers and alumina seals. Tubes were autoclaved for 15 minutes at 121° C. Ten tubes of each medium component were made to gain accurate results. The pressure tubes were then inoculated with 10% inocula. The effect of each medium component on the bacterial growth rate and its doubling time within a range of selective concentrations was evaluated over a 9 hour period at 25° C. Growth rate and the doubling time were evaluated by means of optical density measurements. The optical density of each sample was measured at a 660 nm wavelength on a Spectrophotometer every hour (UV/Vis Spectrophotometer, Philips, Pu 8628).

3.3. Results and Discussion

3.3.1. Growth of Denitrifying Bacteria in Basal Media

In order to evaluate the maximum growth rate achieved, the selected denitrifying bacterium was primarily grown on a basal medium. Two basal media: sodium format and sodium acetate media were prepared following the procedures given in Section 3.2.1. Figs. 3.1 (a) and (b) show the bacterial growth rate over a 9 h static incubation in the sodium formate basal and sodium acetate basal media respectively. In the sodium formate basal medium the bacteria reached a final biomass concentration of 0.19 O.D.Units, whereas a final biomass concentration of 0.31 O.D.Units was achieved in the sodium acetate basal medium. The results in both sodium formate and acetate basal media show relatively slow growing bacteria. Bacteria grown in the sodium formate medium achieved a growth rate of 0.13 h^{-1} with a doubling time of 5.1 h. In contrast, a 0.17 h^{-1} growth rate and a 4 h doubling time were obtained when using a sodium acetate medium. In order to enhance the bacterial growth rate as well as achieve higher yields of biomass, the basal medium had to be reformulated.

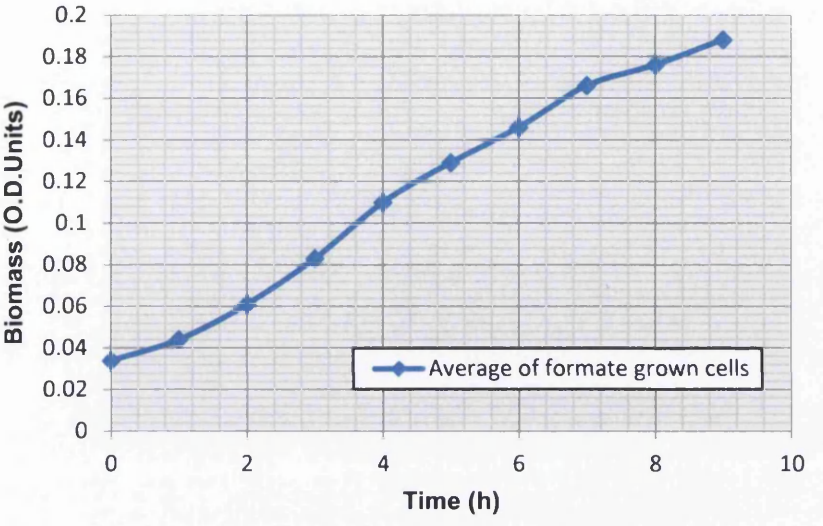

(a)

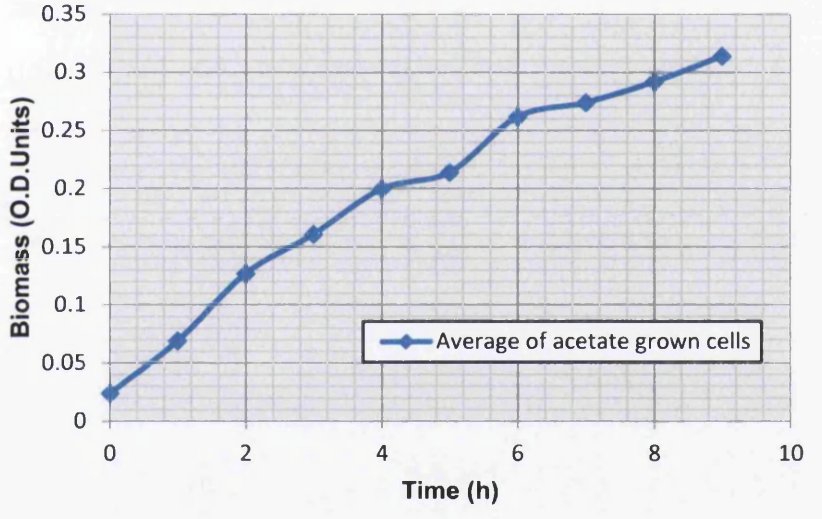

(b)

Figure 3-1: Bacterial growth on two basal media: (a) Sodium formate basal medium and (b) Sodium acetate basal medium.

3.3.2. Optimisation of the Growth Rate of Denitrifying Bacteria

In order to maximise the growth rate of the bacteria used in this study, optimisation of its growth media was carried out. The optimisation was evaluated on the two

media studied (sodium formate and sodium acetate) in two different ways. Firstly, the effect of each medium component was studied in a selected range of concentrations. Furthermore, medium component concentrations, based on equations of chemical reactions, were used to evaluate the bacterial growth rate.

3.3.2.1. Effect of a Selective Range of Concentrations of Different Medium Components on Bacterial Growth

3.3.2.1.1. Sodium Formate Medium

The bacterial growth rate and its doubling time of different sodium formate, sodium nitrate and potassium dihydrogen orthophosphate concentrations are shown in Figs. 3.2 (a) and (b) respectively. The final biomass of the bacterial growth after 9 hours incubation, with respect to the concentration of the medium chemical components, is given in Appendix B.1. The concentration of sodium formate, sodium nitrate and potassium dihydrogen orthophosphate were increased by a range of 0% to 1.5% in steps of 0.25%. It is clear that the growth rate improves as the concentration increases. However, higher concentrations inhibit the bacterial growth. A significant improvement in the growth rate, from 0.11 h^{-1} to 0.16 h^{-1}, was achieved when a potassium dihydrogen orthophosphate concentration of 1% was used. However, growth inhibition was observed when the concentration of potassium dihydrogen orthophosphate exceeded 1%. A similar trend of the bacterial growth rate is shown with respect to sodium formate concentrations. Furthermore, the increase in the sodium nitrate concentration up to 1.25% resulted in an enhancement in the growth rate, from 0.1 h^{-1} to 0.17 h^{-1}, which reflects an approximately 2.5 h reduction in the doubling time. However, a drop in the growth rate was realised if the sodium nitrate

concentration increased further. It is clear that sodium formate strongly supports the bacterial growth compared to the sodium nitrate and potassium dihydrogen orthophosphate.

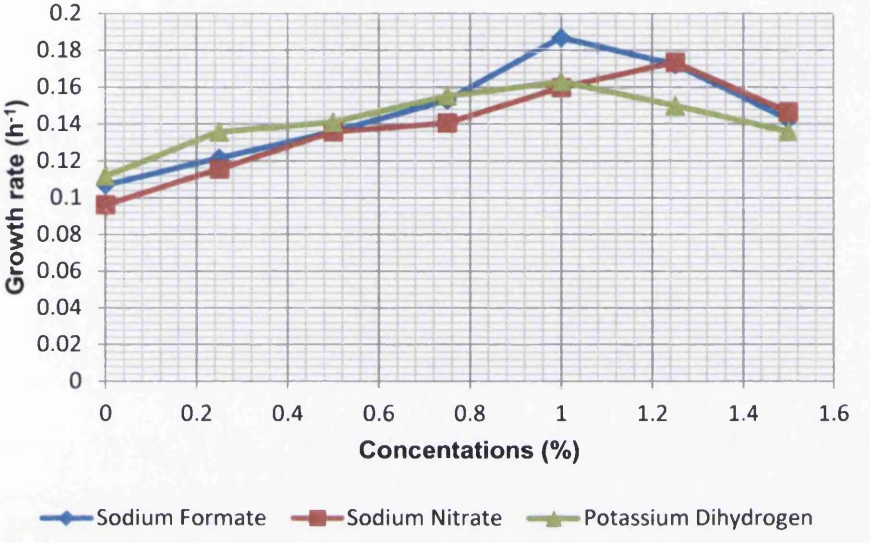

(a)

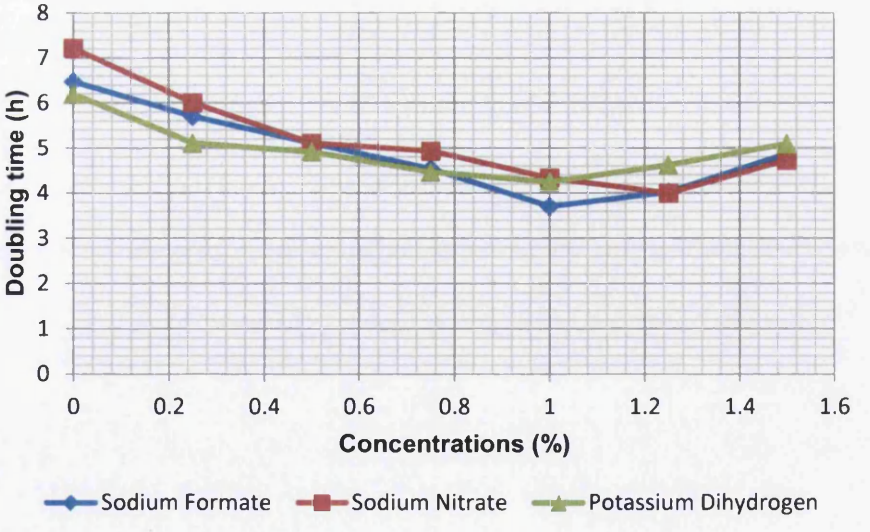

(b)

Figure 3-2: (a) Growth rates of bacteria in different medium components (Sodium Formate, Sodium Nitrate and Potassium Dihydrogen) with different concentrations; (b) Doubling times.

Figs. 3.3 (a) and (b) show the bacterial growth rates and the doubling times with different amounts of yeast extract and ammonium sulphate. The ammonium sulphate concentration was increased in a range of 0% to 0.5% in steps of 0.1%. A number of yeast extract concentrations between 0% and 0.75% were used.

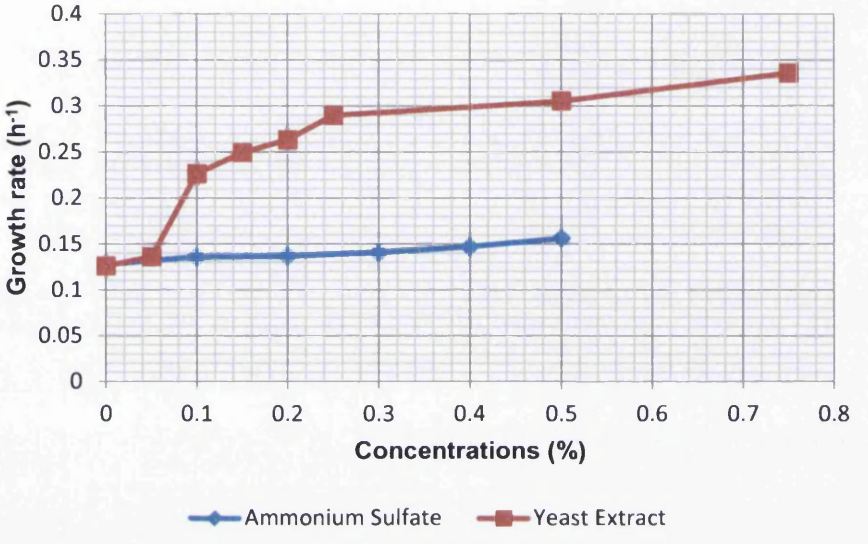

(a)

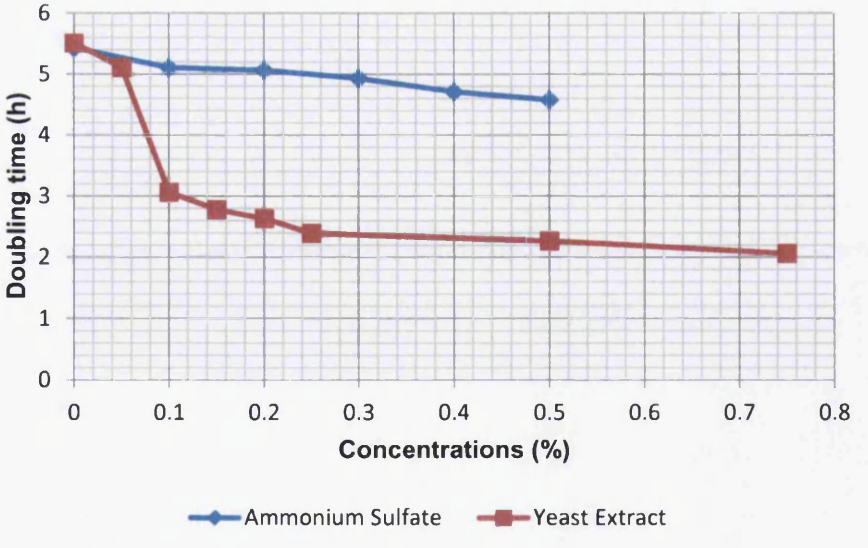

(b)

Figure 3-3: (a) Growth rates of bacteria in different medium components (ammonium sulphate and yeast extract) with different concentrations; (b) Doubling time.

The results indicate that increases in yeast extract levels offer beneficial support to the bacterial growth rate, whereas the growth rate remains relatively unaffected by increasing the ammonium sulphate concentration. Further, the bacterial growth rate was considerably enhanced from 0.13 h^{-1} to 0.34 h^{-1} approximately as a result of an increase in the yeast concentration from 0% to 0.75%.

Table 3-3 outlines the bacterial growth rates and the doubling times based on the type of water used. Three types of water: distilled, tap and 50 % mixed (tap + distilled) water were used, and the growth rates achieved were 0.13 h^{-1}, 0.1 h^{-1} and 0.12 h^{-1} respectively. According to the results, distilled water is preferred over the other types of water.

TABLE 3-3: Growth rates and doubling times of bacteria with different types of water.

Type of water	Growth rate (h^{-1})	Doubling Time (h)
Distilled water	0.13	5.1
Tap water	0.1	6.81
Mixed water	0.12	5.84

It is manifest that chemical compounds have a direct influence on the bacterial growth rate. An optimised medium was tested through the selection of component concentrations that give the maximum growth rate. Concentrations of chemical components used in the sodium formate medium are outlined in Table 3.4. The bacterial growth rate on the optimised medium was 0.4 h^{-1} and the doubling time reduced to 1.74 h. The final biomass achieved was 0.94 (see Fig. 3.4). The sodium

formate medium was also studied without using yeast extract, and a slow growth of the bacteria was observed, as shown in Fig. 3.5.

TABLE 3-4: Optimum sodium formate medium concentration.

1	Sodium Formate ($H-COONa$)	1%
2	Sodium Nitrate ($NaNO_3$)	1.25%
3	Potassium Dihydrogen Orthophosphate (KH_2PO_4)	1%
4	Ammonium Sulphate ($(NH_4)_2SO_4$)	0.5%
5	Yeast Extract	0.75%
6	Water (H_2O)	1 L

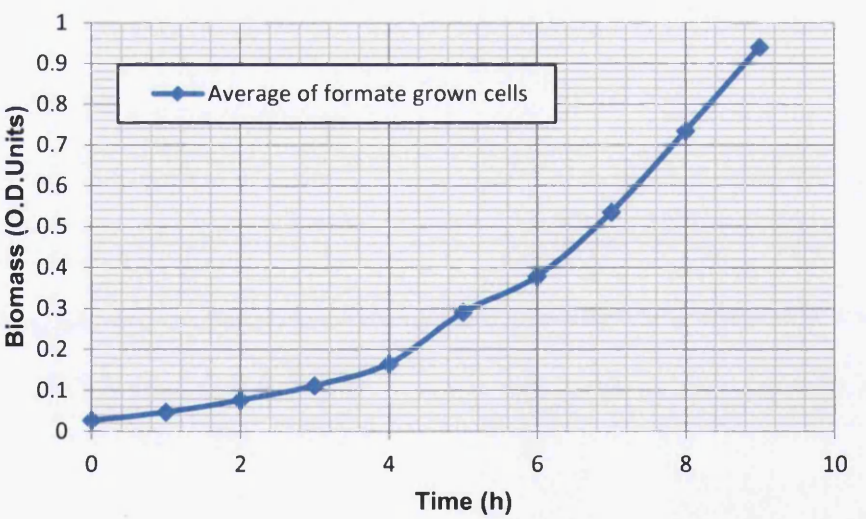

Figure 3-4: Bacterial growth on the optimum sodium formate medium.

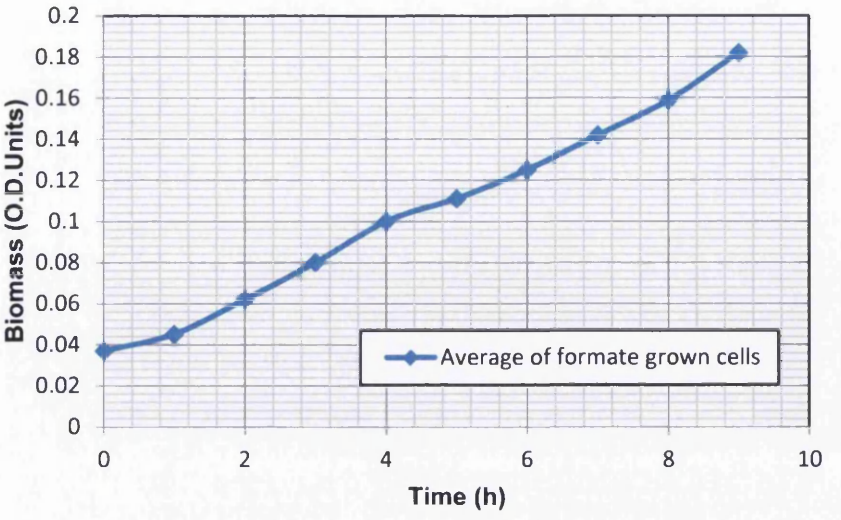

Figure 3-5: Bacterial growth on the sodium formate medium without using yeast extract.

3.3.2.1.2. Sodium Acetate Medium

Fig 3.6 (a) shows the effect of sodium acetate, sodium nitrate and potassium dihydrogen orthophosphate on bacterial growth rates. The corresponding doubling times are shown in Fig 3.6 (b). Appendix B.2 outlines the final biomass achieved after 9 hours incubation in terms of concentrations. A concentration range of 0% to 1.5% was considered in sodium acetate, sodium nitrate and potassium dihydrogen orthophosphate. A bacterial growth rate enhancement was observed when the medium component concentrations were increased. However, the bacteria cannot stand concentrations higher than 1.25% of both sodium acetate and sodium nitrate. Potassium dihydrogen orthophosphate concentrations higher than 1% can also inhibit the growth rate. Furthermore, improvement based on increasing the sodium acetate is higher than that achieved when the sodium nitrate and potassium dihydrogen orthophosphate concentrations were increased. For example, the increase in the sodium acetate and sodium nitrate concentrations, from 0% to 1.25%, obtained

growth rate improvements of 0.24 h^{-1} and 0.2 h^{-1} respectively. These growth rate improvements reflected in doubling time reductions of 2.9 h and 3.52 h respectively. An improvement in the growth rate from 0.15 h^{-1} to 0.2 h^{-1}, together with a reduction in the doubling time, from 4.7 h to 3.5 h, were achieved by increasing the potassium dihydrogen orthophosphate concentrations from 0% to 1%.

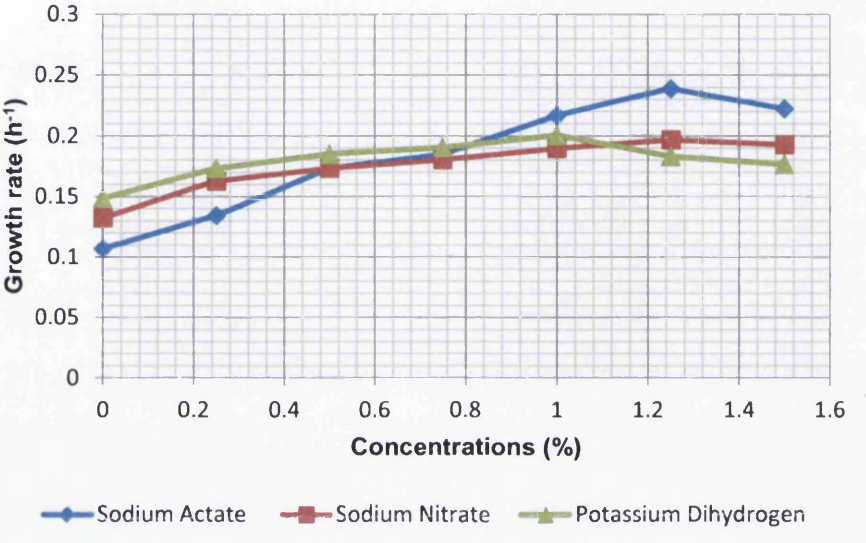

(a)

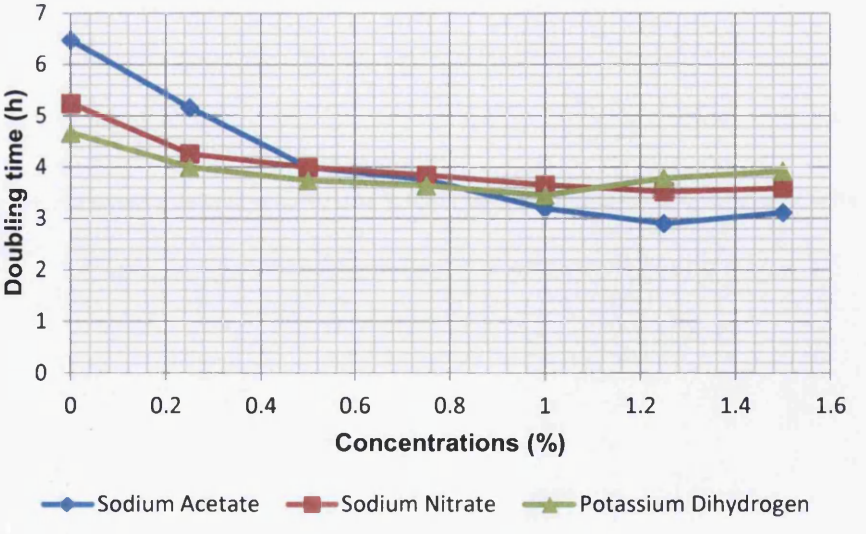

(b)

Figure 3-6: (a) Growth rates of bacteria in different medium component (Sodium Acetate, Sodium Nitrate and Potassium Dihydrogen) with different concentrations; (b) Doubling time.

The results in Fig 3.7 indicate that ammonium sulphate does not support the bacterial growth rate as much as the significant enhancement of the growth rate based on yeast extract.

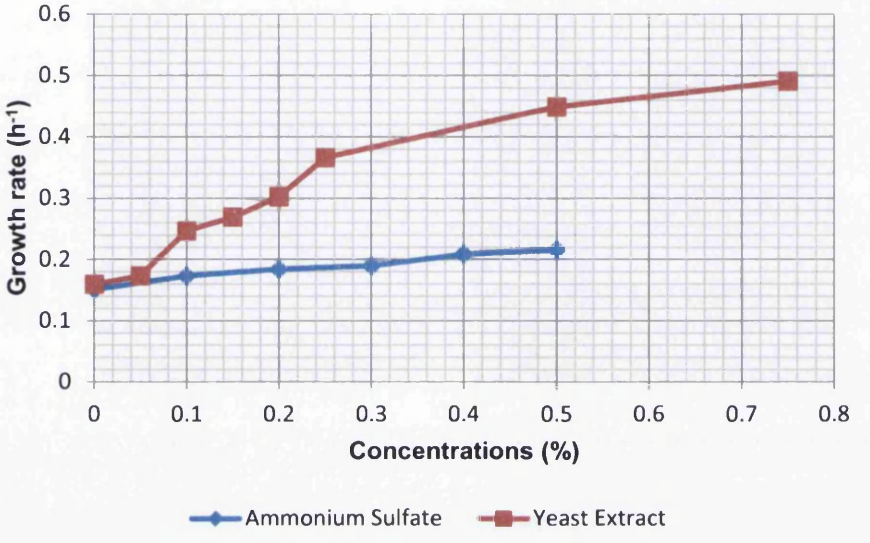

(a)

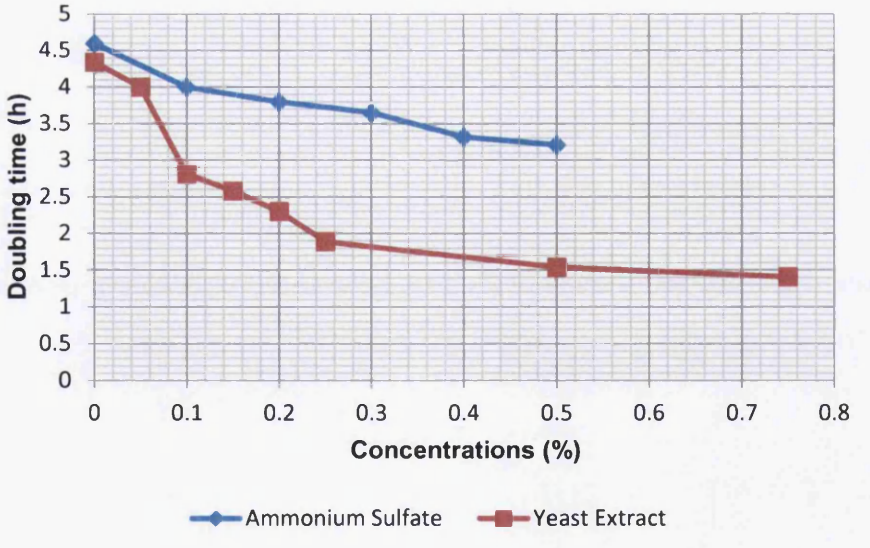

(b)

Figure 3-7: (a) Growth rates of bacteria in different medium component (ammonium sulphate and yeast) with different concentrations; (b) Doubling time.

Increasing the yeast extract concentration from 0% to 0.5% reduced the doubling time from 4.34 h to 1.54 h, whereas a reduction in the doubling time from 4.6 h to 3.2 h was achieved through the increase of the ammonium sulphate concentration from 0% to 0.5%. In addition, the use of distilled water helped achieve a growth rate of 0.17 h^{-1} in comparison with a 0.13 h^{-1} growth rate obtained when tap water was used (see Table 3-5).

TABLE 3-5: Growth rates and doubling times of bacteria with different types of water.

Type of water	Growth rate (h^{-1})	Doubling Time (h)
Distilled water	0.17	4
Tap water	0.13	5.53
Mixed water	0.14	5.02

The component concentrations, shown in Table 3-6, were used to test for the optimum sodium acetate medium, where the concentration with the best growth rate was selected.

TABLE 3-6: Optimum sodium acetate medium concentration.

1	Sodium Acetate ($CH_3 \cdot COONa \cdot 3H_2O$)	1.25%
2	Sodium Nitrate ($NaNO_3$)	1.25%
3	Potassium Dihydrogen Orthophosphate (KH_2PO_4)	1%
4	Ammonium Sulphate ($(NH_4)_2SO_4$)	0.5%
5	Yeast Extract	0.75%
6	Water (H_2O)	1 L

The bacterial growth rate on the optimised sodium acetate medium was 0.52 h^{-1} and the doubling time reduced to 1.3 h. The final biomass obtained was 1.43, as shown in Fig. 3.8. This sodium acetate medium was also studied without using yeast extract, and a bacterial growth rate of 0.2 h^{-1} and a final biomass of 0.27 were obtained (see Fig. 3.9).

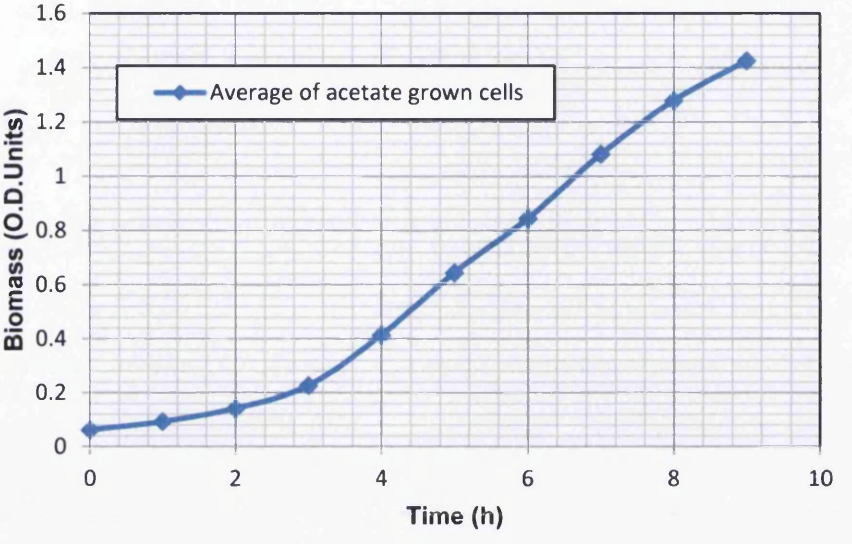

Figure 3-8: Bacterial growth on the optimum sodium acetate medium.

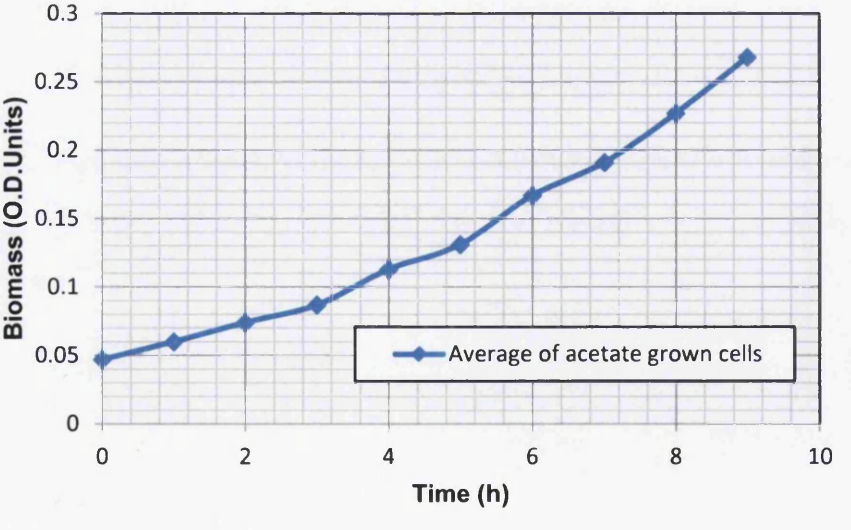

Figure 3-9: Bacterial growth on the sodium acetate medium without using yeast extract.

3.3.2.2. Effect of Certain Concentrations of Balanced Medium Components on Bacterial Growth

Concentrations of balanced medium components were used to assess the bacterial growth rates. The concentrations of the medium components, sodium acetate, sodium formate and yeast extract were measured based on equations of chemical reactions in proportion to 0.912% nitrate concentration (which corresponds to 1.25% sodium nitrate concentration). This sodium nitrate concentration (1.25%) was selected as it gave the best growth rate, compared to those produced using other concentrations of sodium nitrate (see Fig. 3.2 (a) and Fig 3.6 (a)). The concentrations of both ammonium sulphate and potassium dihydrogen orthophosphate were selected as 0.5% and 1% respectively, according to the results discussed earlier. Table 3.7 outlines the concentrations of the chemical components used in this case study. The two media (sodium formate and sodium acetate) were studied, tested and compared.

TABLE 3-7: Concentrations of chemical components measured based on equations of chemical reactions

1	Sodium Acetate ($\boldsymbol{CH_3 \cdot COONa \cdot 3H_2O}$)	0.76%
2	Sodium Formate ($H - COONa$)	1%
3	Sodium Nitrate ($NaNO_3$)	1.25%
4	Potassium Dihydrogen Orthophosphate (KH_2PO_4)	1%
5	Ammonium Sulphate ($(NH_4)_2SO_4$)	0.5%
6	Yeast Extract	0.42%
7	Water (H_2O)	1 L

3.3.2.2.1. Sodium Formate Medium

The sodium formate medium, prepared using deliberate concentrations of chemical components, was examined, and its growth rates evaluated. A growth rate of 0.32 h^{-1} was achieved, together with a doubling time of 2.2 h and a final biomass of 0.64 (see Fig. 3.10). However, the bacterial growth rate reduced to almost 0.22 h^{-1} when the sodium formate was removed, as shown in Fig. 3.11. The medium was also tested without sodium nitrate, and a growth rate of 0.27 h^{-1} was achieved.

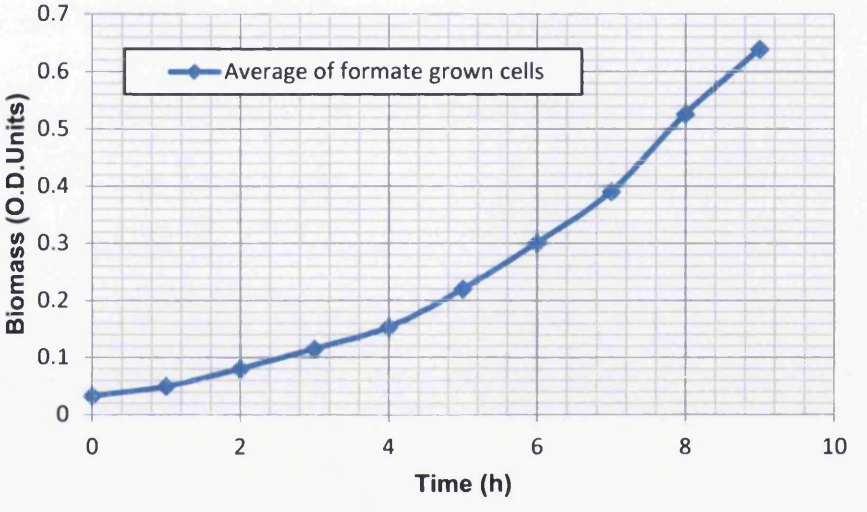

Figure 3-10: Bacterial growth on the sodium formate medium prepared using balanced concentrations of chemical components.

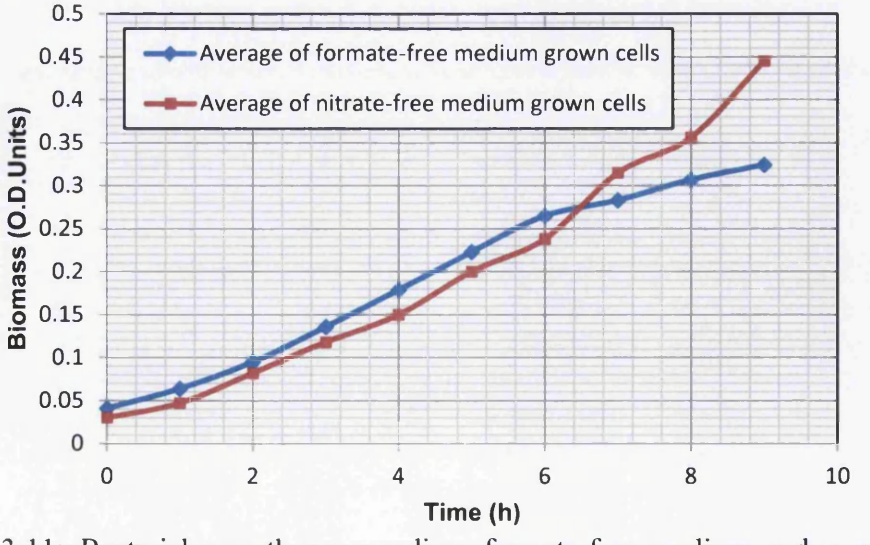

Figure 3-11: Bacterial growth on a sodium formate-free medium and a sodium nitrate-free medium.

In order to study the effects of yeast extract concentrations on the growth rate of the medium, prepared using 1.25% sodium nitrate and 1% sodium formate, a concentration range of yeast extract from 0% to 0.5%, in steps of 0.1%, was used. The bacteria growth rate, doubling time and final biomass achieved are drawn in Table 3.8. A gradual increase in the growth rate, from 0.12 h^{-1} to 0.34 h^{-1}, was achieved when the yeast extract concentration was increased from 0% to 0.5%.

TABLE 3-8: Characteristics of a sodium formate medium with different yeast extract concentrations.

Yeast extract concentration (w/v, %)	Growth rate (h^{-1})	Doubling Time (h)	Final biomass
0	0.12	5.74	0.14
0.1	0.24	2.85	0.4
0.2	0.26	2.7	0.44
0.3	0.28	2.44	0.51
0.4	0.3	2.3	0.58
0.5	0.34	2.06	0.69

3.3.2.2.2. Sodium Acetate Medium

Concentrations of chemical components were measured based on the equations from chemical reactions (see Table 3.7), and were used to prepare a sodium acetate medium. The bacterial growth rate achieved and its doubling time were 0.47 h^{-1} and 1.47 h respectively. The final biomass, reached over a period of 9 h, was 1.32, as shown in Fig. 3-12.

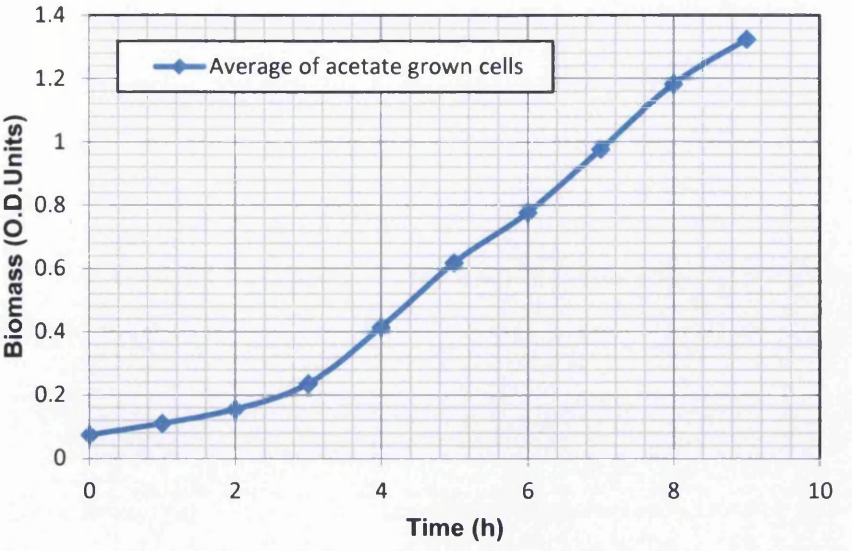

Figure 3-12: Bacterial growth on a sodium acetate medium prepared using balanced concentrations of chemical components.

The effect of sodium acetate and sodium nitrate on bacterial growth was studied. The medium was first tested without using sodium acetate. The results showed that removing sodium acetate incurred a reduction in the bacterial growth rate from 0.47 h^{-1} to 0.22 h^{-1}, which also reflected an increase in the doubling time by 1.7 h (see Fig. 3.13). However, a decrease in the growth rate from 0. 47 h^{-1} to 0.35 h^{-1} was observed when sodium nitrate was removed (see Fig. 3.13). This drop in the bacterial growth rate also reflected an increase of almost 0.5 h in the doubling time.

The effect of yeast extract concentrations on bacterial growth was also studied. A range of concentrations from 0% to 0.5% in steps of 0.1% was used. Table 3.9 outlines the bacterial growth rate, doubling time and final biomass achieved. The results indicated that lower yeast extract concentrations result in higher doubling times and lower yields of biomass.

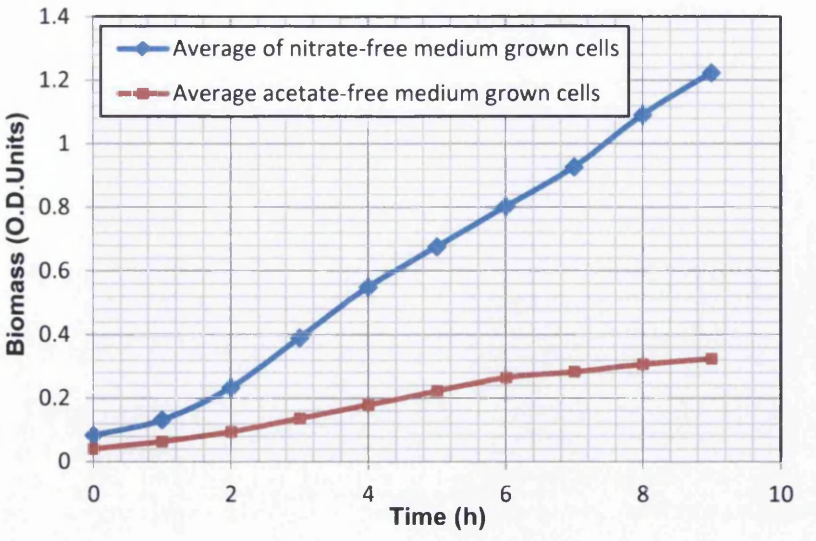

Figure 3-13: Bacterial growth on sodium acetate-free medium and sodium nitrate-free medium.

TABLE 3-9: Characteristics of a sodium acetate medium with different yeast extract concentrations

Yeast extract concentration (w/v, %)	Growth rate (h^{-1})	Doubling Time (h)	Final biomass
0	0.13	5.22	0.26
0.1	0.27	2.57	0.59
0.2	0.32	2.15	0.69
0.3	0.39	1.8	0.71
0.4	0.42	1.64	0.99
0.5	0.44	1.7	1.07

3.4. Summary

Medium optimisation was achieved through evaluations of the influence of various concentrations of chemical components on bacterial growth. Two media: sodium formate and sodium acetate were investigated. The assessment was carried out with two different approaches. In the first, a selected range of concentrations of each component was used to evaluate bacterial growth rates. The results showed that an optimised medium can be achieved using a sodium nitrate concentration of 1.25%, a potassium dihydrogen concentration of 1%, an ammonium sulphate concentration of 0.5% and a yeast extract concentration of 0.75% in 1 L distilled water. A growth rate of 0.4 h^{-1} was obtained in a sodium formate medium at 1% concentration, whereas a 0.52 h^{-1} growth rate was achieved in a sodium acetate medium using a concentration of 1.25%. The second approach assessed the growth rate on a medium that was prepared using balanced component concentrations, based on equations from known chemical reactions. The results showed that the use of 1% potassium dihydrogen, 0.5% ammonium sulphate and 0.42% yeast extract in a sodium formate medium with sodium nitrate and sodium formate concentrations of 1.25% and 1%, respectively, in 1 L distilled water achieved a growth rate of 0.32 h^{-1}. It was also demonstrated that using a sodium acetate medium with sodium nitrate, sodium acetate, potassium dihydrogen, ammonium sulphate and yeast extract concentrations of 1.25%, 0.76%, 1%, 0.5% and 0.42%, respectively, obtained a growth rate of 0.47 h^{-1}. The results confirm that with the two approaches considered, sodium acetate is a directly utilisable substrate that is more readily metabolisable than formate.

4. BIOLOGICAL DENITRIFICATION IN MICROBIAL FUEL CELLS

4.1. Introduction

Removal of nitrate can be accomplished by the process of biological denitrification in which nitrate is reduced to gaseous nitrogen products, which are then released into the atmosphere (Payne 1973). The atmosphere is composed primarily of dinitrogen gas. Biological treatment is a candidate method that can support and encourage the growth of naturally occurring bacteria, which help convert nitrate to nitrogen gas. It is important to be noted that these sorts of bacteria are not harmful and would not cause illness or threaten public health. However, additional filtration and disinfection must be carried out on biologically treated water to ensure protection of public health. Using such a method has a significant benefit, especially given there is no or little waste generated. This chapter aims to study the biological removal of nitrate using a mediatorless dual chambered MFC in which a mixed bacterial culture in the cathode performs denitrification. This is done by making use of electrons supplied by a mixed bacterial culture oxidising acetate at the anode. Five electrons e^- are required to convert one molecule of nitrate to nitrogen gas, as shown in equation (2.5).

The results obtained in Chapter Three proved that acetate can greatly support the denitrification rate. Therefore, acetate is used as an organic substrate that serves as the carbon (nutrient) and energy source for the biological process. The substrate affects the integral composition of the bacterial community in the anode biofilm, as well as the MFC's performance, including its power density and coulombic efficiency (Chae *et al.* 2009). Both chambers of the MFC used in this study were treated with inocula from soil collected from an area around Swansea University. It has been found that a single gram of soil may contain 1×10^3 to 1×10^6 species of

bacteria (Gans *et al.* 2005, Torsvik *et al.* 2002, Tringe *et al.* 2005). In the previous chapter, a soil sample was tested and showed a resultant diversity within the bacterial community, including denitrifying bacteria. This chapter aims to achieve a higher nitrate reduction rate possible by using 100% microbial fuel cells enriched with soil inocula only (i.e., stream, river or lake sediment, digester sludge, sewage and wastewater treatment plant were not used here). The MFC's performance was examined under closed and open circuit conditions. The denitrification activity at various acetate and nitrate concentrations was also investigated. Furthermore, nitrate reduction rates as a function of external resistance was studied. The results confirmed that denitrification activity was greatly dependent on acetate concentration, and over 92% of nitrate can be removed at an acetate concentration of 272 mg/L under closed circuit conditions through an external resistance of 500 Ω.

4.2. Materials and Methods

4.2.1. Microbial Fuel Cell Design and Setup

An H-shape MFC, which consisted of two separated chambers joined with a glass tube containing a 4.7 cm × 4.5 cm diameter proton exchange membrane (PEM), was constructed. The volume of each chamber was approximately 200 ml with a 50 ml headspace. Anodic and cathodic chambers were operated in anaerobic conditions, where the top of each chamber was sealed with a rubber stopper. A platinum wire was introduced from the top of each chamber through the rubber stopper to solder one end of a rectangular prism shaped graphite felt (GF) electrode, having a surface area of 40 cm^2 and a weight of 0.719 g. Given that the rectangular prism-shaped

electrode (SA) had a length (L) of 4 cm, a width (W) of 0.5 cm and a height (H) of 4 cm, the outer surface area was calculated as

$$SA = 2LW + (2L + 2W)H. \quad (4.1)$$

$$SA = 2 \times 4 \times 0.5 + (2 \times 4 + 2 \times 0.5) \times 4 = 40\ cm^2. \quad (4.2)$$

Each chamber has two side ports to allow the provision of fresh substrate, as well as purging nitrogen, and to allow the removal of the treated one.

4.2.2. Microbial Fuel Cell Inoculation and Operation

4.2.2.1. Preparation of Soil Inocula

A soil sample was obtained from an area around Swansea University. The sample was collected from a depth of 3 cm using a clean spatula and bag, and was then delivered to a laboratory within 5 min. An inoculum solution was prepared by adding 10 g soil to a 250 ml flask that contained 70 ml of an autoclaved solution. The latter was prepared with 1 g CH_3-$COONa$-$3H_2O$ and 3 g KNO_3 in 500 ml distilled water, and then autoclaved at 121° C for 15 min. The inoculum solution was shaken and kept for 20 min before used.

4.2.2.2. Medium Preparation

The mixed culture of soil inoculum was simultaneously inoculated into each chamber during the MFC start up. Both anode and cathode chambers were similarly filled with an artificial wastewater medium. This artificial wastewater medium, which was prepared according to Lee *et al.* (2003), contained inorganic salts dissolved in 990 ml of 5 mM phosphate buffer and 10 ml of a trace mineral solution. The chemical

components of the inorganic salts are listed in Table 4.1. The ingredients of the trace mineral solution in 1L distilled water are outlined in Table 4.2.

TABLE 4-1: Components of the inorganic salts medium

Components	Concentrations (mg/L)
KH_2PO_4	15
$(NH_4)_2SO_4$	30
$NaHCO_3$	105
$FeCl_3 \cdot 6H_2O$	0.25
$MgSO_4 \cdot 7H_2O$	50
$CaCl_2$	3.75
$MnSO_4 \cdot H_2O$	5

TABLE 4-2: Components of the trace mineral solution

Components	Concentrations (g/L)
Nitrilotriacetic acid	1.5
$FeSO_4 \cdot 7H_2O$	0.1
$MnCl_2 \cdot 4H_2O$	0.1
$COCl_2 \cdot 6H_2O$	0.17
$ZnCl_2$	0.1
$CaCl_2 \cdot 2H_2O$	0.1
$CuCl_2 \cdot 2H_2O$	0.02
H_3BO_3	0.01
Na_2MoO_4	0.01
Na_2SeO_4	0.017
$NiSO_4 \cdot 6H_2O$	0.026
$NaCl$	1

The phosphate buffer solution used to form the basis of the salt solution was prepared as a mixture of KH_2PO_4 and K_2HPO_4. The salt solution was autoclaved at 121° C for 15 min and left to cool. Nitrogen gas was then purged for 30 min to remove oxygen. The solution's pH was checked and adjusted to 7 in each chamber through the addition of 1 M HCl or 1 M $NaOH$. The former (HCl) was used to reduce pH, while the latter ($NaOH$) was used to increase pH.

4.2.2.3. Enrichment Procedure

In order to maximise the growth of the biofilm-forming organisms, enrichment was conducted in three different modes for three months, following the procedure given in Borole *et al.* (2009). The MFC reactor was first operated in a fed-batch mode under a closed circuit condition through 10 KΩ in the first month. This essential growth mode allowed the microorganisms to grow at a constant load using acetate as a carbon source in the anodic chamber and nitrate as an electron acceptor in the cathodic chamber. This was facilitated through the weekly addition of 2 mM (169.5 mg/L) sodium acetate $CH_3 - COONa - 3H_2O$ and 8.4 mM (847.9 mg/L) potassium nitrate (KNO_3) into the anodic and cathodic chambers respectively. The second mode was performed as starvation mode for a month, where the addition of a carbon source was stopped and the nitrate fed was carried out weekly. The main goal of this mode was to enable consumption of carbon source added in the first mode.

The mode was also given a selection of organisms that were capable of either using residual acetate or internally storing carbon to be subsequently used for cellular maintenance needs. This purpose was achieved by replacing the medium solution in both chambers after two weeks of the starvation mode period, which helped avoid sodium and nitrite accumulations in the anode and cathode chambers respectively.

Furthermore, the weekly addition of the carbon source was restarted and the external load was reduced from 10 KΩ to 500 Ω to allow a higher current to flow between the electrodes for the rest of the enrichment period. This resulted in higher availability of an electron acceptor in the cathode and offered the opportunity of the growth of exoelectrogenic organisms. During the enrichment process, both chambers were purged with gaseous nitrogen for 10 min after each fuel addition in order to obtain anaerobic conditions. Furthermore, the solution in each chamber was continuously mixed using a magnetic stirrer (B&T Flatspin, Stirrer) to enhance mass transfer. The experiment was conducted at room temperature. The enrichment process was completed and the MFC operation was then started, and this is discussed next.

4.2.2.4. MFC Operation

The power generated by an MFC is computed as the production of cell voltage across an external resistance due to the current flow through the resistor. The MFC system is operated at a steady state when the power generated equals the power consumed for an extended time. In steady state MFC systems, sustainable power can be generated as the product of a steady current passing through a fixed load and a constant voltage drop across this load. Due to the possibility of many steady conditions in an MFC system, it is important to define the condition in which the MFC produces the maximum sustainable current, as well as computing the maximum sustainable power. In order to obtain a steady state condition, the MFC system was initially conducted through an external resistance of 500 Ω in several batch modes using acetate as the carbon source and nitrate as the electron acceptor under anaerobic conditions. The cell voltage was measured every hour using a digital multimeter connected to a personal computer through a data acquisition system

(34405A, Agilent). The nutrient medium was completely replaced at the operation start up and when the voltage dropped to less than 5 mV as an end of batch. Previous study (Sukkasem *et al.* 2008) found that a stable MFC system was achieved when the voltage output was reproducible after replacing the medium at least twice. In this study, a stable voltage generation (sustainable voltage) of 30 mV approximately was produced after three batches. Furthermore, in order to define the steady state that provides the maximum power output, a polarization curve was obtained by measuring the stable voltage generated at various external resistances.

Polarization and power density curves were discussed in Section 2.2.8.3. In this study, a single cycle method was used to obtain the polarization curve, and the external resistance was varied from 10 Ω to 10 KΩ in steps of 250 Ω at an interval of 10 min using a resistor box (DECADE Resistance box type RB701). The cell voltage was measured at each resistance. Current and power were calculated with respect to the voltage and resistance based on Ohm's law, using equations (2.21) and (2.22) respectively. Current and power densities were also calculated, by normalising the current and voltage through an electrode surface area, using equations (2.24) and (2.23) respectively. The coulombic efficiency (CE), based on total acetate added, was calculated using equation (2.31).

A series of batch-mode MFC tests were performed to investigate the effect of nitrate and acetate concentrations on the MFC's performance and its denitrification activities. The operation of these tests was carried out under closed circuit through 500 Ω external resistance. Furthermore, the effect of external resistance on the denitrification process was studied by operating the MFC under three different loads. Nitrate reduction and nitrite accumulation rates were studied and evaluated throughout the tests.

4.2.3. Chemical Analysis

4.2.3.1. Nitrate Concentration

Nitrate concentrations were determined by an ultraviolet (UV) spectrophotometric screening method proposed by Clesceri *et al.* (1999). This method helps screening samples with low organic matter content. A rapid determination of NO_3^- concentration was achieved through the measurement of UV absorption at 220 nm. However, the sample absorbance was also measured at 275 nm to avoid the interference of the dissolved organic matter, as well as correcting the NO_3^- value. This is due to the fact that dissolved organic matter may also absorb at 220 nm, whereas NO_3^- does not absorb at 275 nm. The corrected UV-light absorbance of NO_3^- (A_{corr}) in the sample was calculated as (Beschkov *et al.* 2004)

$$A_{corr} = A_{220} - 2 \times A_{275}, \tag{4.3}$$

where A_{220} and A_{275} are the absorbance readings at 220 nm and at 275 nm respectively. In order to remove the insoluble particles (including cells and other medium components) the samples were centrifuged for 15 min at 8000 rpm before the photometric determination of NO_3^-. 1 ml of 1 M HCl was then added to the samples (each of 50 ml), and the light absorbance was read against distilled water. A NO_3^- calibration curve was obtained following Beer's law for concentrations up to 11 mg/L and used to actually determine the NO_3^- concentration in the samples.

Beer's law indicates that the absorbance is directly proportional to the concentration of a solution. A stock nitrate solution was prepared by dissolving 0.7218 g KNO_3 in 1 L distilled water. Eleven standard solutions of NO_3^- in the range of 0 to 4 mg $NO_3^- - N/L$ were prepared through the dilution of the following volumes of nitrate solution: 0, 2, 4, 6, 8, 10, 12, 14, 16, 18, 20 ml to 50 ml distilled

water. Each NO_3^- standard was treated in the same manner as the sample. A standard curve was constructed by plotting the absorbance of each standard solution of NO_3^- against its corresponding $NO_3^- - N$ concentration, as shown in Fig. 4.1. Sample concentrations can be directly obtained from the standard curve using corrected sample absorbances calculated by equation (4.1). Note that most laboratories usually report nitrate content in parts per million (ppm) of nitrate-nitrogen ($NO_3^- - N$); however, this thesis reports results in ppm NO_3^-. The conversion of $NO_3^- - N$ to NO_3^- can be achieved through multiplication of the factor 4.4, where for example 10 $NO_3^- - N$ is equal to 44 NO_3^-.

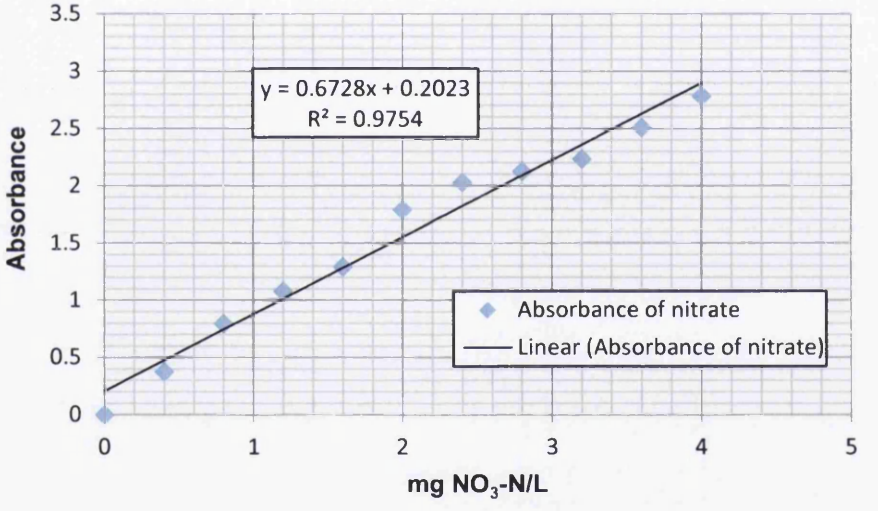

Figure 4-1: Standard curve for nitrate.

4.2.3.2. Nitrite Concentration

Nitrite concentrations were obtained using a development spectrophotometric method proposed by Merino (2009). A concentration of nitrite present in a sample can be determined by diazotizing with sulphanilamide and coupling with N-(1-naphtyl)-ethylenediamine dihydrochloride to form a highly coloured azo dye that is measured at 540 nm. Distilled water was used to prepare all reagents as follows:

1. Reagent 1, which is a nitrite stock solution (2,000 mg NO_2^-/L), is prepared by dissolving 0.6003 g of sodium nitrite in 200 ml of distilled water. This solution can be stable for at least 3 months at 4° C.
2. Reagent 2, which is a nitrite working solution (100 mg NO_2^-/L), is prepared daily when needed by diluting 5 ml of the nitrite stock solution (reagent 1) to 100 ml of water.
3. Reagent 3, which is a hydrochloric acid HCl (37%) (1.0 mol/L), is prepared by diluting 83 ml HCl to 1,000 ml of water.
4. Reagent 4, which is an ammonia buffer solution NH_3 (25%) with pH 11, is prepared by adding 75 ml ammonia to 825 ml of water. The pH was then adjusted to 11 with HCl (reagent 3). Finally, the resulting solution is diluted to 1,000 ml.
5. Reagent 5, which is known as Carrez solution I, is made by dissolving 150 g potassium hexacyanoferrate (II) trihydrate, $K_2[Fe(CN)_6].3\,H_2O$ in water and diluting to 1,000 ml. Note that this solution (reagent 5) should be stored in a brown bottle.
6. Reagent 6, which is known as Carrez solution II, is prepared by dissolving 230 g of zinc acetate dehydrate, $Zn(CH_3COO)_2.2\,H_2O$ in water and diluting to 1,000 ml.
7. Reagent 7, which is called colour reagent I, is prepared by dissolving 2 g sulphanilamide in water, adding 150 ml HCl (reagent 3), and then diluting to 200 ml.
8. Reagent 8, which is called colour reagent II, is prepared by dissolving 0.2 g N-(1-naphthyl)-ethylenediamine dihydrochloride in 200 ml of water. Note

that this solution should be stored in a dark bottle and replaced monthly or as soon as a brown colour develops.

A test sample was prepared by adding 60 ml of hot water (50-60° C) to 5 ml of the laboratory sample. For clarification, the two solutions: 4 ml Carrez solution I (reagent 5) and 4 ml Carrez solution II (reagent 6) were added to the test sample, with swirling after each reagent addition. The test sample was then transferred to a centrifuge cup and centrifuged for 10 min at 4,000 rpm. The clear supernatant was filtered using a filter paper (Whathman, Germany) and was diluted to 100 ml with water. To determine the nitrite, 20 ml of the test sample was transferred to a 100 ml volumetric flask, and 10 ml of ammonia buffer (reagent 4) was added. 2 ml of the colour reagent I (reagent 7) was added and mixed to develop the colour. The resulting solution was kept at room temperature for 5 min before adding 2 ml of the colour reagent II (reagent 8). It was then diluted to 100 ml with water and left to stand for between 10 min and 2 h. The sample absorbance was measured at 540 nm using a spectrophotometer (UV-Visible spectrometer). The instrument was adjusted against water. The actual nitrite concentration present in the sample was obtained from a calibration graph. The latter was prepared by making use of six standard solutions of the nitrite working solution (reagent 2) in the range of 0 to 1.2 mg NO_2^-/L. The following volumes of nitrite working solution were used: 0, 1, 2, 3, 4 and 6 ml, each placed into a separate flask. A standard solution with each volume was prepared, following the procedure of the test sample preparation described above. A standard curve was established through plotting the absorbances of standard solutions of NO_2^- against their nitrite standard concentration (which is in

mg NO_2^-/L), as shown in Fig. 4.2. Nitrite concentration of the test sample $(x_{NO_2^-})$ was determined using the calibration graph as

$$x_{NO_2^-} = \frac{Abs_{(s1)} - Abs_{(b11)}}{b_1} \times F, \tag{4.4}$$

where $Abs_{(s1)}$ $Abs_{(b11)}$ are the absorbances of the sample and the blank respectively, b_1 is the gradient of the calibration graph and F is the dilution factor, which is 5 in the method (plus any dilution of the test sample).

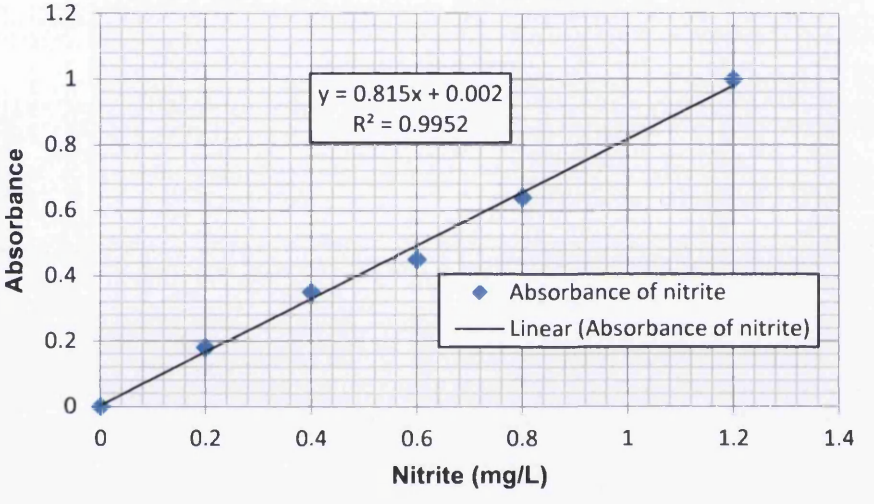

Figure 4-2: Standard curve for nitrite.

4.3. Results and Discussion

4.3.1. MFC Performance under Closed/Open Circuits

In order to investigate and evaluate the performance of an MFC reactor under closed and open circuit conditions, a batch-mode using 122 mg/L of acetate and 520 mg/L of nitrate concentrations was operated at each condition. The results are presented in terms of electricity generation, Coulombic efficiency, nitrate reduction and nitrite

accumulation rates. Nitrate reduction and nitrite accumulation rates were determined based on the methods discussed in Section 4.2.3. The system was first operated under an open circuit condition for a period of time, and the voltage output was measured every hour until the end of the batch. An illustration of the voltage output measured over the time period is shown in Fig. 4.3. An open cell voltage (OCV) maximum of 349.92 mV was obtained. The OCV of an MFC is the maximum voltage that can be achieved at infinite external resistance. In the cathode chamber, the total amount of NO_3^- removed was 68.36% (355.5 mg NO_3^-/L), and the nitrite accumulation was 18.16 mg NO_2^-/L at the end of the batch. It has to be noted that nitrite accumulation is shown as one of the main problems in biological denitrification due to the inhibited effect of nitrite ions on bacterial growth (Almeida *et al.* 1995). Furthermore, the MFC reactor was operated with a closed circuit through an external resistance of 500 Ω. The results showed a higher reduction rate of 87.5% (455.12 mg NO_3^-/L) and lower nitrite accumulation of 6.63 mg/L, compared to that obtained in open circuit mode where electron transfer is unavailable.

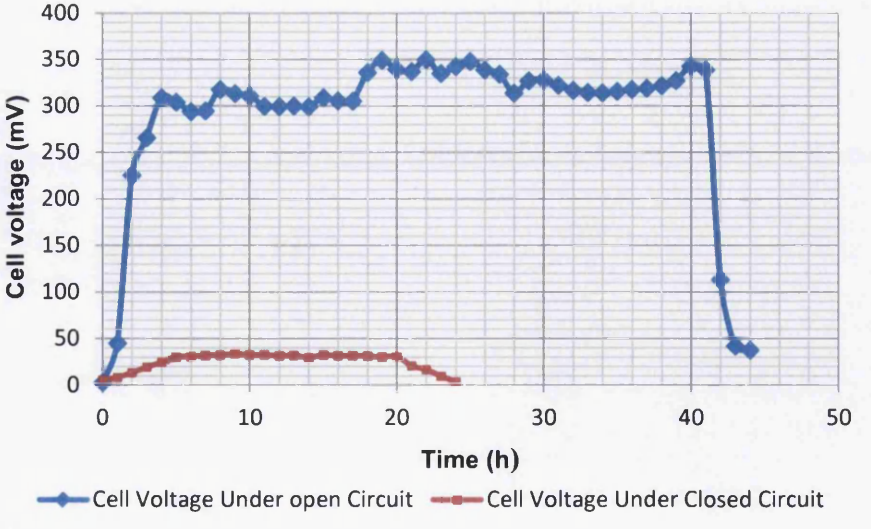

Figure 4-3: Electricity generation by a batch-mode MFC under both open and closed circuit conditions using acetate in the anode chamber and nitrate in the cathode chamber.

This is in congruence with that reported in Jia *et al.* (2008), where the amount of nitrate removal in the closed circuit MFC was 2.5 higher than that obtained in the open circuit MFC. The maximum cell voltage achieved through an external resistance of 500 Ω was 33.95 mV. The coulombic efficiency, which indicates the ratio between the coulombs recovered and the total coulombs in the substrate, was about 1.42%, illustrating that a substantial fraction of acetate was lost without current generation.

4.3.2. Electrochemical Properties

The maximum power density was evaluated through the examination of a polarization curve, which characterises voltage as a function of current. The power production over a range of current densities was obtained by changing the external resistance R_{ext} using a resistor box, when the voltage production became stable. The MFC reactor was initially operated under an open circuit condition. Once the reactor achieved a stable voltage output of 0.349 V, the resistor box was switched on and the external resistance was varied from 10 Ω to 10 kΩ in steps of 250 Ω every 10 min and the cell voltage was measured at each resistance. Current and power levels were calculated with the voltage and resistance based on Ohm's law. Current and power densities were calculated by normalising the current and voltage through an electrode surface area. Polarization and power density curves are displayed in Fig. 4.4 (a). The polarization curves illustrating the three characteristic regions of voltage drop in the MFC are shown in Fig. 4.4 (b). These regions include a rapid voltage decrease due to the flow of current through high external resistance, an almost constant decrease in voltage and a second significant voltage drop at high current densities. The decrease

in the cell voltage is a consequence of electrode overpotentials (activation, bacterial metabolic and mass transfer losses) and ohmic losses.

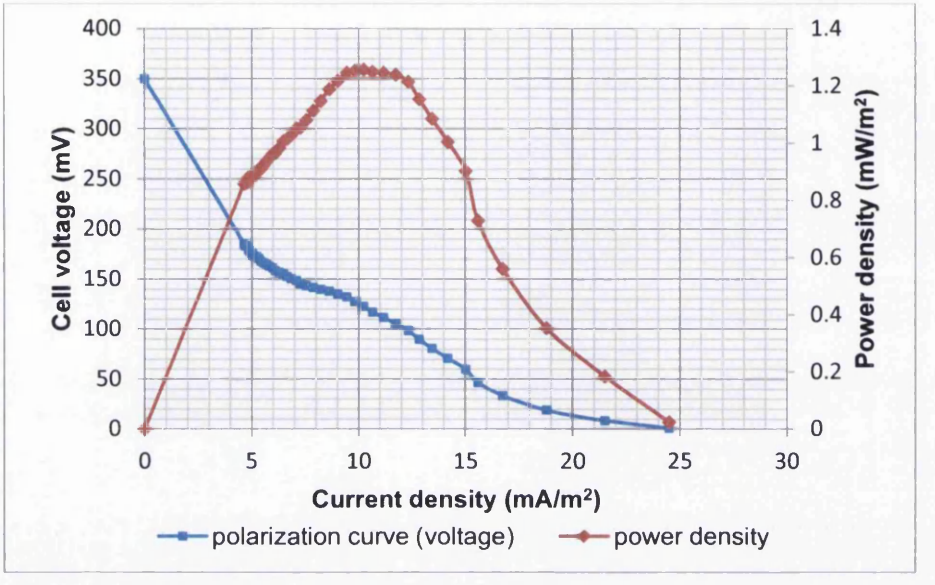

(a)

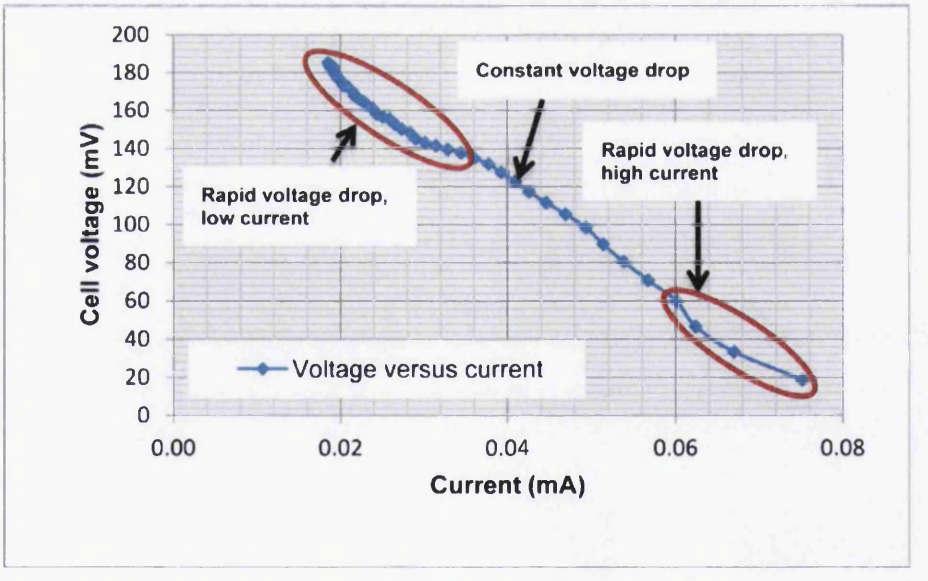

(b)

Figure 4-4: (a) Polarization curves. (b) The three characteristic regions of voltage drop.

The maximum power density obtained was 1.26 mW/m^2 at a current density of 10.23 mA/m^2. This is a slightly lower than that reported in Jia *et al.*, (2008); where the highest power density achieved was 1.7 mW/m^2 at a current density of 15 mA/m^2. This is a result of two factors. Firstly, Jia *et al.*, (2008) used a graphite-Mn(IV) and a graphite-Fe(III) electrode as an node and a cathode respectively; however, we used a pure GF electrode here in both chambers. Modification of GF electrodes using nanomaterials and the improvements observed is discussed in Chapter 6. Furthermore, the results achieved in this study were based on the enrichment of soil inocula only; however anaerobic digester sludge was used in Jia *et al.*, (2008). Based on the slope of the linear region of the polarization curve, an internal resistance R_{int} of 2893 Ω could be determined. It is also shown in Fig. 4.4 (a) that the power output was maximal when $R_{int} = R_{ext} = 3000$ Ω.

4.3.3. Denitrification Activity

4.3.3.1. Effects of Nitrate Concentrations on Denitrification Activity

The effects of different nitrate concentrations on denitrification activity, voltage output and coulombic efficiency were investigated at a fixed external resistance of 500 Ω. The MFC system was operated with a number of batches at a range of nitrate concentrations between 470 mg/L to 670 mg/L in steps of 50 mg/L in the cathodic chamber, while a fixed acetate concentration of 122 mg/L was added in the anodic chamber at the beginning of each batch. An illustration of typical profiles of cell voltages produced is shown in Fig. 4.5.

The denitrification activity was examined through the measurement of nitrate and nitrite concentrations at the end of each batch. The denitrification activity

(including nitrate reduction and nitrite accumulation rates), current generation and coulombic efficiency achieved are outlined in Table 4.3. The results showed that both nitrate removal and nitrite accumulation rates exhibited an increase with the increase of nitrate concentration. Increasing the nitrate concentration from 470 mg/L to 670 mg/L improved the denitrification activity by almost 2% (from 87.32% to 89.3%). However, an increase in nitrite accumulation by a factor of approximately 3 (from 5.15 mg/L to 16.93 mg/L) was incurred. Furthermore, an increase in the coulombic efficiency from 1.29% to 1.6% was observed. Previous work (Jia *et al.* 2008) suggested that the current production was dependent on glucose and nitrate. The results in our experiments confirmed this suggestion and also demonstrated that the denitrification rate was supported by the current production (which was dependent on nitrate). However, the system was also operated with the absence of nitrate as an electron acceptor in the cathodic chamber, and a low electrical current was observed. The CE obtained in this case (i.e., when the system operated without nitrate) was 0.72%.

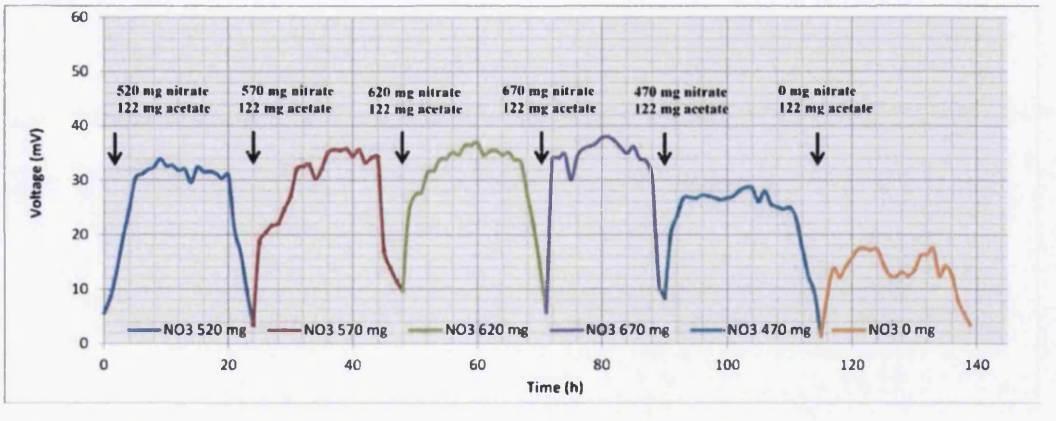

Figure 4-5: Effect of nitrate concentrations on voltage generation.

TABLE 4-3: Nitrate removal and nitrite accumulation of several closed batches fed with 122 mg/L acetate and different nitrate concentrations.

Nitrate concentration (mg/L)	Nitrate removal		Nitrite accumulation mg/L	Average current (μA)	Coulombic efficiency (%)
	mg/L	%			
470	410.39	87.32	5.153	46	1.29
520	455.12	87.524	6.626	52.4	1.42
570	500.3	87.8	10.31	54	1.46
620	547.26	88.27	12.52	61	1.58
670	598.21	89.3	16.93	65	1.6

4.3.3.2. Effect of Acetate Concentrations on Denitrification Activity

To investigate the effect of acetate on the MFC performance, the fuel cell was fed with several batches at different acetate concentrations in the anodic chamber. Acetate concentrations of 72, 122, 172, 222 and 272 mg/L were used. Each batch was performed with an external resistance of 500 Ω at a nitrate concentration of 520 mg/L in the cathodic chamber. Cell voltage profiles produced are shown in Fig. 4.6. The denitrification rate, current production and coulombic efficiency obtained are given in Table 4.4. The addition of sodium acetate can allow the bacteria to provide more electrons and to increase the voltage output. This was observed as an increase in the cell voltage when the concentration of acetate was increased. Meanwhile, increasing acetate concentration resulted in an increase in the current generation as well as in the CE. This is because there was less time for acetate to be lost during competing physical and biological processes. This agrees very well with that demonstrated in Kim *et al.*, (2005). In the cathodic chamber, an increase in the

nitrate removal from 85.6% to 92.23%, together with a decrease in the nitrite accumulation from 7.4 mg/L to 5.2 mg/L, were observed when the acetate concentration increased from 72 mg/L to 272 mg/L. This indicates that when acetate concentration of 272 mg/L was used, 1.08% of the nitrate removed was turned into nitrite based on equation (2.7).

The remaining 91.15% (474.97 mg/L) of the nitrate removed was possibly converted into nitrogen gas, in accordance with equation (2.5). The experimental results proved that the sodium acetate highly supports the denitrification activity. However, the MFC performance was evaluated in the absence of sodium acetate and a denitrification rate of 71.7% was achieved while producing low cell current. This is due to the bacteria making use of the carbon stored internally by the cells from the previous batches, where carbon sources are used. It has to be noted that operating the MFC system in carbon starvation mode (i.e., without using a carbon source) during the enrichment forced the bacteria to store carbon internally.

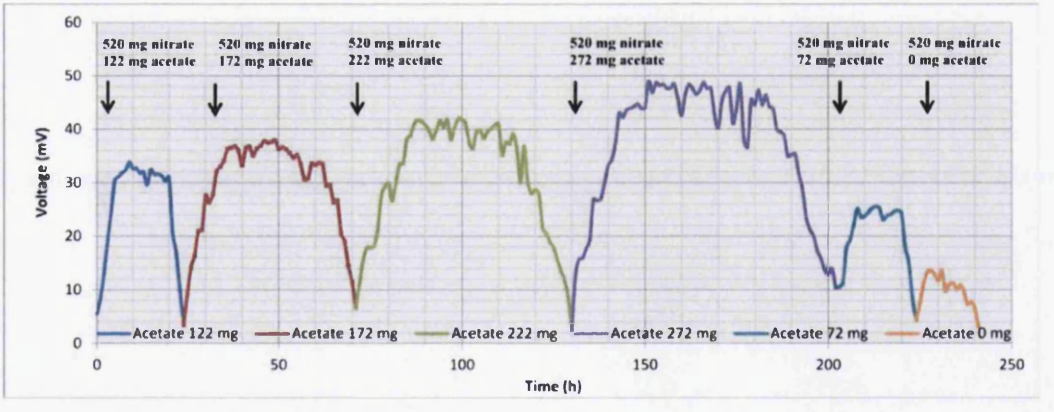

Figure 4-6: Voltage generation using acetate at different concentrations.

TABLE 4-4: Nitrate removal, nitrite accumulation, average current and CE of several closed batches fed with 520 mg/L nitrate and different acetate concentrations.

Acetate concentration (mg/L)	Nitrate removal		Nitrite accumulation mg/L	Average current (μA)	Coulombic efficiency (%)
	mg/L	%			
72	445.01	85.6	7.4	41	1.33
122	455.12	87.5	6.6	52.4	1.42
172	466.8	89.8	6.4	59	2.25
222	472.3	90.83	5.89	63	2.31
272	480.17	92.2	5.2	74	2.7

4.3.3.3. Effect of External Resistance on Denitrification Activity

To investigate the effect of electricity generation on the denitrification process, further experiments were conducted with an MFC under different external resistances: 500, 5000 and 10000 Ω. Sodium acetate and nitrate concentrations of 122 mg/L and 520 mg/L respectively were used. Average currents of 52 μA (500 Ω), 22 μA (5 KΩ) and 14 μA (10 KΩ) were produced, as shown in Fig. 4.7. The results confirmed that the denitrification rate is strongly dependent on the cell current produced, which was varied here by external resistance. The nitrate removal, nitrite accumulation and CE achieved by the MFC under different external resistances are given in Table 4.5. It was observed that using higher resistance led to low cell current, resulting in lower nitrate removal rates and higher accumulation rates. This was possibly due to insufficient electron donors being available on the cathode.

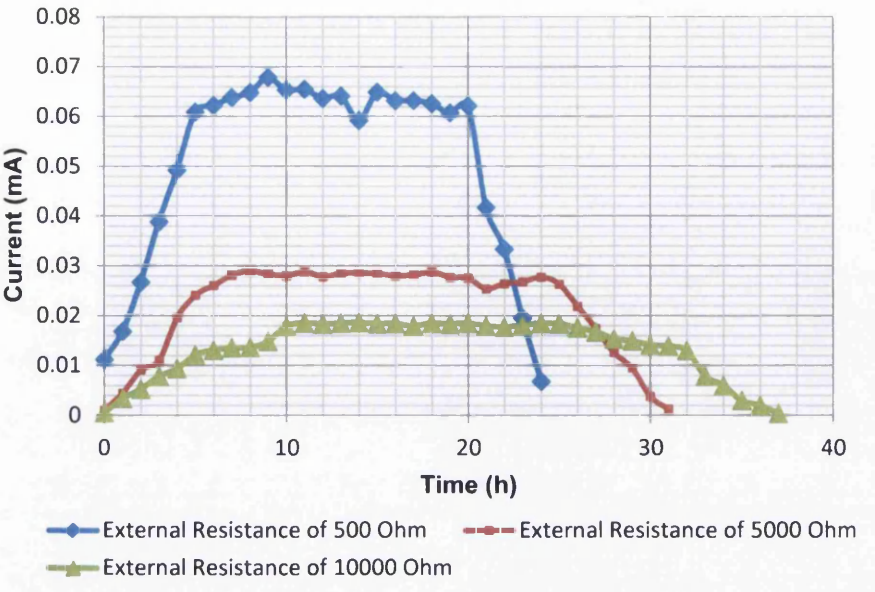

Figure 4-7: Current generation of an MFC under different external resistances: 500, 5000 and 10000 Ω.

TABLE 4-5: Nitrate removal, nitrite accumulation, average current and CE of several closed batches fed with 520 mg/L nitrate and 122 mg/L acetate concentrations under different external resistances: 500, 5000 and 10000 Ω

External resistance (Ω)	Nitrate removal		Nitrite accumulation mg/L	Average current (μA)	Coulombic efficiency (%)
	mg/L	%			
500	455.12	87.5	6.6	52.4	1.42
5,000	434.98	83.65	7.61	22.2	0.78
10,000	412.5	79.33	8.34	14	0.58

4.4. Summary

In this chapter, the performance of an MFC system was investigated and evaluated at different acetate and nitrate concentrations under closed and open circuit conditions. The effect of external resistance on the MFC's performance was also studied. The

results were presented in terms of power production, Coulombic efficiency, nitrate removal and nitrite accumulation rates. The results suggested that the denitrification rate is strongly dependent on the current generation. The latter was affected by external resistance levels, as well as acetate and nitrate concentrations. Increasing the relative nitrate concentrations enhanced the nitrate reduction rate at the expense of increasing the nitrite accumulation rate.

In contrast, an increase in the nitrate removal, together with a reduction in the nitrite accumulation, was observed when the acetate concentration increased. The results demonstrated that over 92% of nitrate was removed when an acetate concentration of 272 mg/L was used. However, there was an accumulation of nitrite of 1.08% at the end of the test. The coulombic efficiency was almost 2.7%, demonstrating that a substantial fraction of substrate was lost without current generation. Higher external resistances would, however, inhibit the denitrification activity as a result of producing lower electrical currents. In addition, a polarization curve was drawn through the variation of the external resistance using a resistor box, and a maximum power density of 1.26 mW/m^2 was obtained at a current density of 10.23 mA/m^2.

5. CHARACTERISTICS OF THE MICROBIAL COMMUNITY ON THE ELECTRODE SURFACE

5.1. Introduction

Denitrification bacteria play a critical role in the removal of nitrogen compounds from water and wastewater. Therefore analysis of the microbial community related to denitrification is very important to understand the nitrate removal process, and this is investigated in this chapter. The microbial community attaches to the electrode and forms a biofilm on its surface. This biofilm facilitates efficient biological electron transfers in the MFC. The biofilm is a collection of bacterial cells attached to a surface, creating an extracellular matrix. Bacteria can develop a plurality of electron transfer strategies through their associated biofilms (Rabaey *et al.* 2004). The formation of these biofilms plays an important role in the evolution of electrode potential in MFCs. It has been reported that acetate has an efficient impact on the composition of the microbial community attached to the MFC's anode (Logan and Regan 2006). Many researchers have focused on electrochemically active biofilms, including isolation of electrogenic bacteria (Logan *et al.* 2006), and microbial community analysis of the electrochemically active biofilm (Kim *et al.* 2007) and the mechanisms of electron transfer (Lovley and Phillips 1988). The environmental factors, such as temperature, pH and oxygen, can also affect microbial growth.

In order to understand the physiology of the exoelectrogenic denitrifier bacteria and the ecology of the communities on the cathodic electrode biofilms, dilution of microbial communities attached to the electrode was used to isolate and identify dominant populations of bacteria existing in the MFC's cathodic electrode. The biofilm formed on the anodic electrode was also investigated.

5.2. Materials and Methods

5.2.1. Bacteria Isolation from the Electrode Surface

A small piece of almost 1 cm^2 from both MFC anode and cathode electrodes was cut and crushed separately into a tube containing 10 ml autoclaved distilled water under sterilised conditions. Cell suspension was obtained by vortexing for 2 min, and serial dilutions were made in 10-fold steps to 10^{-8} in sterile tubes containing 9 ml of autoclaved distilled water. Petri plates of sterilised nutrient agar medium with nitrate were used for the isolation of the bacteria by inoculating the plates with 1 ml bacterial suspension from each dilution. A nutrient agar medium containing beef extract (3 g/L), peptone (5 g/L) and agar (15 g/L) in 1 L distilled water was supplemented with nitrate in the form of potassium nitrate (1 g/L). The medium was adjusted to pH 7. This medium (nutrient agar medium) is a complex medium because it contains ingredients with unknown amounts of nutrients. This can support the growth of a wide range of microbes. The plates were then incubated at 25° C for 7 days in an oxoid anaerobic jar system. The latter was used to produce an oxygen-free environment to cultivate anaerobic bacteria on plating agar media, as previously detailed in Section 3.2.2. Nine colonies were picked up from the incubated mixed culture plates. Three colonies of the nine selected were isolated from the anode electrode and the six remaining were taken from the cathode electrode. Each colony was transferred to a new petri plate containing a similar medium. The isolated bacteria were incubated at 25° C for 2 days under anaerobic conditions. A Gram stain was used to identify the types of bacteria, and biochemical tests were then performed for each isolate under sterilised conditions. A cryopreservation method was used to preserve all isolated bacteria, as described in Section 3.2.3.

In order to present the advantages of the acetate medium (described in Chapter Three), all isolates were subcultured on that medium and incubated at 25° C for 7 days under anaerobic conditions. A comparison with the bacteria isolated and studied in Chapter Three was considered. One of the denitrifier bacteria isolated from the cathode electrode biofilm was selected and re-inoculated back into the MFC cathode chamber to enrich the cathodic chamber. The selection was based on their higher ability to transform nitrate into nitrogen gas and the greatest proliferation observed. Furthermore, in order to investigate the ability of the selected denitrifier bacteria to reduce nitrate and produce power in a pure culture, a new MFC reactor was operated and enriched following the procedure described in Section 4.2.2 (using the same artificial wastewater medium). In this MFC, the cathode compartment was inoculated with a pure culture of the selected denitrifier bacteria, whereas the anode compartment was inoculated with the bacterial suspension obtained from the previous MFC anode biofilms. Both compartments were kept anoxic by purging with nitrogen gas. The MFC system was enriched for a period of three months using 2 mM (169.5 mg/L) sodium acetate in the anodic chamber and 8.4 mM (847.9 mg/L) potassium nitrate in the cathodic chambers. The voltage across 500 Ω was measured every hour using a digital multimeter connected to a personal computer through a data acquisition system. The current and power levels were calculated, as previously described in Chapter Three.

5.2.2. Gram stain test

A Gram stain test is used to distinguish between gram-positive and gram-negative bacteria, which have distinct and consistent differences in their cell walls. Gram-positive bacteria have a thick layer cell wall made of peptidoglycan over almost 50%

- 90% of the cell envelope, which are stained purple by crystal violet. In contrast, Gram-negative bacteria have a thinner layer of 10% of cell envelope, which are stained pink by the counter-stain. The Gram stain test was performed by heat fixing a bacterial smear to a slide. The cells were then stained with the primary stain, crystal violet, followed by fixation with iodine. After adding the iodine, the cells were decolorised with alcohol. Subsequently, the cells were stained with the secondary stain, safranin, and were then analysed under the oil immersion lens of a microscope. Finally, the bacteria could be classified based on the colour shown: where it was Gram positive they appeared dark purple, whereas the cell is Gram negative if the colour was pink. The Gram stain was also used to identify bacterial shape.

5.2.3. Bacteria Identifications through Biochemical Tests

5.2.3.1. Nitrate Reductase Test

The denitrification activity of the isolated bacteria was carried out using the nitrate reductase test. This test aims to differentiate between bacteria based on their ability to reduce nitrate to nitrite or nitrogenous gases. It first performs through the detection of nitrite in the medium after incubation with the bacteria by using sulphanilic acid and alpha-naphthylamine. The sulphanilic acid denotes as nitrate reagent A in this study, while alpha-naphthylamine is represented by nitrate reagent B. Nitrite, if present in the medium, will react with sulphanilic acid (nitrate reagent A) forming a colourless complex known as nitrite-sulphanilic acid. This colourless complex will then yield a red precipitate (prontosil) when an alpha-naphthylamine (nitrate reagent B) is added. The absence of red colour (after the addition of both nitrate reagents A and B) indicates that nitrite is not present in the medium. This can be explained as

either that the nitrate has not been reduced by the bacteria (i.e., the bacteria is nitrate negative) or the bacteria have not only reduced nitrate to nitrite, but have also reduced nitrite to nitrogenous gases (i.e., the bacteria is nitrate positive). A small amount of zinc powder can then be added to the incubated medium for more discrimination. Zinc powder can help reduce nitrate (if it is still there) to nitrite, and a red colour will develop in the incubated medium within 15 min. Furthermore, the nitrate medium was introduced to Durham tubes to detect gas production. The success of the nitrate reduction test depends on providing the bacteria with an optimised growth medium, the correct temperature and anoxic conditions. The test was performed as follows:

1. Sulphanilic acid solution (nitrate reagent A) was prepared through dissolving 8 g of sulphanilic acid in 1 L of 5N acetic acid. The latter was made of 287.086 ml acetic acid stock solution (99.5%) diluted to 1000 ml with distilled water. The reagent can be stored at room temperature for up to 3 months in dark brown glass containers. Wrapping the bottle with aluminium foil can ensure darkness.
2. Alpha-naphthylamine solution (nitrate reagent B) was prepared by dissolving 6 g of N,N-Dimethyle-1-naphthylamine in 1 L 5N acetic acid. Reagent B can be stored at 2° C to 8° C for up to 3 months in dark brown glass containers. The bottle may be wrapped with aluminium foil to ensure darkness.
3. The nitrate broth medium was made by mixing 3 g/L of beef extract, 5 g/L of peptone and 1 g/L of potassium nitrate in 1 L distilled water. The medium prepared was then buffered to pH 7. 10 ml of the nitrate broth was added into 15 ml tubes fitted with Durham tubes. The tubes were then autoclaved for 15 min at 121° C.

4. The tubes were inoculated with the isolated bacteria and were incubated at 37° C for 2 days. A negative control tube without any bacteria was also made.
5. Almost 10 drops of both nitrate reagents A and B were added into each tube. The tubes were shaken well to mix the reagents with the medium.
6. A small amount of zinc powder would be added to the broth if no colour change was observed.

5.2.3.2. Catalase Test

The catalase test is used to detect the catalase enzyme in the bacteria through the decomposition of hydrogen peroxide to release oxygen and water. The presence of catalase enzyme can be confirmed if gas bubbles are observed (Mac-Faddin 1980). The catalase enzyme is present in most cytochrome-containing aerobic and facultative anaerobic bacteria (Doelle 1969). The test was performed as follows:

1. A 100 ml solution of 30% hydrogen peroxide was made using distilled water. This solution is unstable and should be stored in a fridge in a dark bottle.
2. A microscope slide was placed inside a sterile petri plate to limit catalase aerosols.
3. A sterile inoculating loop was used to collect a small amount of isolated bacteria colony (24 h old) and placed onto the microscope slide.
4. A drop of 30% H_2O_2 was added onto the bacteria on the microscope slide (without mixing). The petri plate was immediately covered with a lid to limit the aerosols, and the results were then recorded. Positive results indicate the presence of catalase where gas bubbles are shown, whereas no bubble formation represents a catalase-negative reaction.

5.2.3.3. Oxidase Test

The oxidase test can help determine the presence of oxidase enzymes in the bacteria (Steel 1961). This test is based on the ability of the bacteria to produce an intracellular oxidase enzyme. Some bacteria may produce more than one type of oxidase enzyme, which all participate in the cellular respiration process and catalyse removal of hydrogen from a substrate using oxygen as a hydrogen acceptor. The active substrate in an oxidase reagent, known as N,N,N,N-Tetramethyl-p-phenylenediamine dihydrochloride, acts as an artificial electron acceptor for the enzyme oxides, and this is often referred to as Kovac's oxidase reagent. The oxidase enzymes can oxidise the colourless reagent, forming the coloured compound Wurster's blue, which is a purple compound which is readily visible. The following procedure was performed:

1. Kovac's oxidase reagent was made by dissolving 1% of N,N,N,N-Tetramethyl-p-phenylenediamine dihydrochloride in warm water, following the procedure given in Naz *et al.* (2009) and Steel (1961). The reagent should be stored at a room temperature in a dark bottle.
2. A piece of filter paper was placed into a sterile petri plate. The filter paper was then moistening with oxidase reagent.
3. A single colony from the agar plate (one day old) was transferred and smeared onto this filter paper.
4. The results were then taken within 30 sec. A positive oxidase result is recorded if a purple colour is observed, while it is negative if the colour does not change.

5.3. Results and Discussion

5.3.1. Bacteria Identification

Bacteria often tend to grow and form a layer of biofilm on the surface of an object. The biofilm thickness depends on the nutrient conditions. The bacterial biofilm attached on the surface of both anode and cathode electrodes were revealed by using a Hitachi S-4800 scanning electron microscopy (a Hitachi S-4800 SEM), and their images are shown in Fig. 5.1 and Fig. 5.2 respectively. Imaging using SEM was done to confirm the presence of bacterial biofilm on the MFC electrodes. A small piece of 1 cm^2 of both electrodes was cut and used for imaging. The results showed heavy colonisations of bacteria on the surfaces of both electrodes. Furthermore, single colonies of bacterial species were isolated from each electrode biofilm to identify microbial species. Unknown bacteria are often identified through a series of tests including Gram stains, streaks for isolation and biochemical tests. The biochemical tests can help identify the bacteria since they have slightly different metabolic processes and contain different enzymes (Harley 2008). In this experiment, nine unknown isolates were identified, based on the biochemical tests and physiological characterisations, and the results are given in Table 5.1. Three colonies were isolated from the anode electrode biofilm, while six colonies were isolated from the cathode electrode biofilm. The Gram stain test indicated that most of the bacteria, including A2, A3, C2, C3, C4 and C5, were Gram-negative, while the others remaining (A1, C1 and C6) were Gram-positive. This test also showed that the majority of the bacteria, including A1, A3, C2, C3, C4 and C5, were rods.

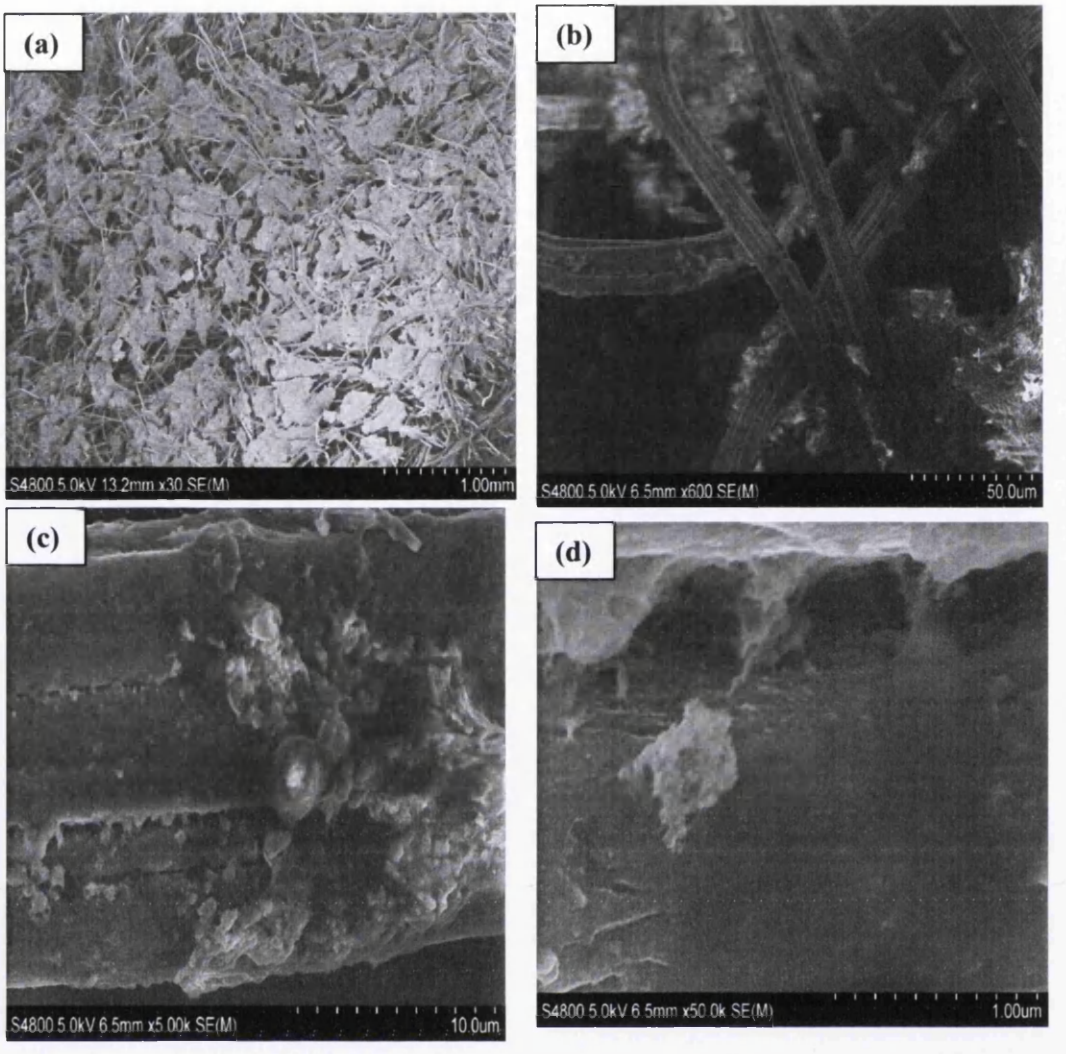

Figure 5-1: SEM images of bacterial biofilms on the surface of the anode GF electrode fibres, used during MFC evaluations, with different magnifications: (a) x30, (b) x600 (c) x5k and (d) x50k.

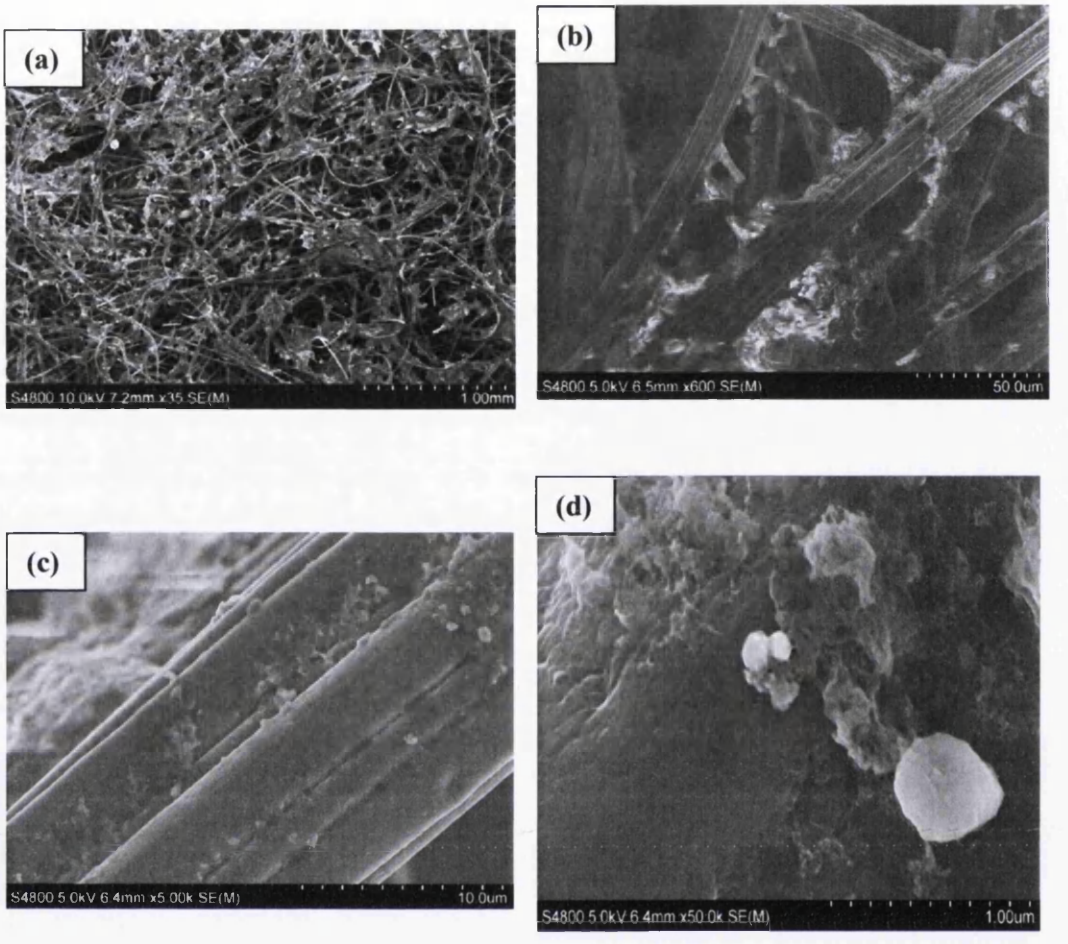

Figure 5-2: SEM images of bacterial biofilms on the surface of the cathode GF electrode fibres, used during MFC evaluations, with different magnifications: (a) x35, (b) x600 (c) x5k and (d) x50k.

TABLE 5-1: Biochemical tests and morphological characteristics of isolated denitrifying bacteria.

Isolation Number	A1	A2	A3	C1	C2	C3	C4	C5	C6	Bacteria isolated and tested in Chapter 3
Compartment	Anode	Anode	Anode	Cathode	Cathode	Cathode	Cathode	Cathode	Cathode	From soil
Growth in nutrient agar (NA) supplemented with nitrate	+	+	+	+	+	+	+	+	+	+
Growth in the acetate medium (AM) designed in Chapter 3	+	+	+	+	+	+	+	+	+	+
Colony colour and shape on (NA)	Orange	Beige	Beige	Beige	Beige	Bright and shiny beige	Bright and shiny beige	Orange	Beige	Beige
Colony colour and shape on (AM)	Orange	Bright and shiny beige	Dark beige	Orange	Dark beige	Beige	Beige	Dark beige	Dark beige	Beige
Gram stain	+	-	-	+	-	-	-	-	+	-
Cell shape	Rods	Coccus	Rods	Coccus	Rods	Rods	Rods	Rods	Coccus	Rods
Catalase test	+	+	+	+	+	+	+	+	+	+
Oxidase test	-	+	+	-	-	-	+	+	+	-
Nitrate reductase test	+	+	-	+	+	+	+	+	+	+
Gas production	-	+	-	+	+	+	-	-	-	+
Anaerobic growth	+	+	+	+	+	+	+	+	+	+
Aerobic growth	+	+	+	+	+	+	+	+	+	+
Growth in 25 °C	+	+	+	+	+	+	+	+	+	+
Growth in 37 °C	+	+	+	+	+	+	+	+	+	+

The catalase and oxidase tests examined the ability of bacteria to live in an aerobic lifestyle. The former test revealed that all isolated bacteria have catalase, and therefore are able to breakdown hydrogen peroxide. However, the latter test showed that some bacteria, such as A1, C1, C2 and C3, lack the ability to produce cytochrome oxidase, while the others (including A2, A3, C4, C5 and C6) gave positive results. The production of cytochrome oxidase or cytochrome catalase assumes that the bacterium is either an aerobic or facultative anaerobic. For more discrimination, the growth of all isolates was tested under strictly anaerobic and aerobic conditions, and the results confirmed that all bacteria are able to grow under

both conditions, but with different efficiencies. Therefore, the isolates were identified as facultative anaerobic bacteria. Furthermore, the nitrate test was performed, and the results showed a red colour after the addition of both reagents A and B when testing some bacteria, such as A1, C4, C5 and C6. This illustrates that these bacteria contain nitrate reductase enzyme, and therefore they have the ability to reduce nitrate to nitrite. However, some of the other bacteria (including A2, C1, C2 and C3) lacked the red colour after adding both reagents A and B, and also no colour was developed in the incubated medium after the addition of zinc powder. This observation indicates that these bacteria have not only reduced nitrate to nitrite, but have also reduced nitrite to nitrogenous gases. The latter were detected in Durham tubes. According to the results obtained so far the bacteria, including A1, A2, C1, C2, C3, C4, C5 and C6, were characterised as nitrate positive bacteria. However, only the isolates A2, C1, C2 and C3 were able to perform a complete denitrification. The isolate A3 was examined and the results showed a red colour after the addition of zinc powder, illustrating that A3 are nitrate-negative bacteria. Furthermore, the ability of the bacteria to grow at two different temperatures: 25° C and 37° C was studied, and the results showed that all isolates were able to grow at both temperatures. Finally, the bacteria were identified through the use of Bergey's manual of systematic bacteriology, according to the results obtained through the colonies morphology and biochemical tests. The isolates C2 and C3 were shown as straight rods, cells stain Gram negative, facultative anaerobic, oxidase negative and catalase positive, and therefore they were categorised as Enterobacteriaceae. The bacterium C1 was cells coccus, Gram positive, facultative anaerobic, oxidase negative and catalase positive, and therefore it was classified as Micrococcaceae. The isolate A2 was identified as Thiosphaera, since it was cocci cells, that are gram negative, facultative anaerobic,

oxidase positive and catalase positive. In addition, the results showed that denitrifying bacteria were not only found in the cathode biofilm, but also in the anode biofilm. This observation is coherent with previous work in the literature (Sukkasem et al. 2008).

5.3.2. MFC Performance with Cathodic Pure Culture

In this section, the capability of the isolated denitrifier bacteria to improve the performance of the MFC system proposed in Chapter Four was examined. One of the isolated denitrifier bacteria (C2) was selected and then injected back into the MFC system to enrich the cathodic chamber, and no improvement was observed in both nitrate reduction rate and power production. This is because the biofilm thickness inhibited the injected bacteria covering the outer surface of the biofilm from accepting electrons from the electrode. Furthermore, in order to investigate the ability of these isolated denitrifier bacteria to reduce nitrate and produce power in a pure culture, a new MFC system was operated with the injection of the selected denitrifier bacteria in the cathodic chamber. The anodic chamber was inoculated by a mixed bacteria isolated from the anode electrode biofilm, which was established over a period of 9 months with the feed of acetate. It was found that a pure culture produced current densities lower than or equal to those obtained using a mixed culture (Nevin *et al.* 2008). This was also realised in this study, as shown in Fig. 5.3. A maximum voltage of 12.4 mV was achieved, which accounted for 36% approximately of that produced by the mixed bacterial experiment. This result is in agreement with that demonstrated in Feng *et al.* (2009), where the maximum voltage obtained from isolated strains accounted for 45% to 55% of the mixed bacterial voltage. The nitrate reduction rate achieved was 56.2%, and this is almost 31% lower

than that obtained by the mixed bacterial experiment. The reduction in the voltage obtained and the nitrate removal rate is attributed to the lack of a number of synergistic interactions that occurred in the original mixed cultures.

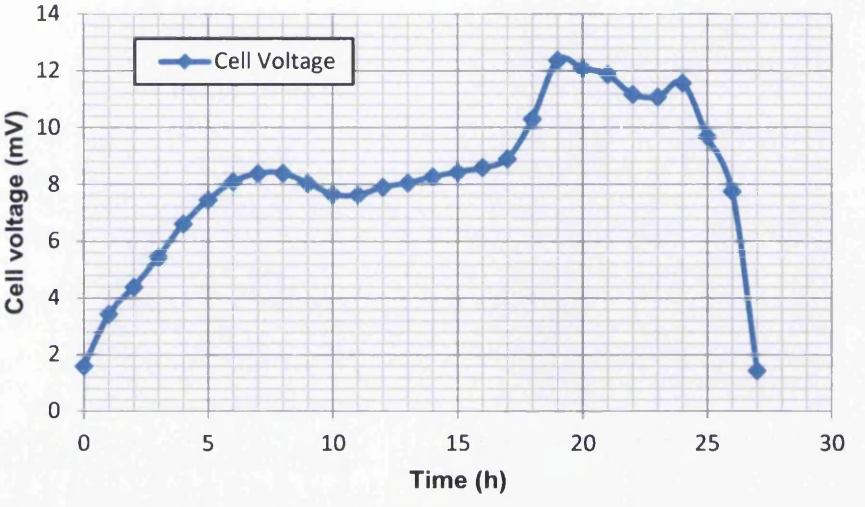

Figure 5-3: Current generation of an MFC with cathodic pure culture under 500 Ω.

5.3.3. Comparisons and Results Discussion

A medium prepared for denitrifiers must allow growth of a large number of denitrifiers that are as diverse as possible. Therefore, the composition of the growth media previously designed in Chapter Three for denitrifiers was chosen to support a wide range of bacteria. These compositions included sodium acetate, sodium nitrate, potassium dihydrogen orthophosphate, ammonium sulphate, yeast extract and agar. All the isolates were incubated in this medium in order to evaluate its ability to support bacterial growth. It was observed that all the isolates were able to grow in this medium (see Table 5.1). From the results of bacteria isolated and tested in this

chapter and Chapter Three, it can be concluded that the characterisation of the isolate C2 is similar to that of the bacteria isolated and tested in Chapter Three.

5.4. Summary

In this chapter, a number of bacteria were isolated from both the anode and cathode electrodes that were used in the MFC system operated and evaluated in Chapter Four. The isolates were tested through biochemical tests and their morphological characteristics identified. A diversity of nitrate reducing bacteria was observed throughout the test; however, just four isolates were shown to deliver complete denitrification. One of these four isolates, named in this study as C2, was realised to have characteristics similar to that of the bacteria isolated and tested in Chapter Three, and therefore it was selected for further investigation. The selected bacterium was re-inoculated back into the cathode chamber of the MFC (studied in Chapter Four) for enrichment, though no improvement was observed in both the nitrate reduction rate or power production. The ability of the chosen bacterium to reduce nitrate and produce power in a pure culture was also investigated. A maximum voltage of almost 36% of that produced by the mixed bacterial experiment was achieved, and this agreed with a previous study in the literature. This result demonstrated that the entire denitrification process might include activities contributed to by a number of different bacterial groups.

6. ELECTROCHEMICAL CHARACTERISATIONS AND CONDUCTIVITY MODIFICATIONS OF A GRAPHITE FELT ELECTRODE

6.1. Introduction

Carbon has attracted interest as an electrode material due to many advantages, including high electrical and thermal conductivities, chemical stability, wide potential range and low cost. Carbon based materials such as graphite felt (GF), carbon fibres and carbon cloth have been widely used as electrode materials for electrochemical properties due to their stability, high surface area and availability at a reasonable cost. GF electrodes have been attractive materials due to their interesting characteristics in applications, such as electrosynthesis and metal recovery. However, they have low electrochemical activity due to poor kinetics and reversibility that limit their use as active electrode materials. Therefore, great attention has been paid to the modification of such electrode materials in order to improve their electrochemical properties. The modification of the electrode surface area may also improve such aspects as bacterial adhesion, hence increasing the electron transfer from bacteria to the electrode surface. This chapter aims to investigate the electrochemical behaviours of a GF electrode using a cyclic voltammetry method, and to enhance the redox behaviours through the modification of the GF electrode surface with carbon nanomaterials, including single-wall carbon nano tubes (SWCNTs), graphitised carbon black (GCB), carbon nanofibres (CNFs) and graphitised carbon nanofibres (GCNFs). Among the nanomaterials used, GCNFs yielded the best electrochemical properties. Therefore, this was used to improve MFC performance, and a good improvement was observed.

6.2. Materials and Methods

6.2.1. Specific Geometric Surface Area (SGSA) of Graphite Felt Electrode

A graphite felt electrode (GFE) consists of fibres randomly dispersed with a large distributed void space between them. The dimensions of the GFE were measured using a ruler, and its fibres measured under an optical microscope using an ocular micrometer lens. The ocular lens contains a glass disk with fine divisions that are not numbered and is used to measure objects within its field of view (i.e., the total area visible through the microscope). The scale unites of the ocular lens decrease with the increase of magnification. Therefore, the calibration of the ocular micrometer was determined through the use of a stage micrometer. The latter is a microscope slide with a finely divided scale marked on the surface and is used to calibrate an optical system. The stage micrometer contains 10 divisions of 0.1 mm, forming a total length of 1 mm. The length of a single division on the ocular micrometer and consequently the length and diameter of the carbon fibres were determined as follows:

1. Magnification of 10X was selected, and the stage micrometer was placed on the microscope stage.
2. The scale of the ocular lens was superimposed over that of the stage micrometer.

   The length in millimeters (mm) of a single division on the ocular micrometer was calculated by dividing the length (in mm) - covered in the stage micrometer - by the number of divisions on the ocular lens. The full length of the ocular scale covered 10 divisions of the stage micrometer, resulting in an

equivalent total length of (10 × 0.1 mm) = 1 mm long. The ocular scale of 1 mm long contains 100 divisions, and therefore each division equals 0.01 mm.

3. The stage micrometer was removed, and the slide with carbon fibres on the top was placed on the microscope stage under the same magnification. Based on the division space determined in step 2, the lengths and diameters of one hundred fibres were calculated and then used to determine the average dimensions (i.e., the average length and diameter) of the fibre. For example, a fibre covering 50 divisions long and 2 divisions width of the ocular scale corresponds to a total length of 50 × 0.01 = 0.5 mm and a diameter of 2 × 0.01 = 0.02 mm.

The apparent density of the GFE (δ_E) was calculated by dividing the weight of the electrode by its volume. The specific geometric surface area (SGSA) of the GFE can be derived from the surface area of the fibre (S_F) and the volume of the GFE (V_E) according to (Shut and Chung 1996)

$$SGSA = S_F/V_E. \tag{6.1}$$

The GFE has a shape of rectangular prism, and therefore its volume V_E can be calculated as

$$V_E = LWH, \tag{6.2}$$

where L, W and H are the length, width and height of the GFE respectively.

Given that,

$$V_F/V_E = \delta_E/\delta_F, \tag{6.3}$$

where V_F is the volume of the fibre, δ_E is the electrode apparent density and δ_F is the density of the fibre.

Substituting equation (6.3) into equation (6.1), the SGSA can be given as

$$SGSA = (\delta_E/\delta_F)(S_F/V_F). \quad (6.4)$$

The fibre has a cylindrical shape of length ($\mathcal{L}$) and radius (r), and therefore its surface area (S_F) and volume (V_F) can be calculated by

$$S_F = 2\pi r\mathcal{L}. \quad (6.5)$$

$$V_F = \pi r^2\mathcal{L}. \quad (6.6)$$

Substituting equations (6.5) and (6.6) into equation (6.4), the SGSA can be given as

$$SGSA = (\delta_E/\delta_F)(2/r). \quad (6.7)$$

6.2.2. Cyclic Voltammetry of Graphite Felt Electrode

This section aims to investigate the electrochemical performance of a GFE using cyclic voltammetry (CV) experiments. The electrochemical experiments were conducted using (EC Epsilon) and a three electrode arrangement. The three electrodes comprised of a working electrode (WE) at which the redox reaction takes place, a reference electrode (RE) through which no current flows and a counter electrode (CE) (an auxiliary electrode) which completes the circuit. The working electrode was graphite felt, the auxiliary electrode was platinum (Pt) and the reference electrode was a Silver/Silver Chloride electrode (Ag/AgCl). These electrodes are connected to a potentiostat that provides the desired potential. The potentiostat was linked up with a personal computer controlled Electro-Chemical application that was used for collecting and calculating the data. The electrochemical experiments were carried out in a one compartment electrochemical cell with a volume of about 25 ml at room temperature and in an oxygen free environment (by bubbling nitrogen through the solution). The electrolyte used in the electrochemical

experiments was 1 mM methyl viologen (MV^{+2}) in a 0.1 M phosphate buffer solution (PBS), which was composed of a mixture of KH_2PO_4 and K_2HPO_4 and with a pH of 7. The methyl viologen (MV^{+2}) has been considered as the simplest redox system in which MV^{+2} reduced to the relatively stable cation radical MV^{+} (Alehashem *et al.* 1995, Steckhan and Kuwana 1974). The MV^{+} is relatively stable in oxygen free solutions, resulting in a deep blue colour, which is evidence of the formation of MV^{+} in the solution, in contrast to the colourless MV^{+2} (Kosower and Cotter 1964, van Dam and Ponjee 1974). The methyl viologen can act as a good electron transfer mediator for a biological system (Steckhan and Kuwana 1974) and can also be electroreduced on a surface of various electrodes (Lilienthal and Smith 1995, Yang and McCreery 1999). Furthermore, the effect of the pH value on electrochemical behaviour was investigated through the use of a range of pH values from 4 to 8, in steps of 1. The interaction between the concentration and the peak current obtained were also studied, where methyl viologen concentrations of 0.25 mM, 0.5 mM, 1 mM, 2.5 mM and 5 mM were used. Moreover, the effect of the PBS concentration was studied, and PBS concentrations of 0.2 M, 0.1 M, 0.05 M, 0.01 M, 0.005 M and 0.001 M were used. In addition, in order to study the correlation between the redox mechanism and the surface area used, the graphite (carbon) felt electrode was cut into multiple pieces with different surface areas: (3mm × 2mm × 1mm), (4mm × 3mm × 2mm), (4mm × 4mm × 2mm), (7mm × 3mm × 2mm), (5mm × 5mm × 2mm) and (5mm × 6mm × 2mm). The electrochemical experiments were performed as follows:

1. A solution of 0.1 M phosphate buffer in 25 ml distilled water of pH 7 was prepared, and a 1 mM methyl viologen (MV^{+2}) concentration was then made in the 0.1 M phosphate buffer solution (i.e., using the phosphate buffer

solution as diluents). The resultant solution was poured into an electrochemical cell with a volume of about 25 ml.

2. The three electrodes were carefully connected to an external cell box in the faraday cage and were then fitted into the electrochemical cell, by making sure that all electrodes were submerged but not touching the cell bottom.
3. The computer programme was set to the following conditions: an initial potential (IP) of -200 mV, a final potential (FP) of -200 mV, a switching potential (SP) of -900 mV, and a scan rate (SR) of 20, 50, 100, 200 or 250 mVs^{-1} at room temperature.
4. The solution in the cell was purged with nitrogen for 2 min, while stirring through the use of a small magnetic stirrer to achieve anoxic conditions.
5. The experiment was run and a voltammogram was taken.
6. Steps 1 to 5 were repeated with different pH values of 4, 5, 6 and 8.
7. Steps 1 to 5 were repeated with different methyl viologen concentrations of 0.25 mM, 0.5 mM, 2.5 mM and 5 mM, while using a pH value of 7.
8. Steps 1 to 5 were repeated with different phosphate buffer concentrations of 0.2 M, 0.05 M, 0.01 M, 0.005 M and 0.001 M, while using a 1 mM methyl viologen concentration and adjusting the pH value to 7 in all the phosphate buffer concentrations.
9. Steps 1 to 5 were repeated with different surface areas of the graphite (carbon) felt electrode. All the pieces of the graphite (carbon) felt electrodes were washed with distilled water before being used.

6.2.3. Cyclic Voltammetry of the Graphite Felt Modified Electrode

Graphite felt has a large specific surface area and good stability (Li *et al.* 2006). However, it has a lower electrochemical activity that leads to a limited voltage efficiency and a lower power density, compared to the other materials used in the MFC system. It has been reported that the electrochemical activity of the GF can be improved by treating the GF with concentrated sulphuric acid (Sun and Skyllas-Kazacos 1991). Alternative novel modification techniques were also developed to enhance the GF electrochemical activity material, as shown in Sun and Skyllas-Kazacos (1992). This work aims to improve the electrochemical activity of the GF electrode through the use of carbon nanomaterials. The electrochemical behaviours of a GF electrode modified with different carbon nanomaterials were evaluated via cyclic voltammetry. The carbon electrode surface area can be enlarged by dispersing the carbon nanomaterials on the surface of the electrode to form a randomly dispersed array of high surface area. Furthermore, it has been demonstrated that carbon nanomaterials have the ability to facilitate the electron transfer process during the electroreduction and electrooxidation of electroactive species such as NADH and hydrogen peroxide (Hrapovic *et al.* 2003, Wang and Musameh 2003), and during the enzyme-substrate interaction (Gooding *et al.* 2003). Additionally, the porous structure of the carbon nanomaterials can give the electrode better wetting properties (Nugent *et al.* 2001). This can allow the analyte to diffuse into the carbon nanomaterial bundles with lower friction (Verweij *et al.* 2007). Four types of carbon nanomaterials were used in this study to modify the GF electrode. These carbon nanomaterials include single-walled carbon nanotubes (SWCNTs), graphitised carbon black (GCB), carbon nanofibres (CNFs) and graphitised carbon nanofibres

(GCNFs). The electrochemical performance of the modified GF electrodes was investigated and evaluated through cyclic voltammetry. The experiments were performed as follows:

1. The tests were performed in 1 mM methyl viologen (MV^{+2}) in a 0.1 M phosphate buffer solution of pH 7 at a room temperature.
2. Four graphite felt electrodes were cut into a similar size of 4 mm × 4 mm × 2 mm and washed with distilled water before treating.
3. Suspensions of carbon nanomaterials were prepared by mixing 0.7 mg of each nanomaterial with 700 µL of N,N.Dimethylformamide (DMF) as the dispersing agent and agitating the mixture using a sonicating tip (Ultrasonic processor, Sonics Vibra Cell) for 1 h. Close to 10 µL of the resultant solution (i.e., the nanomaterial and DMF solution) were dropped directly onto the GF electrode surface and were allowed to dry at 40° C for 45 min to evaporate the solvent.
4. The electrodes were tested following steps 1 to 5 described in the procedure given in Section 6.2.2.

6.2.4. MFC performance using modified electrodes

In contrast to the microbial fuel cell studied and evaluated in Chapter Four with both anode and cathode graphite felt electrodes, in this section a two compartment MFC reactor was established, as previously described in Chapter Four, with the exception of using the new GF electrodes modified with GCNFs in both chambers. In this modified MFC system, the cathode and anode compartments were inoculated with the bacterial suspension isolated from the previous MFC cathode and anode biofilms

respectively. Both compartments were kept anoxic by purging with nitrogen gas. The modified MFC system was enriched for a period of three months. The voltage across an external resistance of 500 Ω was measured every hour using a digital multimeter connected to a personal computer through a data acquisition system. The current and power were calculated using equations (2.21) and (2.22) respectively.

6.3. Results and Discussion

6.3.1. Determination of Specific Geometric Surface Area (SGSA) of Graphite Felt Electrode

SEM photographs of the GF electrode were taken at various magnifications in order to study the structural properties of the GF. The SEM images displayed in Fig. 6.1 show randomly dispersed cylindrical fibres, and each fibre composes of a group of thinner fibres. An electrode (with dimensions of length × width × height = 4 cm × 0.5 cm × 4 cm) was used, and therefore its apparent density δ_E was calculated by dividing its weight of 0.71 g by its volume of 8 cm^3. One hundred samples of fibres were taken and their dimensions measured, as shown in Fig. 6.2. According to the results obtained, it was assumed that the electrode comprises cylindrical fibres of 1mm length and 0.01 mm diameter. The number of fibres contained in an electrode can be calculated by dividing the volume of the electrode by the volume of the fibre. With the assumption of a cylindrical fibre having a length of 1mm and a diameter of 0.01 mm, the volume of the fibre was calculated using equation (6.6) as 7.85×10^{-5} mm^3. Consequently, an electrode of 8 cm^3 volume has 101910828 fibres approximately, where each has a weight of 7×10^{-9} g. The latter was calculated by

dividing the mass of the GF electrode by the number of fibres. Given the weight and volume of the fibre, its density (δ_F) was calculated as 8.92×10^{-5} g/mm^3. Finally, the SGSA of the fibre based porous carbon was calculated using equation (6.7) as about 4004.5 cm^2/cm^3.

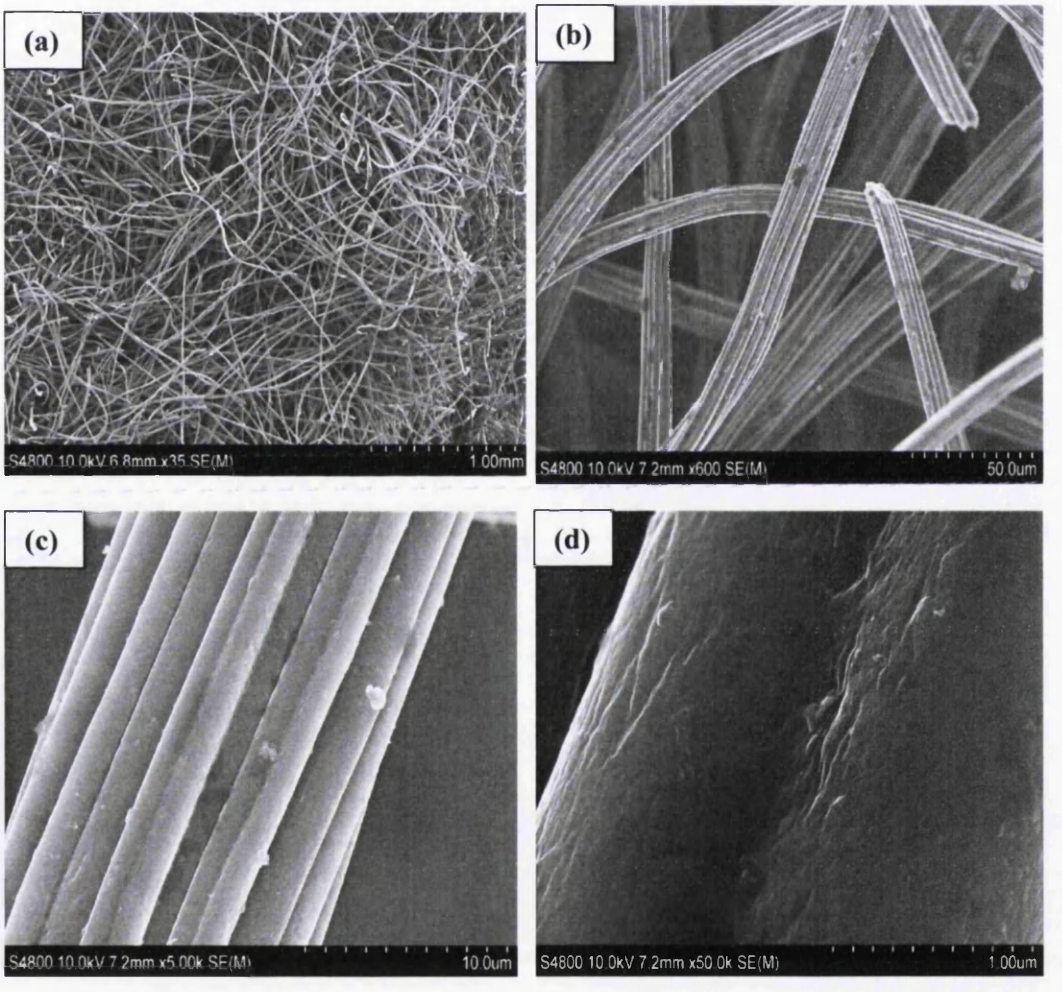

Figure 6-1: SEM micrographs of GF electrode fibres at different magnifications: (a) x35, (b) x600, (c) x5k and (d) x50k.

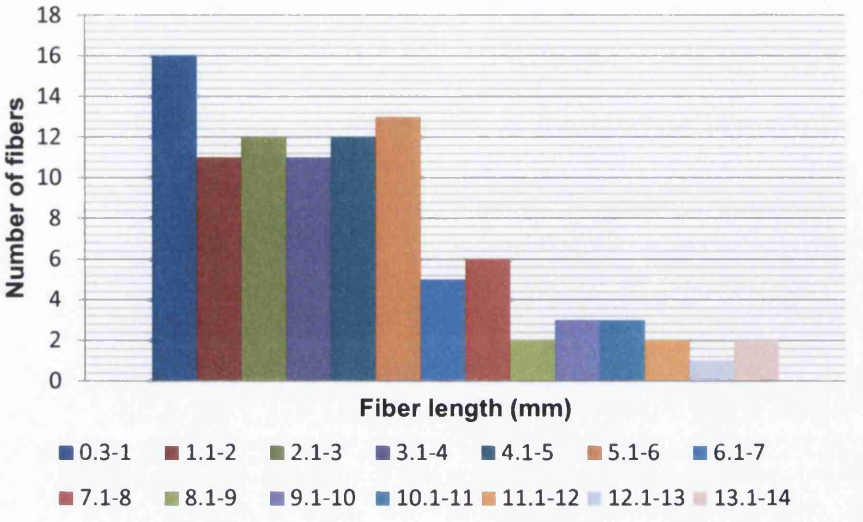

Figure 6-2: Lengths of different fibres

6.3.2. Electrochemical Performance of the Graphite Felt Electrode: Investigation and Enhancement

Cyclic voltammograms can give information about the current and potential behaviour of an electrode in an aqueous solution. However, they may be different for the same system, depending on the electrode's properties, scan rates, electrolyte pH and concentrations used. In this section, an investigation of the electrochemical behaviour of both modified and unmodified GF electrodes through the use of cyclic voltammetry techniques was carried out.

6.3.2.1. Cyclic Voltammetry of the Unmodified Graphite Felt Electrode

In order to investigate the electrochemical properties of the unmodified GF electrode, cyclic voltammetry was used to examine the reduction of 1 mM methyl viologen in 0.1 M of phosphate buffer solution at pH 7 on the surface of the unmodified GF

electrode. A graphite felt working electrode of 4 mm × 4 mm × 2 mm surface area was used. The experimental conditions were fixed at an initial potential (IP) of -200 mV, final potential (FP) of -200 mV and switching potential (SP) of -900 mV at room temperature. The electrochemical behaviour of the unmodified GF electrode was examined at various scan rates (SRs), and the cyclic voltammograms obtained are displayed in Figs 6.3 (a) and (b). The magnitude of the anodic and cathodic peaks current $I_{Pa}^{\leftarrow}$ and $I_{Pc}^{\rightarrow}$, and their associated peak potentials, $E_{Pa}^{\leftarrow}$ and $E_{Pc}^{\rightarrow}$ respectively, are very important parameters in cyclic voltammetry. On the forward scan, the potential was scanned in a negative direction, and the cathodic current was produced due to the electrode process, where the potential is sufficiently negative to reduce MV^{+2}. The cathodic current rose until the concentration of MV^{+2} at the working electrode surface was depleted, and the cathodic peak current appeared. The cathodic current then declined with time. The cathodic peak current obtained at a scan rate of 20 mVs^{-1} was 0.47 mA. Furthermore, the scan direction was switched to positive at -900 mV to establish the reverse scan. The anodic current was produced when the electrode became a sufficiently strong oxidant to oxidise the MV^{+} at the electrode surface. It rapidly increased until the concentration of MV^{+} at the electrode surface was diminished, causing a decline in the anodic current with time, which resulted in an anodic peak current of 0.39 mA. The ratio of the anodic and cathodic peaks current was just lower than unity. This is because some of the reduced species could not be re-oxidised on the time scale of a cyclic voltammetric experiment during the reverse direction. These reduced species were produced in the forward reduction process and diffused into the bulk solution due to the difference in concentrations, which derived the reduced species away from the electrode.

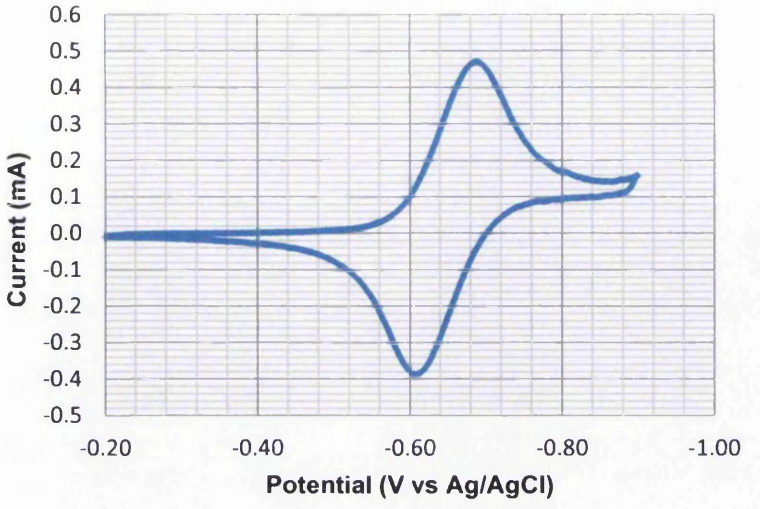

(a)

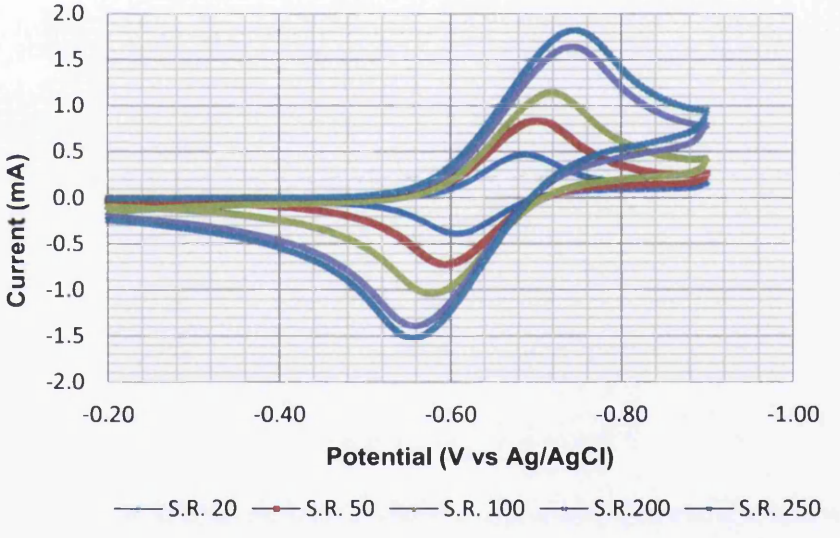

(b)

Figure 6-3: Cyclic voltammograms of 1 mM MV^{+2} in a 0.1 M phosphate buffer solution (pH 7.0) (a) at a scan rate of 20 mVs^{-1} (b) at scan rates of 20, 50, 100, 200 and 250 mVs^{-1}.

A linear relationship of the peak currents with respect to the square root of the scan rate $(\nu_s)^{1/2}$ was also observed, as shown in Fig 6.4. This indicated that the electrode

reaction of MV in the bulk was controlled by diffusion (mass transfer). The formal standard potential (i.e., the midpoint potential) can be calculated as

$$E^{o'} = \frac{E_{Pa}^{\leftarrow} + E_{Pc}^{\rightarrow}}{2}. \quad (6.8)$$

In our experiment at a scan rate of 20 mVs^{-1}, the midpoint potential was -0.65 V and the peak potentials separation ΔE_p (calculated using equation (2.45) was 80 mV. The ΔE_p exhibited an increase with the increase of the scan rate, suggesting that the GF electrode reaction was a quasi-reversible electron transfer process.

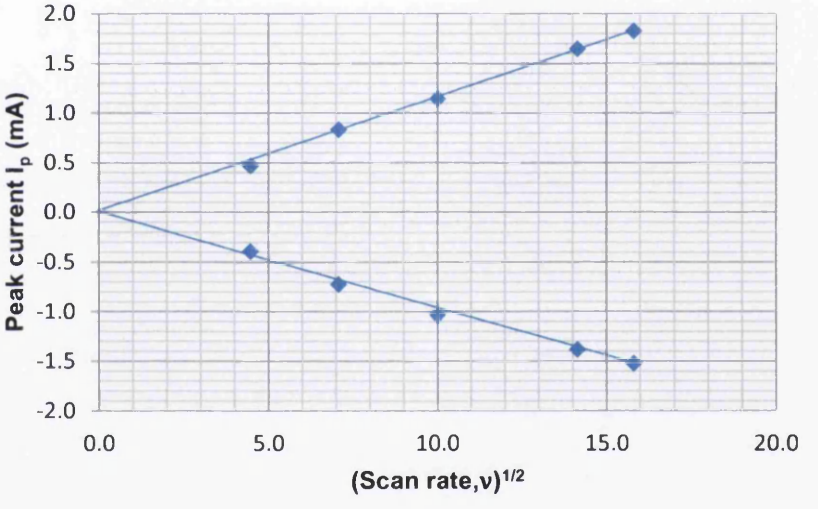

Figure 6-4: The peak current I_p of both forward and reverse waves as a function of $(\boldsymbol{\nu_s})^{1/2}$.

In addition, 30 circles of cyclic voltammograms for 1 mM methyl viologen in 0.1 M phosphate buffer solution at pH 7 at a scan rate of 20 mVs^{-1} on the unmodified GF electrode were performed. The results showed a slight decrease in the peak current and peak potential, illustrating a good stability of the graphite felt electrode. The effect of the pH value of the bulk solution on the electrochemical behaviour of the

unmodified GF electrode was also investigated, and the results are shown in Fig 6.5. The results showed a gradual increase in both peak cathodic and anodic currents when the pH value increased from 4 to 7 in steps of 1. However, a slight increase in the peak potentials separation was induced. Increasing the pH value up to 8 caused a drop in the redox peak current, compared to those obtained at pH 7. It was clearly seen that the maximum reduction and oxidation peak currents were obtained at pH 7, due to the highest dissociative ability of methyl viologen on the GF electrode surface, hence increasing the rate of electron transfer. Moreover, the effect of the working electrode surface area on the redox mechanism was studied, and the results revealed an increase in the peak current with increases in the surface area, as shown in Fig 6.6.

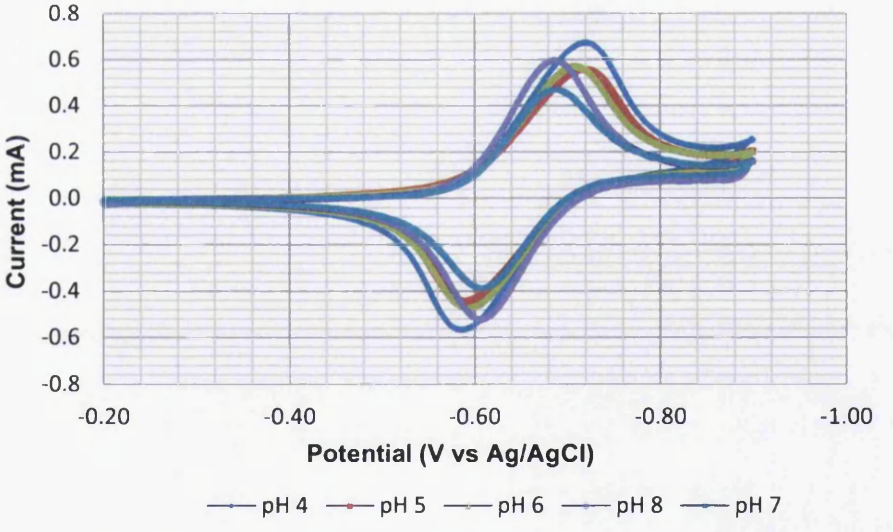

Figure 6-5: Cyclic voltammograms of 1 mM MV^{+2} in 0.1 M phosphate buffer on GFE at different pH values: 4, 5, 6, 7 and 8. Scan rate is 20 mVs^{-1}.

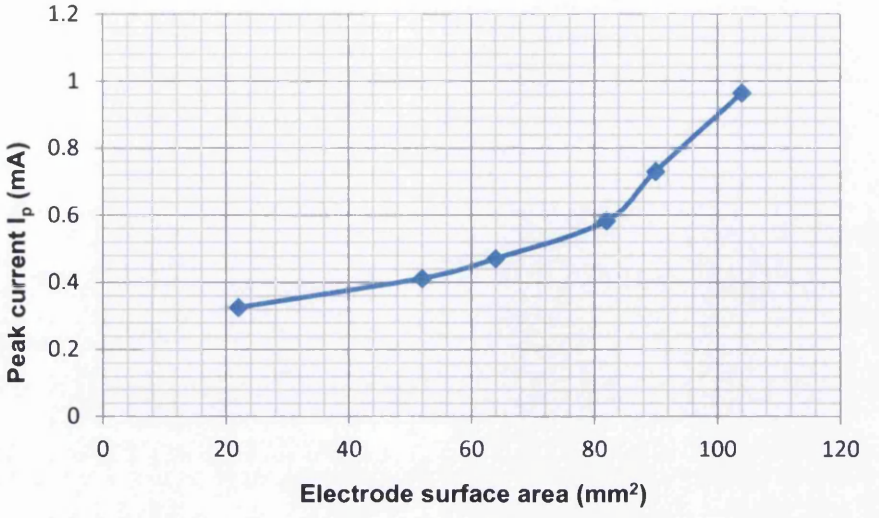

Figure 6-6: Peak current values of 1 mM methyl viologen in 0.1 M phosphate buffer on GFE with different surface areas using a scan rate of 20 mVs^{-1}.

The impact of the concentrations of both methyl viologen and the phosphate buffer on the electrochemical behaviour of the GF electrode was also investigated, and the results shown in Fig 6.7 and Fig 6.8 respectively.

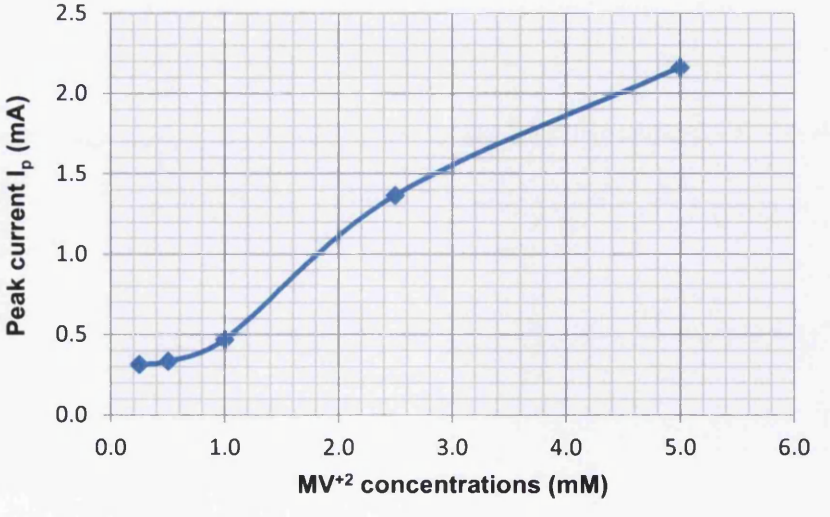

Figure 6-7: Concentration dependence of I_p of methyl viologen in a 0.1 M phosphate buffer (pH 7) using a scan rate of 20 mVs^{-1}.

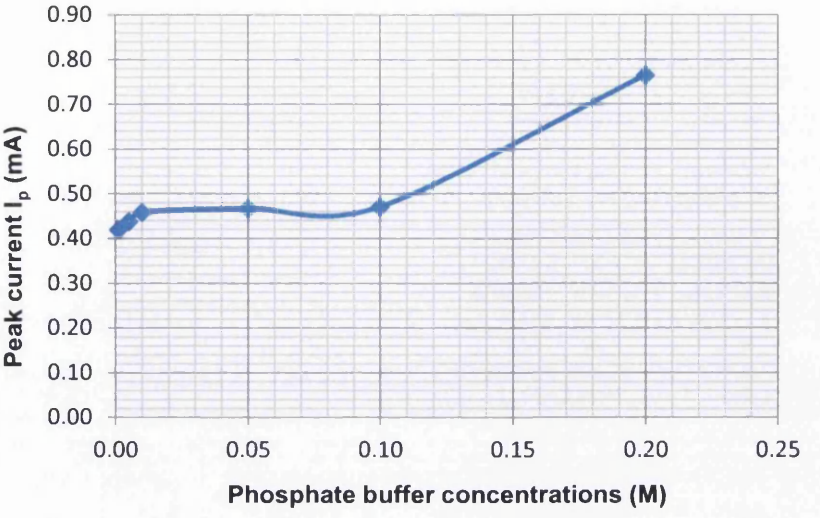

Figure 6-8: Peak current I_p in different phosphate buffer concentrations (pH 7) using a scan rate of 20 mVs^{-1}.

A significant increase in the peak current of almost 1.84 mA was achieved when the methyl viologen concentration was increased from 0.25 mM to 5 mM. It was also manifest that increasing the phosphate buffer concentration from 0.001 M to 0.1 M allowed a slight increase in the peak current of about 0.05 mA. However, a considerable increase of 0.3 mA approximately was obtained when the phosphate buffer concentration was further increased by 0.1 M.

6.3.2.2. Cyclic Voltammetry of a Modified Graphite Felt Electrode with Carbon Nanomaterials

The electrochemical behaviour of a modified GF was investigated by using cyclic voltammetry. The GF electrode was modified with carbon nanomaterials, including SWCNTs, GCB, CNFs and GCNFs, which are promising materials that can provide great stability and high conductivity. Cyclic voltammograms of methyl viologen redox reactions on different modified GF electrodes were recorded and compared in

Fig. 6.9. A comparison of the kinetic methyl viologen redox reactions on the unmodified GF electrode was also considered. The results indicated an improvement in the electrochemical activity of the methyl viologen on the modified electrodes compared to the unmodified electrode. This led to a significant increase in the redox peak current, as shown in Fig 6.10. An electrode modified with graphitised carbon nanofibres (GCNFs) achieved the best electrochemical performance among the other modified electrodes, due to the largest surface area provided. The maximum I_p obtained with GCNFs modified electrode was 0.778 mA. Therefore, this electrode (the GCNFs modified electrode) was selected for further investigation.

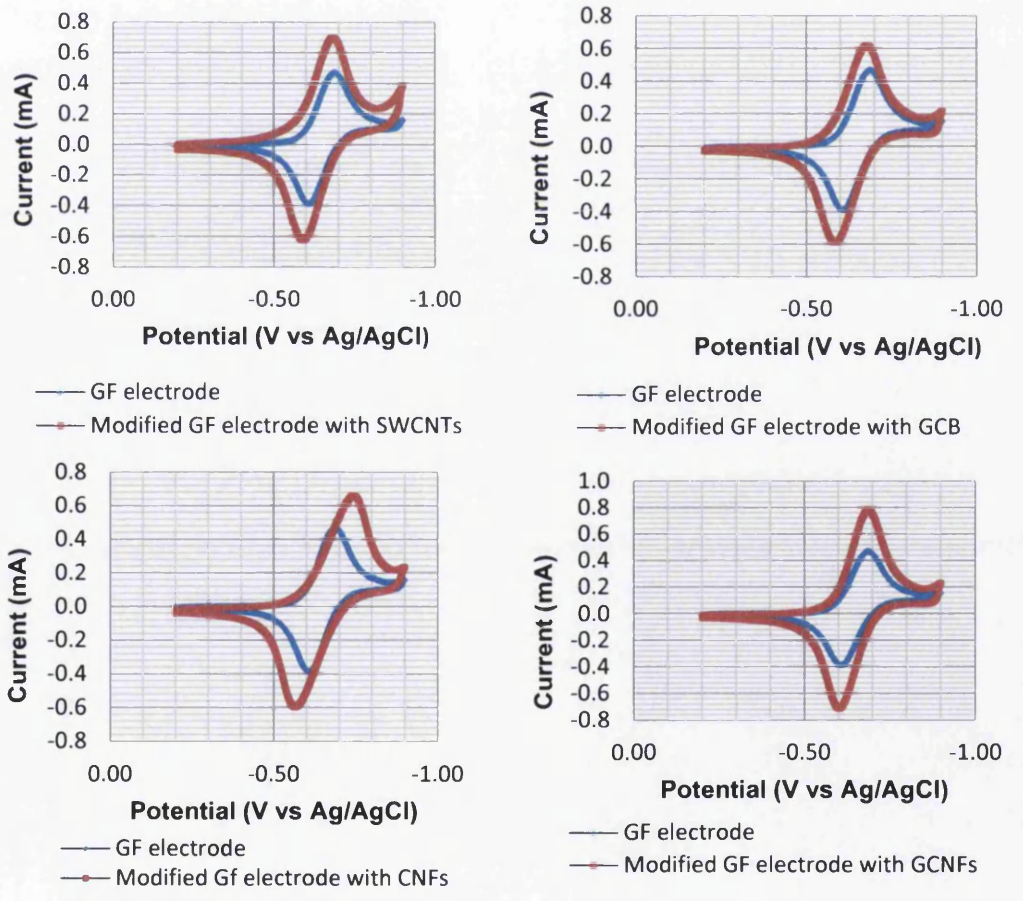

Figure 6-9: Cyclic voltammograms of 1 mM MV^{+2} in a 0.1 M phosphate buffer solution (pH 7.0) on unmodified GFE and modified GFE with SWCNTs, GCB, CNFs and GCNFs using a scan rate of 20 mVs^{-1}.

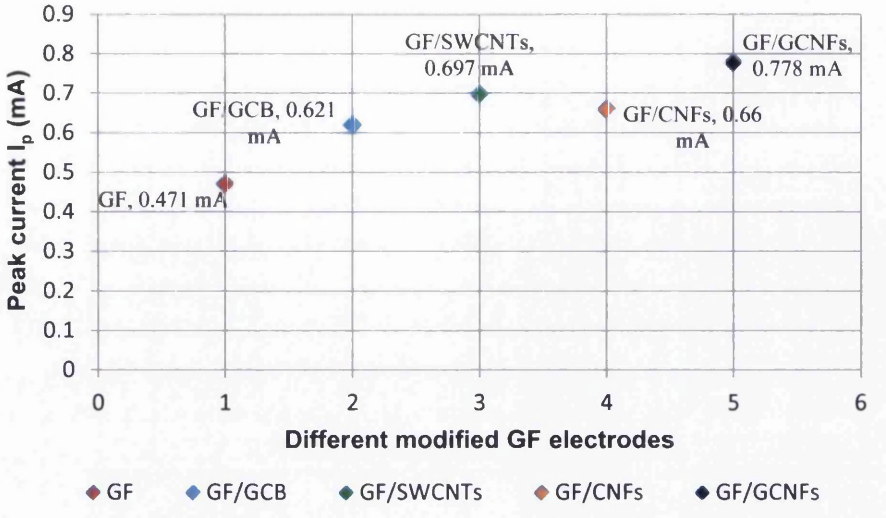

Figure 6-10: Peak current values of 1 mM methyl viologen in 0.1 M phosphate buffer on GFE and GFE modified with different nano-materials using a scan rate of 20 mVs^{-1}.

The ratio of the redox peak current was 0.92 mA, which is higher than that achieved with the unmodified electrode (0.822 mA). However, the peak potential separation obtained with both GCNFs modified and unmodified electrodes was almost the same (85 mA). In order to evaluate the long term stability of the GCNFs modified electrode, cyclic voltammetry experiments were performed at three different scan rates: 20, 50 and 100 mVs^{-1}, and 30 cycles were recorded at each scan. Very small changes were observed in both peak potentials and currents. These observations confirmed that the GCNFs modified electrode has an excellent long term stability to promote the reactions of methyl viologen. In order to check the presence of the carbon nanomaterials on the surface of the GF electrode, a number of scanning electron microscopy (SEM) micrographs were obtained (using an Hitachi S-4800 SEM). The micrographs displayed in Fig. 6.11 showed a random dispersal of the carbon nanomaterials on the surface of the GF electrode.

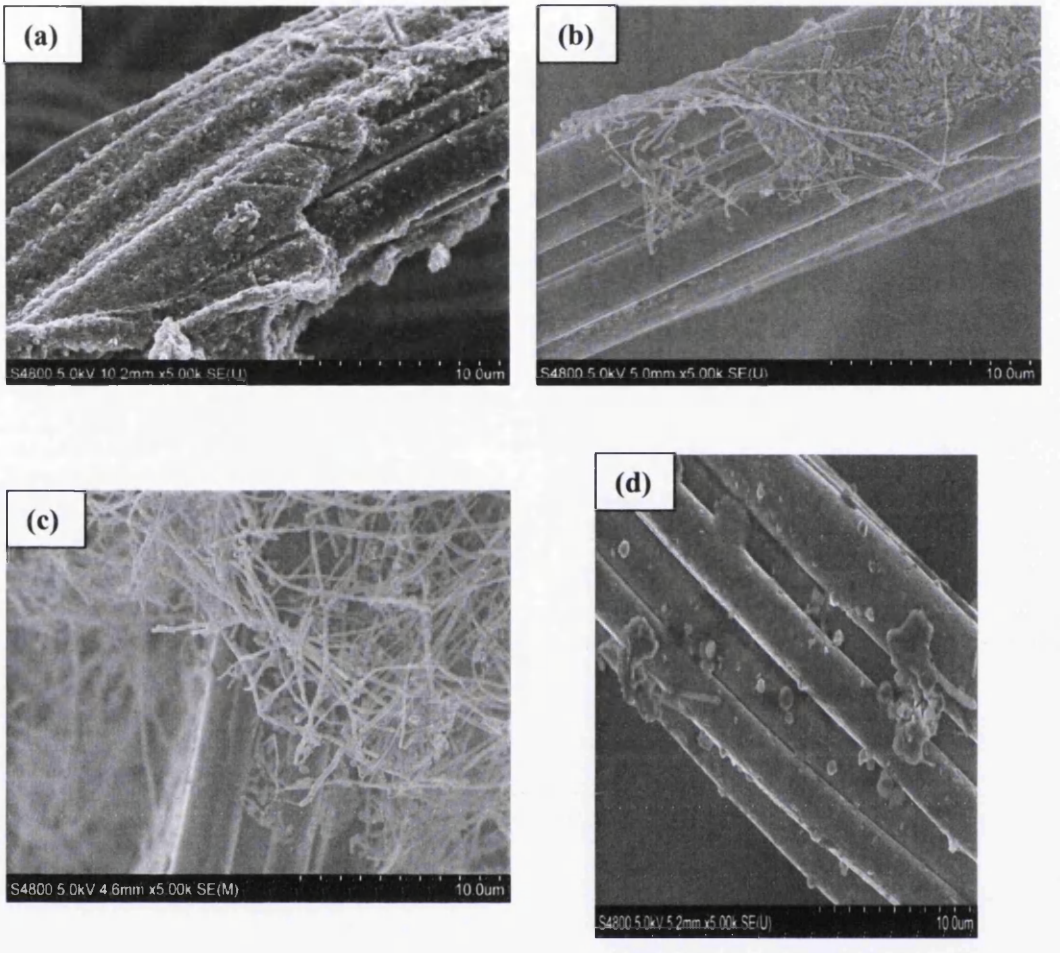

Figure 6-11: SEM images of GF electrode fibres modified with (a) SWCNTs, (b) CNFs, (c) GCNFs and (d) GCB.

6.3.3. MFC Performance with Modified GF Electrodes

The interaction between the bacterial biofilm and the electrode surface area can affect the MFC's performance. The reactants transport, including substrate, electrons and electron accepting species from the bulk to the electrode surface, and the reaction kinetics on the electrodes surfaces can also influence the MFC's performance. The reaction kinetics on the electrode surface and the mass transfer are

affected by the electrode materials (Logan 2008), surface chemical properties of the electrodes (Debabov 2008), size and shape of the electrodes (Aelterman *et al.* 2008) and biofilm condition (Cheng *et al.* 2008). The electrode should provide a good environment for the bacteria to attach to and transport electrons, a large surface area and a high conductivity (Logan 2008). The internal resistance of an MFC consists of two parts, including non-ohmic and ohmic resistances (Fan *et al.* 2008). The former comprises a charge transfer resistance and a diffusion resistance (Larminie and Dicks 2000), and these can be reduced by increasing the electrode surface area, as well as selecting electrodes with good catalytic abilities. Ohmic resistance can be decreased by arranging the electrodes closely, using solutions with high conductivity and using a membrane with low resistivity.

Modification of the GF electrode surface to enhance its reaction kinetics and mass transfer is a good way to improve the MFC's performance. The GF electrode modified with GCNFs yielded the best electrochemical performance and provided the largest surface area compared to the other modified GF electrodes (as shown in the previous section), and therefore it was chosen to enhance the MFC's performance. In an MFC reactor, both anode and cathode were provided by GCNFs modified electrodes. A modified MFC system was enriched following the procedures described in Section 4.2.2 for three months. The maximum voltage obtained using 2 mM (169.5 mg/L) sodium acetate into the anodic chamber and 8.4 mM (847.9 mg/L) potassium nitrate into cathodic chambers was 40.94 mV, as shown in Fig. 6.12. The total amount of nitrate removed was almost 95.3% (495.46 mg/L). The SEM images of the bacterial biofilms, attached to the cathodic GCNFs modified GF electrode, are given in Fig. 6.13.

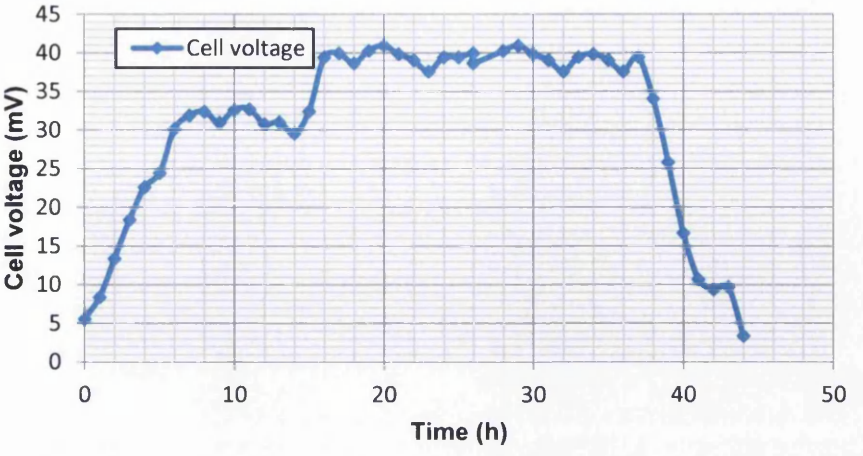

Figure 6-12: Current generation of an MFC with a modified GF electrode under 500 Ω.

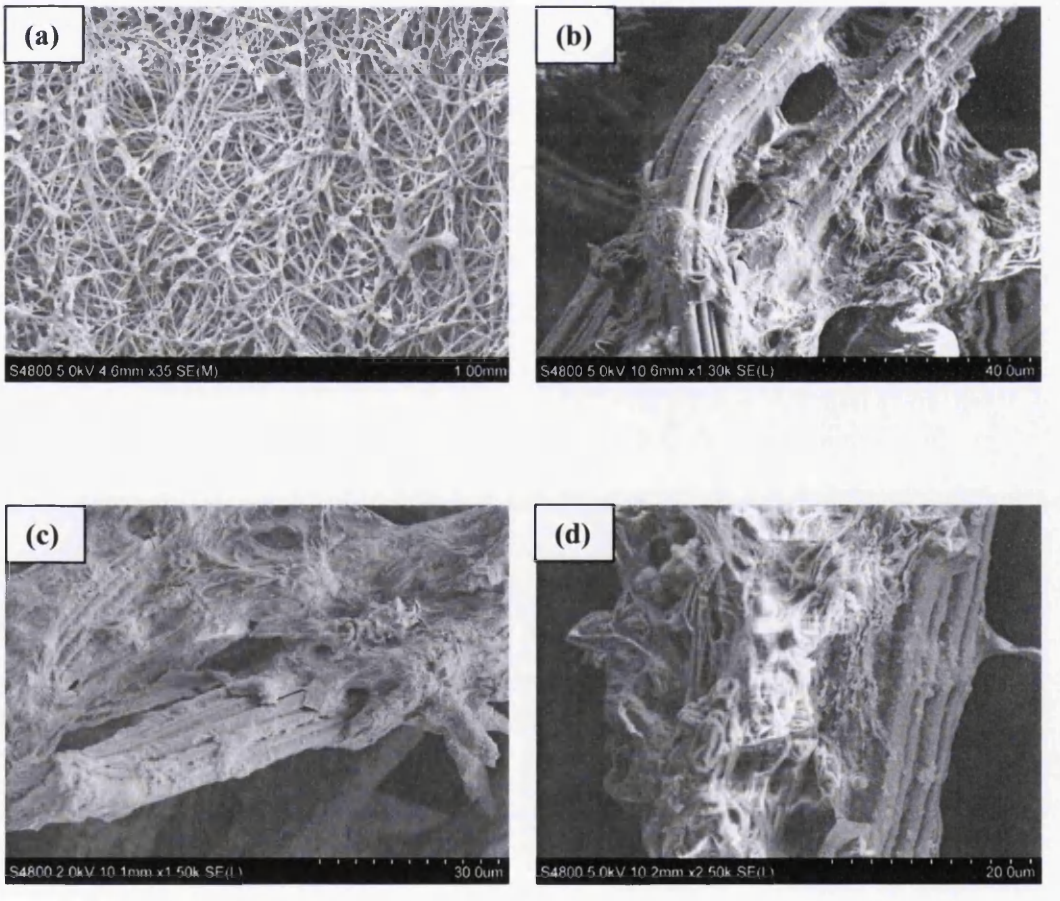

Figure 6-13: SEM micrographs of the biofilms attached to the GCNFs modified cathodic GF electrode fibres, used during the MFC evaluations, at different magnifications: (a) x35, (b) x1.30k, (c) x1.50k and (d) x2.50k.

6.4. Summary

This chapter reported in detail on the redox behaviours of carbon nanomaterials randomly dispersed on graphite felt electrode surfaces. Four nanomaterials, SWCNTs, GCB, CNFs and GCNFs, were used in this study. A cyclic voltammetry technique was used to facilitate the investigation of the redox behaviours. Comparison of the electrochemical properties associated with the unmodified GF electrode was also considered. Experiment results showed the great electrochemical and mechanical advantages of the modified electrodes compared to unmodified electrodes. The GCNFs modified electrode exhibited the best electrochemical activity among the other modified electrodes, due to its having the largest surface area, which greatly increased the rate of electron transfer. Furthermore, an MFC system employing GCNFs modified electrodes was used, and its performance evaluated in terms of power generation and nitrate removal. The results demonstrated that the GCNFs modified MFC system offered about 8% nitrate reduction rate higher than that achieved using unmodified electrodes (the unmodified MFC system removed 87.5% of the nitrate). This is due to the long term stability provided by the GCNFs modified MFC system, where an average of 35 mV was obtained over a period of 44 h.

7. CONCLUSIONS

Nitrogen and nitrate have important environmental impact and there are many problems associated with its release into the environment. Nitrate can be removed from water through the use of physico-chemical methods. However, these processes are not viable and their use is problematic. An alternative promising and versatile approach that can be used for nitrate removal is biological denitrification. However a major drawback is the potential bacterial contamination of treated water, thus the potential need for additional filtration and disinfection to meet current drinking water standards.

The stated aims and objectives of this thesis were to investigate the electrochemical removal of nitrate from water and associated technical problems. The results of the work show that these aims were successfully achieved setting a good platform for future work in this area. The specific outcomes of the work are discussed in the previous chapters, but specific aspects noteworthy of further comment are discussed in the following sections.

7.1. Investigation of Organism Isolated by Traditional Enrichment Processes

Two cultivation media with different carbon sources, including sodium formate and sodium acetate, were designed to allow promotion of high denitrification rates (Chapter Three). Medium optimisation was investigated through studying the complex interactions between medium parameters and their effects on the bacterial growth rates. The results revealed that acetate can be easily converted by bacterial cells and supported good growth (Chapter Three). These bacteria are

electrochemically active and their propagation on acetate provides a good method for generating inocula for MFCs.

7.2. Enrichment Using Electrochemical Methods

In order to perform biological nitrate removal, a mediatorless H-shaped MFC was constructed using bacteria both in the anode and cathode. A mixed bacterial culture in the cathode performed denitrification through the use of electrons supplied by a mixed bacterial culture oxidising acetate in the anode. This configuration represents an anodic (oxidative) reaction in water heavy contaminated with organics, while the reduction of nitrate is carried in relative clean environment, so avoiding the addition of organic matter required of conventional denitrification systems.

The MFC's performance was examined under closed and open circuit conditions (Chapter Four). The results indicated that higher nitrate reduction rates were obtained in the closed circuit MFC compared to that achieved under open circuit conditions. The effects of acetate/nitrate on current generation and nitrate removal, and the denitrification activity as a function of external resistance were also studied. The results demonstrated that the denitrification rate is highly dependent on current production, which is influenced by external resistance, and acetate and nitrate concentrations (Chapter Four). Increases in the nitrate reduction rate through increased the nitrate concentration was observed. However, an increase in the nitrite accumulation rate was also induced which can be problematic due to its toxicity. In contrast, increasing the acetate concentration improved nitrate removal rates and reduced nitrite accumulation (Chapter Four), these results indicating the importance of the feed ratios for the two compartments.

Higher external resistances were shown to inhibit the denitrification activity due to lower electrical currents produced. In addition, a polarization curve was obtained by changing the external resistance using a resistor box, and a maximum power density of 1.26 mW/m^2 was achieved at a current density of 10.23 mA/m^2. This was also compared well with previous findings (Jia *et al.*, 2008).

7.3. Isolation and Characterisation of the Microbial Community Involved in the MFC System

For a good understanding of the nitrate removal process, the microbial community associated with the denitrification was analysed (Chapter Five). The microbial community attached to the electrode surface forming a biofilm that allows an efficient biological electron transfer in the MFC. To isolate and identify dominant populations in the MFC, a series of dilutions of the bacteria attached to the anode and cathode electrodes was carried out. Bacteria identification was achieved through biochemical tests and examination of morphological characteristics. A diversity of nitrate reducing bacteria was found, and some of them were able to perform a complete denitrification (Chapter Five).

Further work would be to gain a more detailed understanding of the microbes involved. This work carried the simplest analysis of microbes present; however the new modern powerful methods based on molecular biology potentially can offer an important insight into the microbial population on the electrode. These methods offer a rapid assessment of the metabolism and interactions and common features of these microbes at the molecular level key to understanding the processes in nanotechnological terms.

7.4. Pure Cultures in MFC

One of the isolated denitrifiers was selected, and its ability of reducing nitrate and generating power in a pure culture was investigated (Chapter Five). The maximum voltage of this strain was almost 36% of that achieved by the mixed bacterial colonies, illustrating that the entire denitrification process might include activities contributed to due to a number of synergistic interactions that occurred in the mixed cultures. Given the complexity of the ammonia/ nitrate metabolisms, it is not surprising to see poor performance with a single organism. Finding good consortia with this approach would reduce the set up times considerably. The observations made during this work were in good agreement with previous results reported in the literature (Nevin *et al.* 2008).

7.5. Modification of Electrodes Using Nanomaterials and Their Improvements as Demonstrated by Dye Reduction Especially with Graphitised Nanomaterials

The electrochemical behaviours of a graphite felt electrode were investigated through the use of the cyclic voltammetry technique (Chapter Six). Enhanced redox behaviours were achieved by modifying the GF electrode surface using carbon nanomaterials, such as SWCNTs, GCB, CNFs and GCNFs. The electrochemical properties associated with the modified GF electrodes were studied, evaluated and compared with those of the unmodified GF electrode. The GCNFs modified electrode offered the best electrochemical activity compared to the other modified electrodes, due to the large surface area provided and the improved electron transfer rate (Chapter Six). Using these types of electrodes should improve the interaction

with the microbes as these particles are much smaller than the felt surfaces giving the microbe more surface to directly interact with.

7.6. The Potential for Further Improvement Electrode Materials and Improvement in Microbe Electrode Interaction

Enhancing the reaction kinetics and mass transfer of the GF electrode through the GCNFs material helped improve the MFC's performance (Chapter Six). The maximum voltage obtained was 40.94 mV and greater than 95% of nitrate was removed, as compared with the unmodified electrode (33.95 mV maximum voltage, 87.5% nitrate removal). In this study only a few conditions of electrode modification were investigated. There are many possibilities that need to be investigated to see if the electrode's performance can be improved further. The optimisation study could have a strong impact on potential development of MFC technology.

7.7. Understanding the Nature of the Interaction of Nanomaterials and Microbes is Fundamental for Further Systematic Improvements

From the previous comments, the study of microbes and their interactions at surfaces modified with nanomaterials is fundamental for further systematic improvements of MFCs and of our understanding of microbial/environmental interactions (and the role of microbes in geochemical processes). Many nanotechnology techniques can be used for measurement and visualisation of the colloidal interactions between the modified electrode surfaces and microbes, together with specific studies of different electrode and microbe surfaces including the molecular components and arrangements such as membranes, cell surfaces and associated proteins and other materials.

8. FUTURE WORK

8.1. Improving Nitrate Reducing MFC

The microbial fuel cell has been shown as an attractive technology for nutrient removal with power generation. In this thesis, a biological nitrate reduction was achieved at a bio-cathode in an acetate-fed MFC, and the results showed an effective application for nitrate removal without relying on an artificial mediator or external power. However, further research is required to overcome some technical limitations relating to low electrical output. These limitations are due to three consequences: Firstly, the low efficiency of transferring electrons from the bacterial cells to the anode, which can be enhanced through the use of molecular analysis techniques, though requiring characterisation of the microbial communities in both MFC chambers, particularly the bacterial group necessary for the most efficient nitrate reduction in the cathodic chamber. This would lead to the need for greater understanding about the gene products involved with electron transfer through studying the gene expression of different bacterial populations under different MFC conditions.

Furthermore, difficult transfer of protons through the system could be due to the thickness of the electrode used. The MFC system studied here was assembled with graphite felt electrodes, which are inexpensive materials. However, they might inhibit proton conduction through the system. Therefore, future research should consider different MFC designs using different electrode materials and shapes in order to explore the most suitable system for real applications. The economic evaluation of the design process should also be considered. Finally, the limitations attributed to the ohmic resistance of the circuit can be suppressed through closely

arranging the electrodes, utilising solutions with high conductivity and using membranes with low resistivity.

In addition, surface analysis techniques, such as X-ray photoelectron spectroscopy, can be used to investigate the presence of adsorbed species on electrode surfaces, as well as clarifying the inductive behaviour shown in electrochemical impedance spectroscopy (EIS) and/or cyclic voltammetry. These methods all speak for study using bio-nanotechnology approached for analysis of the electrode fabrication and function.

8.2. Working towards Potentially important applications

A MFC system has been developed and optimised in this study for nitrate removal in applied situations such as clean water in fishing farming or drinking water, and considerable improvements were achieved. MFCs utilising denitrifying bacteria can also have a special ability to remove nitrogen compound as required in wastewater, as well as producing electricity. However, a large surface area is required for biofilm to build up in such systems. Furthermore, agricultural processing includes huge volumes of wastewaters that are generally considered nontoxic but high in organic matters and nitrogen compounds, causing environmental pollution. The use of bio-electrochemical fuel cell in such field can help obtain energy and treat high organic content wastewater at the same time. Nitrate rich dairy farm waste can be used as feedstock in MFCs in order to reduce the environmental impact of farm wastes. Suitable MFC configurations need to be developed once the underlying limitations have been described (see Section 8.1).

8.3. Nitrate Reduction Using Biochemical Methods: A Study of the Bio-nanotechnology of Cell Electrode Interactions

The general field of bio-electrochemical interactions has a wide range application from health and medicine, biotechnology and environmental engineering. Specifically with this study, these techniques are applied to water purification. However, the activity and reliability of MFC's during the degradation of electron donors can allow the use of MFCs as biosensors for pollutant analysis and in situ monitoring. Biosensors can be constructed in which bacteria are immobilised onto an electrode and protected behind a membrane. The diffusion of nitrogen components through the membrane can be evaluated by measuring the change in potential over the MFC based sensor. Such sensors can be useful as indicators of nitrogen compounds in rivers, at the entrance of wastewater treatment plants, for pollution or illegal dumping detection, or to perform research on polluted sites.

Enhanced nitrate reduction using component of the microbes, including proteins (enzymes) and redox compounds, is a very attractive application of bio-nanotechnology based bio-FCs. This application can be facilitated in two approaches. The first approach uses microorganisms and/or enzymes as catalyst directly in the bio-FCs. While the second approach, which is more efficient in bio-FCs, utilises purified redox enzymes for the targeted oxidation and reduction of specific fuel and oxidiser substrates. The main drawback of these applications is that electron flow is too slow to make a viable fuel cell, due to the difficulty for enzymes to attain direct electrical contact with the electrodes of the cell and to effectively catalyse subsequent reactions. Nanomaterials can help enhance the electrode surface area allowing a strong attachment of enzymes with electrode, and hence improving the

performance and stability of immobilised enzymes as well as the power production. This warrants further investigation.

In addition, the development of micro size MFCs has attracted recent interest; however high internal resistance may limit their power output. Further investigations including exploring electrode properties and device configurations, and analysing the composition and distribution of internal resistances, are essential to improve the micro-sized MFCs for future nitrate reduction applications.

Bibliography

Aelterman P, Rabaey K, Pham HT, Boon N, Verstraete W. 2006. *Continuous Electricity Generation at High Voltages and Currents Using Stacked Microbial Fuel Cells.* Environmental Science & Technology 40: 3388-3394.

Aelterman P, Versichele M, Marzorati M, Boon N, Verstraete W. 2008. *Loading rate and external resistance control the electricity generation of microbial fuel cells with different three-dimensional anodes.* Bioresource technology 99: 8895-8902.

Aida T, Hata S, Kusunoki H. 1986. *Temporary low oxygen conditions for the formation of nitrate reductase and nitrous oxide reductase by denitrifying Pseudomonas sp. G59.* Canadian Journal of Microbiology 32: 543-547.

Alehashem S, Chambers F, Strojek JW, Swain GM, Ramesham R. 1995. *Cyclic Voltammetric Studies of Charge Transfer Reactions at Highly Boron-Doped Polycrystalline Diamond Thin-Film Electrodes.* Analytical Chemistry 67: 2812-2821.

Almeida JS, Júlio SM, Reis MAM, Carrondo MJT. 1995. *Nitrite inhibition of denitrification by Pseudomonas fluorescens.* Biotechnology and Bioengineering 46: 194-201.

Alvarez ML, Ai J, Zumft W, Sanders-Loehr J, Dooley DM. 2000. *Characterization of the Copper−Sulfur Chromophores in Nitrous Oxide Reductase by Resonance Raman Spectroscopy: Evidence for Sulfur Coordination in the Catalytic Cluster.* Journal of the American Chemical Society 123: 576-587.

Aston WJ, Turner APF. 1984. *Biosensors and biofuel cells.* Biotechnologyand Genetic Engineering Reviews 1: 89-120.

Bard AJ, Faulkner LR. 2001. *Electrochemical Methods: Fundamentals and Applications*: John Wiley & Sons, New York.

Bard AJ, Parsons R, Jordan J. 1985. *Standard potential in aqueous solution*: International Union of Pure and Applied Chemistry.

Bazylinski DA, Hollocher TC. 1985. *Evidence from the reaction between trioxodinitrate(II) and nitrogen-15-labeled nitric oxide that trioxodinitrate(II) decomposes into nitrosyl hydride and nitrite in neutral aqueous solution.* Inorganic Chemistry 24: 4285-4288.

Berks BC, Richardson DJ, Robinson C, Reilly A, Aplin RT, Ferguson SJ. 1994. *Purification and characterization of the periplasmic nitrate reductase from Thiosphaera pantotropha.* European Journal of Biochemistry 220: 117-124.

Beschkov V, Velizarov S, Agathos SN, Lukova V. 2004. *Bacterial denitrification of waste water stimulated by constant electric field.* Biochemical Engineering Journal 17: 141-145.

Bitton G. 1994. *Wastewater Microbiology*: Willy-Liss, Inc: USA.

Blackall LL, Burrell PC. 1999. *The Microbiology of Activated Sludge*: Kluwer Academic Publishers.

Blasco R, Castillo F, Martnez-Luque M. 1997. *The assimilatory nitrate reductase from the phototrophic bacterium, Rhodobacter capsulatus E1F1, is a flavoprotein.* FEBS Letters 414: 45-49.

Bond DR, Lovley DR. 2003. *Electricity Production by Geobacter sulfurreducens Attached to Electrodes.* Applied and Environmental Microbiology 69: 1548-1555.

Bond DR, Lovley DR. 2005. *Evidence for Involvement of an Electron Shuttle in Electricity Generation by Geothrix fermentans.* Applied and Environmental Microbiology 71: 2186-2189.

Bond DR, Holmes DE, Tender LM, Lovley DR. 2002. *Electrode-Reducing Microorganisms That Harvest Energy from Marine Sediments.* Science 295: 483-485.

Boogerd FC, Van Verseveld HW, Stouthamer AH. 1983. *Dissimilatory nitrate uptake in Paracoccus denitrificans via a Δ̃gmH+-dependent system and a nitrate-nitrite antiport system.* Biochimica et Biophysica Acta (BBA) - Bioenergetics 723: 415-427.

Borole AP, Hamilton CY, Vishnivetskaya TA, Leak D, Andras C, Morrell-Falvey J, Keller M, Davison B. 2009. *Integrating engineering design improvements with exoelectrogen enrichment process to increase power output from microbial fuel cells.* Journal of Power Sources 191: 520-527.

Brown K, Tegoni M, Prudêncio M, Pereira AS, Besson S, Moura JJ, Moura I, Cambillau C. 2000a. *A novel type of catalytic copper cluster in nitrous oxide reductase.* Nature structural biology 7: 191-195.

Brown K, Djinovic-Carugo K, Haltia T, Cabrito I, Saraste M, Moura JG, Moura I, Tegoni M, Cambillau C. 2000b. *Revisiting the Catalytic CuZ Cluster of Nitrous Oxide (N2O) Reductase.* Journal of Biological Chemistry 275: 41133-41136.

Bryan BA, Jeter RM, Carlson CA. 1985. *Inability of Pseudomonas stutzeri denitrification mutants with the phenotype of Pseudomonas aeruginosa to grow in nitrous oxide.* Applied and Environmental Microbiology 50: 1301-1303.

Bullen RA, Arnot TC, Lakeman JB, Walsh FC. 2006. *Biofuel cells and their development.* Biosensors and Bioelectronics 21: 2015-2045.

Burrell PC, Keller J, Blackall LL. 1998. *Microbiology of a Nitrite-Oxidizing Bioreactor.* Applied and Environmental Microbiology 64: 1878-1883.

Campbell WH. 1999. *Nitrate reductase structure, function and regulation: Bridging the gap between biochemistry and physiology.* Annual Review of Plant Physiology and Plant Molecular Biology 50: 277-303.

Campbell WH. 2001. *Structure and function of eukaryotic NAD(P)H:nitrate reductase.* Cellular and Molecular Life Sciences 58: 194-204.

Cao X, Huang X, Liang P, Boon N, Fan M, Zhang L, Zhang X. 2009. *A completely anoxic microbial fuel cell using a photo-biocathode for cathodic carbon dioxide reduction.* Energy & Environmental Science 2: 498-501.

Carlson CA, Ferguson LP, Ingraham JL. 1982. *Properties of dissimilatory nitrate reductase purified from the denitrifier Pseudomonas aeruginosa.* Journal of Bacteriology 151: 162-171.

Carr GJ, Ferguson SJ. 1990. *The nitric oxide reductase of Paracoccus denitrificans.* Biochem. J. 269: 423-429.

Carter JP, Richardson DJ, Spiro S. 1995. *Isolation and characterisation of a strain of Pseudomonas putida that can express a periplasmic nitrate reductase.* Archives of Microbiology 163: 159-166.

Cast KL, Flora JRV. 1998. *An Evaluation of Two Cathode Materials and The Impact of Copper on Bioelectrochemical Denitrification.* Water Research 32: 63-70.

Cavigelli MA, Robertson GP. 2000. *The Functional Significance of Denitrifier Community Composition in A Terrestrial Ecosystem.* Ecology 81: 1402-1414.

Chae K-J, Mi-Jin C, Jin-Wook LEE, Kyoung-Yeol KIM, S KIMI. 2009. *Effect of different substrates on the performance, bacterial diversity, and bacterial viability in microbial fuel cells.* Bioresource technology 100: 3518-3525.

Chang In S, Hyunsoo M, Orianna B, Jae Kyung J, Ho Il P, H NK, Byung Hong KIM. 2006. *Electrochemically active bacteria (EAB) and mediator-less microbial fuel cells.* Journal of Microbiology and Biotechnology 16: 163-177.

Chang IS, Moon H, Jang JK, Kim BH. 2005. *Improvement of a microbial fuel cell performance as a BOD sensor using respiratory inhibitors.* Biosensors and Bioelectronics 20: 1856-1859.

Chang IS, Jang JK, Gil GC, Kim M, Kim HJ, Cho BW, Kim BH. 2004. *Continuous determination of biochemical oxygen demand using microbial fuel cell type biosensor.* Biosensors and Bioelectronics 19: 607-613.

Chapelle, Francis H. 2001. *Groundwater Microbiology and Geochemistry* 2nd Edition New York: John Wiley and Sons, Inc.

Chaudhuri SK, Lovley DR. 2003. *Electricity generation by direct oxidation of glucose in mediatorless microbial fuel cells.* Nat Biotech 21: 1229-1232.

Cheng KY, Ho G, Cord-Ruwisch R. 2008. *Affinity of Microbial Fuel Cell Biofilm for the Anodic Potential.* Environmental Science & Technology 42: 3828-3834.

Cheng S, Liu H, Logan BE. 2006b. *Increased performance of single-chamber microbial fuel cells using an improved cathode structure.* Electrochemistry Communications 8: 489-494.

Cheng S, Liu H, Logan BE. 2006a. *Increased Power Generation in a Continuous Flow MFC with Advective Flow through the Porous Anode and Reduced Electrode Spacing.* Environmental Science & Technology 40: 2426-2432.

Chiao M, Lam KB, Su Y-C, Lin L. 2002. *A Miniaturized Microbial Fuel Cell. Technical Digest of Solid-State Sensors and Actuators Workshop.* Hilton Head Island.

Choi Y, Song J, Jung S, Kim S. 2001. *Optimization of the performance of microbial fuel cells containing alkalophilic Bacillus sp.* Journal of Microbiology and Biotechnology 11: 863-869.

Clauwaert P, Desloover J, Shea C, Nerenberg R, Boon N, Verstraete W. 2009. *Enhanced nitrogen removal in bio-electrochemical systems by pH control.* Biotechnology Letters 31: 1537-1543.

Clauwaert P, van der Ha D, Boon N, Verbeken K, Verhaege M, Rabaey K, Verstraete W. 2007b. *Open Air Biocathode Enables Effective Electricity Generation with Microbial Fuel Cells.* Environmental Science & Technology 41: 7564-7569.

Clauwaert P, Rabaey K, Aelterman P, De Schamphelaire L, Pham TH, Boeckx P, Boon N, Verstraete W. 2007a. *Biological Denitrification in Microbial Fuel Cells.* Environmental Science & Technology 41: 3354-3360.

Clesceri LS, Greenberg AE, Eaton AD. 1999. *Standard Methods for the Examination of Water and Wastewater.* 20th American Water Works Association,US.

Cohen B. 1931. *The Bacteria Culture as an Electrical Half-Cell.* Journal of Bacteriology 21: 18-19.

Collins PG, Avouris P. 2000. *Nanotubes for electronics.* Scientific American 283: 62-69.

Costerton JW, Lewandowski Z, Caldwell DE, Korber DR, Lappin-Scott HM. 1995. *Microbial Biofilms.* Annual Review of Microbiology 49: 711-745.

Coyne MS, Arunakumari A, Averill BA, Tiedje JM. 1989. *Immunological identification and distribution of dissimilatory heme cd1 and nonheme copper nitrite reductases in denitrifying bacteria.* Applied and Environmental Microbiology 55: 2924-2931.

Davis F, Higson SPJ. 2007. *Biofuel cells—Recent advances and applications.* Biosensors and Bioelectronics 22: 1224-1235.

de Heer WA, Martel R. 2000. *Industry sizes up Nanotubes.* Physics World 13: 49-53.

Debabov V. 2008. *Electricity from microorganisms.* Microbiology 77: 123-131.

DeLong EF, Chandler P. 2002. *Power from the deep.* Nature biotechnology 20: 788-789.

Dias JM, Than ME, Humm A, Huber R, Bourenkov GP, Bartunik HD, Bursakov S, Calvete J, Caldeira J, Carneiro C, Moura JJ, Moura I, Romão MJ. 1999. *Crystal structure of the first dissimilatory nitrate reductase at 1.9 Å solved by MAD methods.* Structure (London, England : 1993) 7: 65-79.

Doelle HW. 1969. *Bacterial metabolism*: Academic Press.

Drysdale G D, et al. 2001. *Assessment of denitrification by the ordinary heterotrophic organisms in an NDBEPR activated sludge sytem.* Water science and technology 43: 147-154.

Du Z, Li H, Gu T. 2007. *A state of the art review on microbial fuel cells: A promising technology for wastewater treatment and bioenergy.* Biotechnology Advances 25: 464-482.

Dworkin M, Falkow S. 2006. *The Prokaryotes: A Handbook on the Biology of Bacteria*: Vol. 7: Proteobacteria: Delta and Epsilon Subclasses. Deeply Rooting Bacteria: Springer.

Emde R, Swain A, Schink B. 1989. *Anaerobic oxidation of glycerol by Escherichia coli in an amperometric poised-potential culture system.* Applied Microbiology and Biotechnology 32: 170-175.

Fan Y, Sharbrough E, Liu H. 2008. *Quantification of the Internal Resistance Distribution of Microbial Fuel Cells.* Environmental Science & Technology 42: 8101-8107.

Fast B, Lindgren PE, Götz F. 1997. *Cloning, sequencing, and characterization of a gene encoding a transport protein involved in dissimilatory nitrate reduction in Staphylococcus carnosus.* Archives of Microbiology 166: 361-367.

Feng Y, Lee H, Wang X, Liu Y. 2009. *Electricity generation in microbial fuel cells at different temperature and isolation of electrogenic bacteria.* Paper presented at Asia-Pacific Power and Energy Engineering Conference (Appeec), vol.1-7, pp. 530–534.

Franks AE, Malvankar N, Nevin KP. 2010. *Bacterial biofilms: the powerhouse of a microbial fuel cell.* Biofuels 1: 589-604.

Frunzke K, Zumft WG. 1986. *Inhibition of nitrous-oxide respiration by nitric oxide in the denitrifying bacterium Pseudomonas perfectomarina.* Biochim. Biophys. 852: 119-125.

Galimand M, Gamper M, Zimmermann A, Haas D. 1991. *Positive FNR-like control of anaerobic arginine degradation and nitrate respiration in Pseudomonas aeruginosa.* Journal of Bacteriology 173: 1598-1606.

Gangeswaran R, Eady RR. 1996. *Flavodoxin 1 of Azotobacter vinelandii: characterization and role in electron donation to purified assimilatory nitrate reductase.* Biochem. J. 317: 103-108.

Gans J, Wolinsky M, Dunbar J. 2005. *Computational Improvements Reveal Great Bacterial Diversity and High Metal Toxicity in Soil.* Science 309: 1387-1390.

Gerber A, Mostert ES, Winter CT, de Villiers RH. 1986. *The effect of acetate and other shortchain carbon compounds on the kinetics of biological nutrient removal.* Water SA. 12(1): 7-11.

Ghafari S, Hasan M, Aroua MK. 2009. *Nitrate remediation in a novel upflow bio-electrochemical reactor (UBER) using palm shell activated carbon as cathode material.* Electrochimica Acta 54: 4164-4171.

Goel RK, Flora JRV. 2005. *Simultaneous Nitrification and Denitrification in a Divided Cell Attached Growth Bioelectrochemical Reactor.* Environmental Engineering Science 22: 440-449.

González PJ, Correia C, Moura I, Brondino CD, Moura JJG. 2006. *Bacterial nitrate reductases: Molecular and biological aspects of nitrate reduction.* Journal of Inorganic Biochemistry 100: 1015-1023.

Gooding JJ, Wibowo R, Liu, Yang W, Losic D, Orbons S, Mearns FJ, Shapter JG, Hibbert DB. 2003. *Protein Electrochemistry Using Aligned Carbon Nanotube Arrays.* Journal of the American Chemical Society 125: 9006-9007.

Gorby YA, Yanina S, McLean JS, Rosso KM, Moyles D, Dohnalkova A, Beveridge TJ, Chang IS, Kim BH, Kim KS, Culley DE, Reed SB, Romine MF, Saffarini DA, Hill EA, Shi L, Elias DA, Kennedy DW, Pinchuk G, Watanabe K, Ishii S, Logan B, Nealson KH, Fredrickson JK. 2006. *Electrically conductive bacterial nanowires produced by Shewanella oneidensis strain MR-1 and other microorganisms.* Proceedings of the National Academy of Sciences 103: 11358-11363.

Gregory KB, Bond DR, Lovley DR. 2004. *Graphite electrodes as electron donors for anaerobic respiration.* Environmental microbiology 6: 596-604.

Guerrero MG, Vega JM, Losada M. 1981. *The Assimilatory Nitrate-Reducing System and its Regulation.* Annual Review of Plant Physiology 32: 169-204.

Guzmán C, Orozco G, Verde Y, Jiménez S, Godínez LA, Juaristi E, Bustos E. 2009. *Hydrogen peroxide sensor based on modified vitreous carbon with multiwall carbon nanotubes and composites of Pt nanoparticles–dopamine.* Electrochimica Acta 54: 1728-1732.

Habermann W, Pommer EH. 1991. *Biological fuel cells with sulphide storage capacity.* Applied Microbiology and Biotechnology 35: 128-133.

Halliday, David, Robert Resnick, Walker. J. 2003. *Fundamentals of Physics.* 6th Edition: New York: John Wiley and Sons, Inc.

Harley JP. 2008. *Laboratory Exercises in Microbiology.* 7th Edition: New York, New York, United States of America: McGraw-Hill Companies.

He Z, Angenent LT. 2006. *Application of Bacterial Biocathodes in Microbial Fuel Cells.* Electroanalysis 18: 2009-2015.

He Z, Minteer SD, Angenent LT. 2005. *Electricity Generation from Artificial Wastewater Using an Upflow Microbial Fuel Cell.* Environmental Science & Technology 39: 5262-5267.

Heilmann J, Logan BE. 2006. *Production of Electricity from Proteins Using a Microbial Fuel Cell.* Water Environment Research 78: 531-537.

Hernandez ME, Newman DK. 2001. *Extracellular electron transfer.* Cellular and Molecular Life Sciences 58: 1562-1571.

Hille R. 1996. *The Mononuclear Molybdenum Enzymes†.* Chemical Reviews 96: 2757-2816.

Hochstein LI, Tomlinson GA. 1988. *The Enzymes Associated with Denitrification.* Annual Review of Microbiology 42: 231-261.

Hochstein LI, Lang F. 1991. *Purification and properties of a dissimilatory nitrate reductase from Haloferax denitrificans.* Archives of Biochemistry and Biophysics 288: 380-385.

Hochstein LI, Betlach M, Kritikos G. 1984. *The effect of oxygen on denitrification during steady-state growth of Paracoccus halodenitrificans.* Archives of Microbiology 137: 74-78.

Holmes DE, Bond DR, Lovley DR. 2004b. *Electron Transfer by Desulfobulbus propionicus to Fe(III) and Graphite Electrodes.* Applied and Environmental Microbiology 70: 1234-1237.

Holmes DE, Nicoll JS, Bond DR, Lovley DR. 2004a. *Potential Role of a Novel Psychrotolerant Member of the Family Geobacteraceae, Geopsychrobacter electrodiphilus gen. nov., sp. nov., in Electricity Production by a Marine Sediment Fuel Cell.* Applied and Environmental Microbiology 70: 6023-6030.

Holzman DC. 2005. *Microbe Power!* Environ Health Perspect 113: A754-A757.

Hooijmans CM, Geraats SGM, van Neil EWJ, Robertson LA, Heijnen JJ, Luyben KCAM. 1990. *Determination of growth and coupled nitrification/denitrification by immobilized Thiosphaera pantotropha using measurement and modeling of oxygen profiles.* Biotechnology and Bioengineering 36: 931-939.

Hrapovic S, Liu Y, Male KB, Luong JHT. 2003. *Electrochemical Biosensing Platforms Using Platinum Nanoparticles and Carbon Nanotubes.* Analytical Chemistry 76: 1083-1088.

Ieropoulos I, Greenman J, Melhuish C. 2003. *Imitating Metabolism: Energy Autonomy in Biologically Inspired Robots.* Proceedings of the 2nd International Symposium on Imitation in Animals and Artifacts: 191-194.

Ieropoulos I, Melhuish C, Greenman J, Horsfield I. 2005b. *EcoBot-II: An artificial agent with a natural metabolism.* Advanced Robotic Systems 2: 295-300.

Ieropoulos IA, Greenman J, Melhuish C, Hart J. 2005a. *Comparative study of three types of microbial fuel cell.* Enzyme and Microbial Technology 37: 238-245.

Iijima S. 1991. *Helical microtubules of graphitic carbon.* Nature 354: 56-58.

Islam S, Suidan MT. 1998. *Electrolytic denitrification: Long term performance and effect of current intensity.* Water Research 32: 528-536.

Jang JK, Pham TH, Chang IS, Kang KH, Moon H, Cho KS, Kim BH. 2004. *Construction and operation of a novel mediator- and membrane-less microbial fuel cell.* Process Biochemistry 39: 1007-1012.

Jia Y-H, Tran H-T, Kim D-H, Oh S-J, Park D-H, Zhang R-H, Ahn D-H. 2008. *Simultaneous organics removal and bio-electrochemical denitrification in microbial fuel cells.* Bioprocess and Biosystems Engineering 31: 315-321.

Kang I, et al. 2006. *Introduction to carbon nanotube and nanofiber smart materials.* Composites Part B: Engineering 37: 382-394.

Karube I, Matsunaga T, Tsuru S, Suzuki S. 1977. *Biochemical fuel cell utilizing immobilized cells of clostridium butyricum.* Biotechnology and Bioengineering 19: 1727-1733.

Kastrau DHW, Heiss B, Kroneck PMH, Zumft WG. 1994. *Nitric oxide reductase from Pseudomonas stutzeri, a novel cytochrome bc complex.* European Journal of Biochemistry 222: 293-303.

Kim BH, Kim HJ, Hyun MS, Park DH. 1999. *Direct electrode reaction of Fe(III)-reducing bacterium, Shewanella putrefaciens.* Journal of Microbiology and Biotechnology 9: 127-131.

Kim BH, Chang IS, Cheol Gil G, Park HS, Kim HJ. 2003. *Novel BOD (biological oxygen demand) sensor using mediator-less microbial fuel cell.* Biotechnology Letters 25: 541-545.

Kim BH, Park HS, Kim HJ, Kim GT, Chang IS, Lee J, Phung NT. 2004. *Enrichment of microbial community generating electricity using a fuel-cell-type electrochemical cell.* Applied Microbiology and Biotechnology 63: 672-681.

Kim HJ, Park HS, Hyun MS, Chang IS, Kim M, Kim BH. 2002. *A mediator-less microbial fuel cell using a metal reducing bacterium, Shewanella putrefaciens.* Enzyme and Microbial Technology 30: 145-152.

Kim JR, Jung SH, Regan JM, Logan BE. 2007. *Electricity generation and microbial community analysis of alcohol powered microbial fuel cells.* Bioresource technology 98: 2568-2577.

Kim JR, Min B, Logan BE. 2005. *Evaluation of procedures to acclimate a microbial fuel cell for electricity production.* Applied Microbiology and Biotechnology 68: 23-30.

Kim N, Choe Y, Jung S, Kim S. 2000. *Effect of initial carbon sources on the performance of microbial fuel cells containing Proteus vulgaris.* Biotechnology and Bioengineering 70: 109-114.

Knowles R. 1982. *Denitrification.* Microbiological reviews 46: 43-70.

Koike I, Hattori A. 1975. *Energy Yield of Denitrification: An Estimate from Growth Yield in Continuous Cultures of Pseudomonas denitrificans under Nitrate-, Nitrite- and Nitrous Oxide-limited Conditions.* Microbiology 88: 11-19.

Konneke M, Bernhard AE, de la Torre JR, Walker CB, Waterbury JB, Stahl DA. 2005. *Isolation of an autotrophic ammonia-oxidizing marine archaeon.* Nature 437: 543-546.

Körner H, Zumft WG. 1989. *Expression of denitrification enzymes in response to the dissolved oxygen level and respiratory substrate in continuous culture of Pseudomonas stutzeri.* Applied and Environmental Microbiology 55: 1670-1676.

Kosower EM, Cotter JL. 1964. *Stable Free Radicals. II. The Reduction of 1-Methyl-4-cyanopyridinium Ion to Methylviologen Cation Radical.* Journal of the American Chemical Society 86: 5524-5527.

Kounaves SP. 1997. "Voltametric techniques." Theory and Intrumentaion. http://www.prenhall.com/settle/chapters/ch37.pdf.

Král P, Shapiro M. 2001. *Nanotube Electron Drag in Flowing Liquids.* Physical Review Letters 86: 131-134.

Krishnan A, Dujardin E, Ebbesen T W, Yianilos P N, Treacy M. M J. 1998. *Young's Modulus of Single-Walled Nanotubes.* Physical review. B, Condensed matter 58: 14013-14019.

Kristjansson J, Hollocher T. 1980. *First practical assay for soluble nitrous oxide reductase of denitrifying bacteria and a partial kinetic characterization.* J. Biol. Chem. 255: 704-707.

Kumita H, Matsuura K, Hino T, Takahashi S, Hori H, Fukumori Y, Morishima I, Shiro Y. 2004. *NO Reduction by Nitric-oxide Reductase from Denitrifying Bacterium Pseudomonas aeruginosa: Characterization of Reaction Intermediates that Applear in the Single Turnover Cycle.* J. Biol. Chem. 279: 55247-55254.

Kurt M, Dunn I J, Bourne J R. 1987. *Biological denitrification of drinking water using autotrophic organisms with H2 in a fluidized-bed biofilm reactor.* Biotechnology and Bioengineering 29: 493-501.

Larminie J, Dicks A. 2000. *Fuel cell systems explained*: John Wiley & Sons, Chichester.

Lee J, Phung NT, Chang IS, Kim BH, Sung HC. 2003. *Use of Acetate for Enrichment of Electrochemically Active Microorganisms and Their 16S rDNA Analyses.* FEMS Microbiology Letters 223: 185-191.

Lee K-C, Rittmann BE. 2003. *Effects of pH and precipitation on autohydrogenotrophic denitrification using the hollow-fiber membrane-biofilm reactor.* Water Research 37: 1551-1556.

Lefebvre O, Al-Mamun A, Ng HY. 2008. *A microbial fuel cell equipped with a biocathode for organic removal and denitrification.* Water Science & Technology 58(4): 881-885.

Lewis K. 1966. *Symposium on bioelectrochemistry of microorganisms. IV. Biochemical fuel cells.* Microbiol. Mol. Biol. Rev. 30: 101-113.

Li Xiao-gang HK, Liu Su-qin, Tan Ning, Chen Li-quan. 2006. *Reaction Mechanism of V(¢ô)/V(¢õ) Redox Couple at Graphite Felt Composite Electrode Bonded with Conductive Carbon Plastic.* Journal of Electrochemistry 12: 368-372.

Lies DP, Hernandez ME, Kappler A, Mielke RE, Gralnick JA, Newman DK. 2005. *Shewanella oneidensis MR-1 Uses Overlapping Pathways for Iron Reduction at a Distance and by Direct Contact under Conditions Relevant for Biofilms.* Applied and Environmental Microbiology 71: 4414-4426.

Lilienthal RR, Smith DK. 1995. *Solvent effects on the redox-dependent binding properties of a viologen-based receptor for neutral organic molecules.* Analytical Chemistry 67: 3733-3739.

Lin JT, Goldman BS, Stewart V. 1994. *The nasFEDCBA operon for nitrate and nitrite assimilation in Klebsiella pneumoniae M5al.* Journal of Bacteriology 176: 2551-2559.

Liu H, Logan BE. 2004. *Electricity Generation Using an Air-Cathode Single Chamber Microbial Fuel Cell in the Presence and Absence of a Proton Exchange Membrane.* Environmental Science & Technology 38: 4040-4046.

Liu H, Ramnarayanan R, Logan BE. 2004. *Production of Electricity during Wastewater Treatment Using a Single Chamber Microbial Fuel Cell.* Environmental Science & Technology 38: 2281-2285.

Liu H, Grot S, Logan BE. 2005b. *Electrochemically Assisted Microbial Production of Hydrogen from Acetate.* Environmental Science & Technology 39: 4317-4320.

Liu H, Cheng S, Logan BE. 2005a. *Power Generation in Fed-Batch Microbial Fuel Cells as a Function of Ionic Strength, Temperature, and Reactor Configuration.* Environmental Science & Technology 39: 5488-5493.

Lloyd D, Boddy L, Davies KJP. 1987. *Persistence of bacterial denitrification capacity under aerobic conditions: The rule rather than the exception.* FEMS Microbiology Letters 45: 185-190.

Logan BE. 2008. *Microbial Fuel Cells*: John Wiley & Sons, Inc., Hoboken, New Jersey.

Logan BE. 2009. *Exoelectrogenic bacteria that power microbial fuel cells.* Nat Rev Micro 7: 375-381.

Logan BE, Regan JM. 2006. *Microbial Fuel Cells—Challenges and Applications.* Environmental Science & Technology 40: 5172-5180.

Logan BE, Murano C, Scott K, Gray ND, Head IM. 2005. *Electricity generation from cysteine in a microbial fuel cell.* Water Research 39: 942-952.

Logan BE, Call D, Cheng S, Hamelers HVM, Sleutels THJA, Jeremiasse AW, Rozendal RA. 2008. *Microbial Electrolysis Cells for High Yield Hydrogen Gas Production from Organic Matter.* Environmental Science & Technology 42: 8630-8640.

Logan BE, Hamelers B, Rozendal R, Schröder U, Keller J, Freguia S, Aelterman P, Verstraete W, Rabaey K. 2006. *Microbial Fuel Cells: Methodology and Technology†*. Environmental Science & Technology 40: 5181-5192.

Lovley DR. 2006a. *Microbial fuel cells: novel microbial physiologies and engineering approaches*. Current Opinion in Biotechnology 17: 327-332.

Lovley DR. 2006b. *Bug juice: harvesting electricity with microorganisms*. Nat Rev Micro 4: 497-508.

Lovley DR. 2008. *The microbe electric: conversion of organic matter to electricity*. Current Opinion in Biotechnology 19: 564-571.

Lovley DR, Phillips EJP. 1988. *Novel Mode of Microbial Energy Metabolism: Organic Carbon Oxidation Coupled to Dissimilatory Reduction of Iron or Manganese*. Applied and Environmental Microbiology 54: 1472-1480.

Lovley DR. 1989. *Requirement for a Microbial Consortium To Completely Oxidize Glucose in Fe(III)-Reducing Sediments*. Applied and Environmental Microbiology 55: 3234-3236.

Luo J, Tillman RW, White RE, Ball PR. 1998. *Variation in denitrification activity with soil depth under pasture*. Soil Biology and Biochemistry 30: 897-903.

Mac-Faddin JF. 1980. *Biochemical tests for identification of medical bacteria*. Baltimore; London: Williams & Wilkins.

Madigan MT, Martinko JM, Parker J. 1997. *Brock Biology of Microorganisms*. 8th Edition: Upper Saddle River, New Jersey : Prentice-Hall, Inc.

Mahne I, Tiedje JM. 1995. *Criteria and methodology for identifying respiratory denitrifiers*. Applied and Environmental Microbiology 61: 1110-1115.

Mergel A, Kloos K, Bothe H. 2001. *Seasonal fluctuations in the population of denitrifying and N2-fixing bacteria in an acid soil of a Norway spruce forest*. Plant and Soil 230: 145-160.

Merino L. 2009. *Development and Validation of a Method for Determination of Residual Nitrite/Nitrate in Foodstuffs and Water After Zinc Reduction*. Food Analytical Methods 2: 212-220.

Meyyappan M. 2005. *Carbon nanotubes science and applications*: CRC Press.

Michalski WP, Hein DH, Nicholas DJD. 1986. *Purification and characterization of nitrous oxide reductase from Rhodopseudomonas sphaeroides f.sp. denitrificans*. Biochimica et Biophysica Acta (BBA) - Protein Structure and Molecular Enzymology 872: 50-60.

Min B, Logan BE. 2004. *Continuous Electricity Generation from Domestic Wastewater and Organic Substrates in a Flat Plate Microbial Fuel Cell*. Environmental Science & Technology 38: 5809-5814.

Min B, Cheng S, Logan BE. 2005a. *Electricity generation using membrane and salt bridge microbial fuel cells.* Water Research 39: 1675-1686.

Min B, Kim J, Oh S, Regan JM, Logan BE. 2005b. *Electricity generation from swine wastewater using microbial fuel cells.* Water Research 39: 4961-4968.

Minkevich IG. 1985. *Estimation of available efficiency of microbial growth on methanol and ethanol.* Biotechnology and Bioengineering 27: 792-799.

Moon H, Chang IS, Jang JK, Kim BH. 2005. *Residence time distribution in microbial fuel cell and its influence on COD removal with electricity generation.* Biochemical Engineering Journal 27: 59-65.

Moon H, Chang IS, Kang KH, Jang JK, Kim BH. 2004. *Improving the dynamic response of a mediator-less microbial fuel cell as a biochemical oxygen demand (BOD) sensor.* Biotechnology Letters 26: 1717-1721.

Moreno-Vivián C, Ferguson SJ. 1998. *Definition and distinction between assimilatory, dissimilatory and respiratory pathways.* Molecular Microbiology 29: 664-666.

Moreno-Vivián C, Cabello P, Martínez-Luque M, Blasco R, Castillo F. 1999. *Prokaryotic Nitrate Reduction: Molecular Properties and Functional Distinction among Bacterial Nitrate Reductases.* Journal of Bacteriology 181: 6573-6584.

Morpeth FF, Boxer DH. 1985. *Kinetic analysis of respiratory nitrate reductase from Escherichia coli K12.* Biochemistry 24: 40-46.

Moura JJG, Brondino CD, Trincão J, Romão MJ. 2004. *Mo and W bis-MGD enzymes: nitrate reductases and formate dehydrogenases.* Journal of Biological Inorganic Chemistry 9: 791-799.

Naz I, Bano A, Ul-Hassan T. 2009. *Morphological, Biochemical and Molecular Characterization of Rhizobia From Halophytes of Khewra Salt Range and Attock.* Pakistan Journal of Botany 41(6): 3159-3168.

Nester EW. 2007. *Microbiology: A human perspective*: McGraw-Hill.

Nevin KP, Lovley DR. 2002. *Mechanisms for Fe(III) Oxide Reduction in Sedimentary Environments.* Geomicrobiology Journal 19: 141-159.

Nevin KP, Richter H, Covalla SF, Johnson JP, Woodard TL, Orloff AL, Jia H, Zhang M, Lovley DR. 2008. *Power output and columbic efficiencies from biofilms of Geobacter sulfurreducens comparable to mixed community microbial fuel cells.* Environmental microbiology 10: 2505-2514.

Newman DK. 2001. *How Bacteria Respire Minerals.* Science 292: 1312-1313.

Newman DK, Kolter R. 2000. *A role for excreted quinones in extracellular electron transfer.* Nature 405: 94-97.

Newman JS. 1973. *Electrochemical systems*: Prentice Hall. New Jersey.

Nugent JM, Santhanam KSV, Rubio A, Ajayan PM. 2001. *Fast Electron Transfer Kinetics on Multiwalled Carbon Nanotube Microbundle Electrodes.* Nano Letters 1: 87-91.

Oh S, Logan BE. 2005. *Hydrogen and electricity production from a food processing wastewater using fermentation and microbial fuel cell technologies.* Water Research 39: 4673-4682.

Oh S, Logan BE. 2006. *Proton exchange membrane and electrode surface areas as factors that affect power generation in microbial fuel cells.* Applied Microbiology and Biotechnology 70: 162-169.

Oh S, Min B, Logan BE. 2004. *Cathode Performance as a Factor in Electricity Generation in Microbial Fuel Cells.* Environmental Science & Technology 38: 4900-4904.

Onnis-Hayden A, Gu AZ. 2008. *Comparisons of Organic Sources for Denitrification: Biodegradability, Denitrification Rates, Kinetic Constants and Practical Implication for Their Application in WWTPs.* Proceedings of the Water Environment Federation 2008: 253-273.

Park DH, Zeikus JG. 2000. *Electricity Generation in Microbial Fuel Cells Using Neutral Red as an Electronophore.* Appl. Environ. Microbiol. 66: 1292-1297.

Park DH, Zeikus JG. 2003. *Improved fuel cell and electrode designs for producing electricity from microbial degradation.* Biotechnology and Bioengineering 81: 348-355.

Park HI, Kim Dk, Choi Y-J, Pak D. 2005. *Nitrate reduction using an electrode as direct electron donor in a biofilm-electrode reactor.* Process Biochemistry 40: 3383-3388.

Park HS, Kim BH, Kim HS, Kim HJ, Kim GT, Kim M, Chang IS, Park YK, Chang HI. 2001. *A Novel Electrochemically Active and Fe(III)-reducing Bacterium Phylogenetically Related to Clostridium butyricum Isolated from a Microbial Fuel Cell.* Anaerobe 7: 297-306.

Paul EA, Clark FE. 1996. *Soil microbiology and biochemistry.* San Diego: Academic Press.

Payne WJ. 1973. *Reduction of nitrogenous oxides by microorganisms.* Microbiol. Mol. Biol. Rev. 37: 409-452.

Philippot L, Hallin S, Schloter M. 2007. *Ecology of denitrifying prokaryotes in agricultural soil.* Advances in Agronomy 96: 249-305.

Piccolino M. 1998. *Animal electricity and the birth of electrophysiology: the legacy of Luigi Galvani.* Brain Research Bulletin 46: 381-407.

Pletcher D, Group SE. 2001. *Instrumental methods in electrochemistry*: Ellis Horwood.

Pommerville J. 2010. *Alcamo's Fundamentals of Microbiology*: Jones & Bartlett Learning.

Priemé A, Braker G, Tiedje JM. 2002. *Diversity of Nitrite Reductase (nirK and nirS) Gene Fragments in Forested Upland and Wetland Soils.* Applied and Environmental Microbiology 68: 1893-1900.

Prosnansky M, Sakakibara Y, Kuroda M. 2002. *High-rate denitrification and SS rejection by biofilm-electrode reactor (BER) combined with microfiltration.* Water Research 36: 4801-4810.

Qiao Y, Li CM, Bao S-J, Lu Z, Hong Y. 2008. *Direct electrochemistry and electrocatalytic mechanism of evolved Escherichia coli cells in microbial fuel cells.* Chemical Communications 11: 1290-1292.

Rabaey K, Verstraete W. 2005. *Microbial fuel cells : novel biotechnology for energy generation.* Trends in biotechnology (Regular ed.) 23: 291-298.

Rabaey K, Lissens G, Siciliano SD, Verstraete W. 2003. *A microbial fuel cell capable of converting glucose to electricity at high rate and efficiency.* Biotechnology Letters 25: 1531-1535.

Rabaey K, Boon N, Höfte M, Verstraete W. 2005a. *Microbial Phenazine Production Enhances Electron Transfer in Biofuel Cells.* Environmental Science & Technology 39: 3401-3408.

Rabaey K, Clauwaert P, Aelterman P, Verstraete W. 2005c. *Tubular Microbial Fuel Cells for Efficient Electricity Generation.* Environmental Science & Technology 39: 8077-8082.

Rabaey K, Ossieur W, Verhaege M, Verstraete W. 2005b. *Continuous microbial fuel cells convert carbohydrates to electricity.* Water Sci Technol 52: 515-523.

Rabaey K, Boon N, Siciliano SD, Verhaege M, Verstraete W. 2004. *Biofuel Cells Select for Microbial Consortia That Self-Mediate Electron Transfer.* Applied and Environmental Microbiology 70: 5373-5382.

Rabaey K, Read ST, Clauwaert P, Freguia S, Bond PL, Blackall LL, Keller J. 2008. *Cathodic oxygen reduction catalyzed by bacteria in microbial fuel cells.* ISME J 2: 519-527.

Rabaey K, Van de Sompel K, Maignien L, Boon N, Aelterman P, Clauwaert P, De Schamphelaire L, Pham HT, Vermeulen J, Verhaege M, Lens P, Verstraete W. 2006. *Microbial Fuel Cells for Sulfide Removal†.* Environmental Science & Technology 40: 5218-5224.

Ramírez-Arcos S, Fernández-Herrero LA, Berenguer J. 1998. *A thermophilic nitrate reductase is responsible for the strain specific anaerobic growth of Thermus thermophilus HB8.* Biochimica et Biophysica Acta (BBA) - Gene Structure and Expression 1396: 215-227.

Rasmussen T, Berks BC, Sanders-Loehr J, Dooley DM, Zumft WG, Thomson AJ. 2000. *The Catalytic Center in Nitrous Oxide Reductase, CuZ, Is a Copper−Sulfide Cluster†.* Biochemistry 39: 12753-12756.

Reddy KR, D'Angelo EM. 1994. *Soil processes regulating water quality in wetlands*: in: W.J. Mitsch (Ed.), Global Wetlands: Old World and New. Elsvier, Amsterdam,The Netherlands, pp. 309-324.

Reddy LV, Kumar SP, Wee Y-J. 2010. *Microbial Fuel Cells (MFCs) - a novel source of energy for newmillennium.* Current Research, Technology and Education Topics in Applied Microbiology and Microbial Biotechnology: 956-964.

Reguera G, McCarthy KD, Mehta T, Nicoll JS, Tuominen MT, Lovley DR. 2005. *Extracellular electron transfer via microbial nanowires.* Nature 435: 1098-1101.

Reimers CE, Tender LM, Fertig S, Wang W. 2000. *Harvesting Energy from the Marine Sediment–Water Interface.* Environmental Science & Technology 35: 192-195.

Reyes F, Roldán MD, Klipp W, Castillo F, Moreno-Vivián C. 1996. *Isolation of periplasmic nitrate reductase genes from Rhodobacter sphaeroides DSM 158: structural and functional differences among prokaryotic nitrate reductases.* Molecular Microbiology 19: 1307-1318.

Reynolds TD, Richards PA. 1996. *Unit operations and processes in environmental engineering*: PWS Pub. Co.

Richardson DJ. 2000. *Bacterial respiration: a flexible process for a changing environment.* Microbiology 146: 551-571.

Richardson JF, Peacock DG. 1994. *Coulson and Richardson's Chemical Engineering* Volume 3 - Chemical and Biochemical Reactors and Process Control (3rd Edition): Elsevier.

Richardson* DJ, Berks BC, Russell DA, Spiro S, Taylor CJ. 2001. *Functional, biochemical and genetic diversity of prokaryotic nitrate reductases.* Cellular and Molecular Life Sciences 58: 165-178.

Rismani-Yazdi H, Carver SM, Christy AD, Tuovinen OH. 2008. *Cathodic limitations in microbial fuel cells: An overview.* Journal of Power Sources 180: 683-694.

Rivas GA, Rubianes MD, Pedano ML, Ferreyra NF, Luque GL, Rodríguez MC, Miscoria SA. 2007. *Carbon Nanotubes Paste Electrodes.* A New Alternative for the Development of Electrochemical Sensors. Electroanalysis 19: 823-831.

Rivett MO, Buss SR, Morgan P, Smith JWN, Bemment CD. 2008. *Nitrate attenuation in groundwater: A review of biogeochemical controlling processes.* Water Research 42: 4215-4232.

Robertson LA, Kuenen JG. 1984. *Aerobic Denitrification: A Controversy Revived.* Archives of Microbiology 139: 351-354.

Robertson LA, Kuenen JG. 1992. *Nitrogen removal from water and waste.* Paper presented at Microbial control of pollution: Society for General Microbiology, Symposium 48.

Rohrback GH, Scott WR, Canfield JH. 1962. *In Proceeding of the 16th Annual Power Sources Conference.* Biochemical full cells, P. 18.

Rosenbaum M, Schröder U, Scholz F. 2005. *In Situ Electrooxidation of Photobiological Hydrogen in a Photobioelectrochemical Fuel Cell Based on Rhodobacter sphaeroides.* Environmental Science & Technology 39: 6328-6333.

Rosenbaum M, Schröder U, Scholz F. 2006. *Investigation of the electrocatalytic oxidation of formate and ethanol at platinum black under microbial fuel cell conditions.* Journal of Solid State Electrochemistry 10: 872-878.

Rowe JJ, Ubbink-Kok T, Molenaar D, Konings WN, Driessen AJM. 1994. *Nark is a nitrite-extrusion system involved in anaerobic nitrate respiration by Escherichia coli.* Molecular Microbiology 12: 579-586.

Rozendal RA, Hamelers HVM, Molenkamp RJ, Buisman CJN. 2007. *Performance of single chamber biocatalyzed electrolysis with different types of ion exchange membranes.* Water Research 41: 1984-1994.

Rozendal RA, Hamelers HVM, Euverink GJW, Metz SJ, Buisman CJN. 2006. *Principle and perspectives of hydrogen production through biocatalyzed electrolysis.* International Journal of Hydrogen Energy 31: 1632-1640.

Sakakibara Y, Nakayama T. 2001. *A novel multi-electrode system for electrolytic and biological water treatments:: electric charge transfer and application to denitrification.* Water Research 35: 768-778.

Sakurai T, Nakashima S, Kataoka K, Seo D, Sakurai N. 2005. *Diverse NO reduction by Halomonas halodenitrificans nitric oxide reductase.* Biochemical and Biophysical Research Communications 333: 483-487.

Sawers RG. 1991. *Identification and molecular characterization of a transcriptional regulator from Pseudomonas aeruginosa PAO1 exhibiting structural and functional similarity to the FNR protein of Escherichia coli.* Molecular Microbiology 5: 1469-1481.

Sayre IM. 1988. *International Standards for Drinking Water.* Am. Water Works Assoc. 80, 53.

Sears HJ, Spiro S, Richardson DJ. 1997. *Effect of carbon substrate and aeration on nitrate reduction and expression of the periplasmic and membrane-bound nitrate reductases in carbon-limited continuous cultures of Paracoccus denitrificans Pd1222.* Microbiology 143: 3767-3774.

Sedlak RI. 1991. *Phosphorus and nitrogen removal from municipal wastewater*: Principles and practice. McGraw-Hill Book Company: USA.

Settle FA. 1997. *Handbook of instrumental techniques for analytical chemistry*: Prentice Hall PTR.

Shantaram A, Beyenal H, Veluchamy RRA, Lewandowski Z. 2005. *Wireless Sensors Powered by Microbial Fuel Cells.* Environmental Science & Technology 39: 5037-5042.

Shapleigh JP, Davies KJP, Payne WJ. 1987. *Detergent inhibition of nitric-oxide reductase activity.* Biochimica et Biophysica Acta (BBA) - Protein Structure and Molecular Enzymology 911: 334-340.

Shoun H, Tanimoto T. 1991. *Denitrification by the fungus Fusarium oxysporum and involvement of cytochrome P-450 in the respiratory nitrite reduction.* Journal of Biological Chemistry 266: 11078-11082.

Shut X, Chung DDL. 1996. *High-strength high-surface-area porous carbon made from submicron-diameter carbon filaments.* Carbon 34(9).

Snyder S, Hollocher T. 1987. *Purification and some characteristics of nitrous oxide reductase from Paracoccus denitrificans.* J. Biol. Chem. 262: 6515-6525.

Steckhan E, Kuwana T. 1974. *Spectroelectrochemical Study of Mediators I. Bipyridylium Salts and Their Electron Transfer Rates to Cytochrome c.* Berichte der Bunsengesellschaft für physikalische Chemie 78: 253-259.

Steel KJ. 1961. *The Oxidase Reaction as a Taxonomic Tool.* Journal of General Microbiology 25: 297-306.

Stolz JF, Basu P. 2002. *Evolution of nitrate reductase: molecular and structural variations on a common function.* ChemBioChem 3: 198-206.

Sukkasem C, Xu S, Park S, Boonsawang P, Liu H. 2008. *Effect of nitrate on the performance of single chamber air cathode microbial fuel cells.* Water Research 42: 4743-4750.

Sun B, Skyllas-Kazacos M. 1991. *Chemical modification and electrochemical behaviour of graphite fibre in acidic vanadium solution.* Electrochimica Acta 36: 513-517.

Sun B, Skyllas-Kazacos M. 1992. *Chemical modification of graphite electrode materials for vanadium redox flow battery application—part II.* Acid treatments. Electrochimica Acta 37: 2459-2465.

Suzuki S, Karube I, Matsunaga T. 1978. *Application of a biochemical fuel cell to wastewaters.* Paper presented at Biotechnology and Bioengineering Symp. 8: 501-511.

Suzuki S, Karube I, Matsuoka H, Ueyama S, Kawakubo H, Isoda S, Murahashi T. 1983. *Biochemical Energy Conversion by Immobilized Whole Cells.* Annals of the New York Academy of Sciences 413: 133-143.

Tans SJ, Verschueren ARM, Dekker C. 1998. *Room-temperature transistor based on a single carbon nanotube.* Nature 393: 49-52.

Tender LM, Reimers CE, Stecher HA, Holmes DE, Bond DR, Lowy DA, Pilobello K, Fertig SJ, Lovley DR. 2002. *Harnessing microbially generated power on the seafloor.* Nature biotechnology 20: 821-825.

Torsvik V, Øvreås L, Thingstad TF. 2002. *Prokaryotic Diversity--Magnitude, Dynamics, and Controlling Factors.* Science 296: 1064-1066.

Tringe SG, et al. 2005. *Comparative Metagenomics of Microbial Communities.* Science 308: 554-557.

Unwin PR. 2007. *Introduction to Electroanalytical Techniques and Instrumentation.* Encyclopedia of Electrochemistry, Wiley-VCH Verlag GmbH & Co. KGaA.

Usuda K, Toritsuka N, Matsuo Y, Kim DH, Shoun H. 1995. *Denitrification by the fungus Cylindrocarpon tonkinense: anaerobic cell growth and two isozyme forms of cytochrome P-450nor.* Applied and Environmental Microbiology 61: 883-889.

Valentini F, Orlanducci S, Terranova ML, Amine A, Palleschi G. 2004. *Carbon nanotubes as electrode materials for the assembling of new electrochemical biosensors.* Sensors and Actuators B: Chemical 100: 117-125.

van Dam HT, Ponjee JJ. 1974. *Electrochemically Generated Colored Films of Insoluble Viologen Radical Compounds.* Journal of the Electrochemical Society 121: 1555-1558.

van Maanen J. M S, Welle I J, Hageman G, Dallinga J W, Mertens P. L. J M, Kleinjans J. C S. 1996. *Nitrate Contamination of Drinking Water : Relationship with HPRT Variant Frequency in Lymphovyte DNA and Urinary Excretion of N-Nitrosamines.* Environmental Health Perspectives 104.

van Rijn J, Tal Y, Schreier HJ. 2006. *Denitrification in recirculating systems: Theory and applications.* Aquacultural Engineering 34: 364-376.

Ventra MD, Evoy S, Heflin JR. 2004. *Introduction to nanoscale science and technology*: Kluwer Academic Publishers.

Verweij H, Schillo MC, Li J. 2007. *Fast Mass Transport Through Carbon Nanotube Membranes.* Small 3: 1996-2004.

Waage P, Gulberg CM. 1986. *Studies concerning affinity.* Journal of Chemical Education 63: 1044-1047.

Wang J. 2006. *Analytical Electrochemistry*: John Wiley & Sons.

Wang J, Musameh M. 2003. *Enzyme-dispersed carbon-nanotube electrodes: a needle microsensor for monitoring glucose.* Analyst 128: 1382-1385.

Ward BB. 1998. Denitrification: diversity of denitrifying bacteria and their functional genes[online]. Available from:http://geoweb.princeton.edu/research/biocomplexity/wardN.html.

Watanabe T, Motoyama H, Kuroda M. 2001. *Denitrification and neutralization treatment by direct feeding of an acidic wastewater containing copper ion and high-strength nitrate to a bio-electrochemical reactor process.* Water Research 35: 4102-4110.

White D. 1995. *The Physiology and Biochemistry of Prokaryotes*: Oxford University Press, New York.

Wong HSP, Akinwande D. 2011. *Carbon Nanotube and Graphene Device Physics*: Cambridge University Press.

Xing D, Zuo Y, Cheng S, Regan JM, Logan BE. 2008. *Electricity Generation by Rhodopseudomonas palustris DX-1.* Environmental Science & Technology 42: 4146-4151.

Yakobson B, Smalley R. 1997. *Fullerene Nanotubes: $C_{1,000,000}$ and Beyond.* American Scientist 85: 324-337.

Yamaoka K, Kato M, Kamihara T. 1994. *Control of Cellular Activity of Dissimilatory Nitrate Reductase in Escherichia coli.* Bioscience, Biotechnology, and Biochemistry 58: 995-997.

Yang H-H, McCreery RL. 1999. *Effects of Surface Monolayers on the Electron-Transfer Kinetics and Adsorption of Methyl Viologen and Phenothiazine Derivatives on Glassy Carbon Electrodes.* Analytical Chemistry 71: 4081-4087.

You S, Zhao Q, Zhang J, Liu H, Jiang J, Zhao S. 2008. *Increased sustainable electricity generation in up-flow air-cathode microbial fuel cells.* Biosensors and Bioelectronics 23: 1157-1160.

Yu M-F, Files BS, Arepalli S, Ruoff RS. 2000. *Tensile Loading of Ropes of Single Wall Carbon Nanotubes and their Mechanical Properties.* Physical Review Letters 84: 5552-5555.

Zhang T, Cui C, Chen S, Ai X, Yang H, Shen P, Peng Z. 2006. *A novel mediatorless microbial fuel cell based on direct biocatalysis of Escherichia coli.* Chemical Communications 21: 2257-2259.

Zhao F, Harnisch F, Schröder U, Scholz F, Bogdanoff P, Herrmann I. 2006. *Challenges and Constraints of Using Oxygen Cathodes in Microbial Fuel Cells.* Environmental Science & Technology 40: 5193-5199.

Zumft WG. 1997. *Cell biology and molecular basis of denitrification.* Microbiology and Molecular Biology Reviews 61: 533-616.

Zumft WG, Gotzmann DJ, Frunzke K, Viebrock A. 1987. *Novel terminal oxidoreductases of anaerobic respiration (denitrification) from Pseudomonas.* In Inorganic Nitrogen Metabolism: 61-67.

Zuo Y, Maness P-C, Logan BE. 2006. *Electricity Production from Steam-Exploded Corn Stover Biomass.* Energy & Fuels 20: 1716-1721.

Zuo Y, Xing D, Regan JM, Logan BE. 2008. *Isolation of the Exoelectrogenic Bacterium Ochrobactrum anthropi YZ-1 by Using a U-Tube Microbial Fuel Cell.* Applied and Environmental Microbiology 74: 3130-3137.

Appendices

Appendix A: Calculation of media component's concentrations based on chemical equations

Balanced chemical equations can be used to determine mass relationships between the reactants consumed and the products formed in a chemical reaction. Therefore, the concentrations of media components, including sodium acetate, sodium formate and yeast extract were determined based on chemical equations, in proportion to the amount of nitrate NO_3^- used in the experiments. Formula calculations for the concentration associated with each medium component are presented in detail next.

A.1. Sodium Acetate

The chemical reaction between the acetate ion (CH_3COO^-) and nitrate (NO_3^-) is given by (van Rijn *et al.* 2006)

$$5CH_3COO^- + 8NO_3^- + 3H^+ \rightarrow 4N_2(g) + 10HCO_3^- + 4H_2O\,. \qquad \text{(A.1)}$$

Equation (A.1) indicates that 5 moles of CH_3COO^- react exactly with 8 moles of NO_3^-.

This mole level of the equation can be converted to masses through the introduction of molar masses, and can be expressed as

$$number\ of\ moles\ of\ the\ substance = \frac{mass\ of\ the\ sample}{molar\ mass\ of\ substance}\,. \qquad \text{(A.2)}$$

The molar mass is the weight of one mole of any chemical substance, an element or compound. The molar mass of a compound, which is a collection of atoms bound together, is the sum of all its associated atomic masses. The molar mass of one mole

acetate ion ($CH_3\,COO^-$) containing two atoms carbon, three atoms hydrogen and two atoms oxygen can be calculated as

$(2\ \text{atoms} \times 12\ \text{grams/mole C}) + (3\ \text{atoms} \times 1.01\ \text{grams/mole H}) +$

$(2\ \text{atoms} \times 16\ \text{grams/mole O}) = 59.03\ \text{grams/mole}\ CH_3COO^-$

Similarly, the molar mass of one mole nitrate (NO_3^-) can be calculated as

$(1\ \text{atom} \times 14.01\ \text{grams/mole N}) + (3\ \text{atoms} \times 16\ \text{grams/mole O}) =$

$62.01\ \text{grams/mole}\ NO_3^-$

A.2. Sodium Formate

The chemical reaction between formate ion ($HCOO^-$) and nitrate (NO_3^-) is given by (Dworkin and Falkow 2006)

$$HCOO^- + NO_3^- + H^+ \rightarrow N_2(g) + CO_2 + H_2O\,. \qquad \text{(A.3)}$$

The equation (A.3) shows that 1 mole of $HCOO^-$ reacts exactly with 1 mole of NO_3^-. The molar mass of one mole formate ion ($HCOO^-$) can be similarly calculated as

$(1\ \text{atom} \times 1.01\ \text{grams/mole H}) + (1\ \text{atom} \times 12\ \text{grams/mole C}) +$

$(2\ \text{atoms} \times 16\ \text{grams/mole O}) = 45.01\ \text{grams/mole}\ HCOO^-$

A.3. Yeast Extract

The chemical reaction between elemental compositions of yeast ($CH_{1.6}N_{0.16}O_{0.5}$) and nitrate (is described by Richardson and Peacock (1994)) is given by (unbalanced stoichiometry)

$$CH_{1.6}N_{0.16}O_{0.5} + NO_3^- \rightarrow CO_2 + H_2O + NH_3 + N_2(g)\,. \qquad \text{(A.4)}$$

The equation (A.4) can be rewritten in a balanced form

$$25CH_{1.6}N_{0.16}O_{0.5} + 21NO_3^- \rightarrow 25CO_2 + 14H_2O + 4NH_3 + 10.5N_2 \qquad \text{(A.5)}$$

Equation (A.5) shows that 25 moles of $CH_{1.6}N_{0.16}O_{0.5}$ react exactly with 21 moles of NO_3^-. The molar mass of one mole $CH_{1.6}N_{0.16}O_{0.5}$ can be calculated as

(1 atom × 12 grams/mole C) + (1.6 atoms × 1.01 grams/mole H) +

(0.16 atoms × 14.01 grams/mole N) + (0.5 atoms × 16 grams/mole O) =

23.9 grams/mole $CH_{1.6}N_{0.16}O_{0.5}$

Appendix B: Final biomass of bacterial growth of media chemical components in a selective range of concentrations after 9 hours incubation

B.1. Sodium Formate Medium

B.1.1. Sodium Format

Concentration (%)	0	0.25	0.5	0.75	1	1.25	1.5
Final biomass (O.D.Units)	0.151	0.182	0.188	0.212	0.23	0.225	0.198

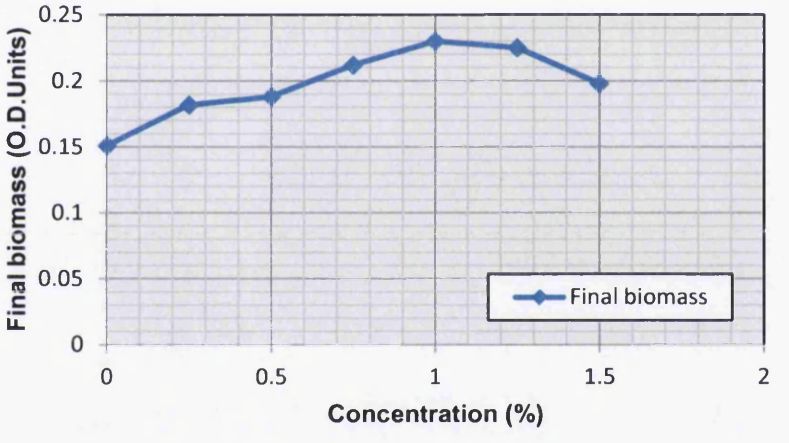

Figure B-1: Final biomass of bacterial growth of the sodium formate medium with different sodium formate concentrations after 9 h incubation.

B.1.2. Sodium Nitrate

Concentration (%)	0	0.25	0.5	0.75	1	1.25	1.5
Final biomass (O.D.Units)	0.163	0.178	0.188	0.194	0.207	0.216	0.199

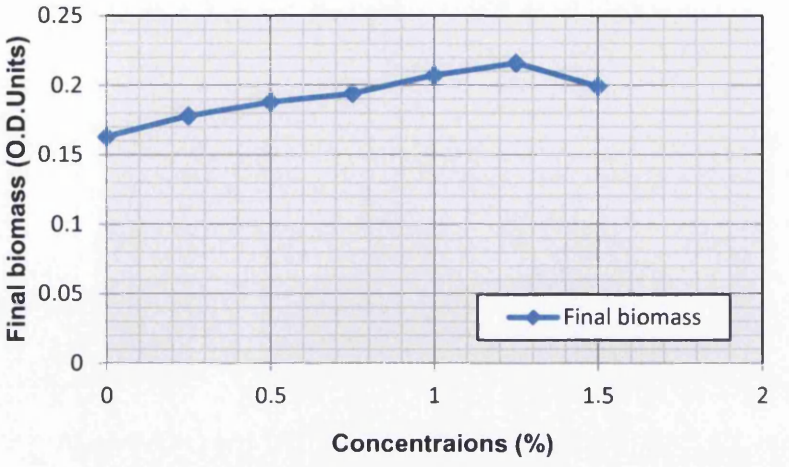

Figure B-2: Final biomass of bacterial growth of the sodium formate medium with different sodium nitrate concentrations after 9 h incubation.

B.1.3. Potassium Dihydrogen Orthophosphate

Concentration (%)	0	0.25	0.5	0.75	1	1.25	1.5
Final biomass (O.D.Units)	0.173	0.188	0.194	0.204	0.213	0.198	0.185

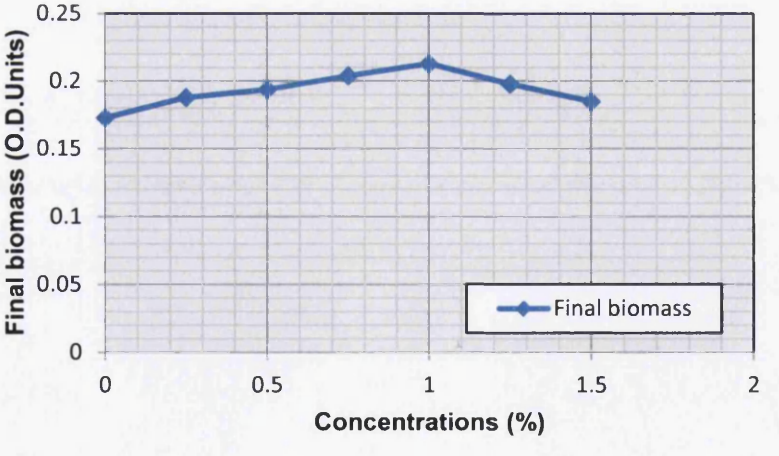

Figure B-3: Final biomass of bacterial growth of the sodium formate medium with different potassium dihydrogen orthophosphate concentrations after 9 h incubation.

B.1.4. Ammonium Sulphate

Concentration (%)	0	0.1	0.2	0.3	0.4	0.5
Final biomass (O.D.Units)	0.177	0.188	0.191	0.196	0.201	0.205

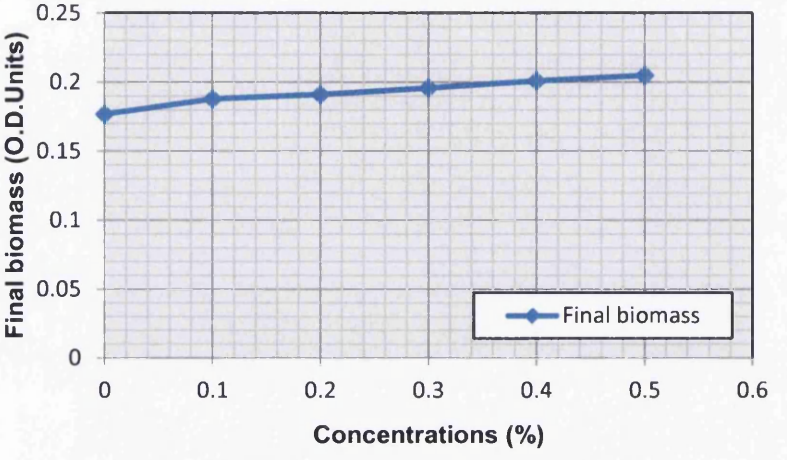

Figure B-4: Final biomass of bacterial growth of the sodium formate medium with different ammonium sulphate concentrations after 9 h incubation.

B.1.5. Yeast Extract

Concentration (%)	0	0.05	0.1	0.15	0.2	0.25	0.5	0.75
Final biomass (O.D.Units)	0.174	0.188	0.384	0.436	0.589	0.69	0.87	0.934

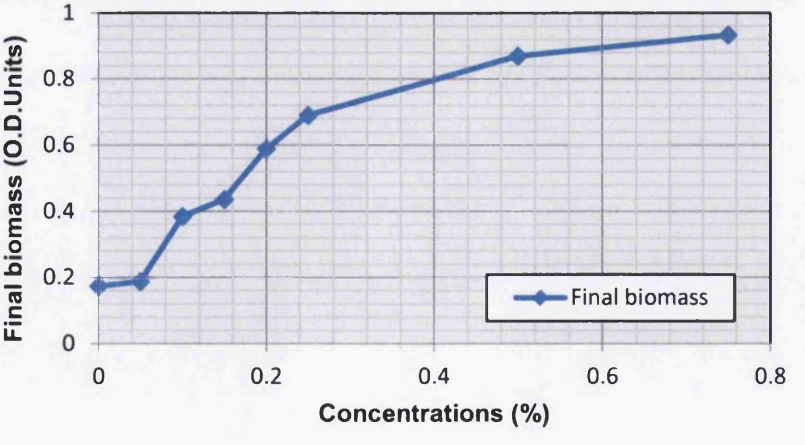

Figure B-5: Final biomass of bacterial growth of the sodium formate medium with different yeast extract concentrations after 9 h incubation.

B.2. Sodium Acetate Medium

B.2.1. Sodium Acetate

Concentration (%)	0	0.25	0.5	0.75	1	1.25	1.5
Final biomass (O.D.Units)	0.151	0.31	0.314	0.341	0.353	0.359	0.358

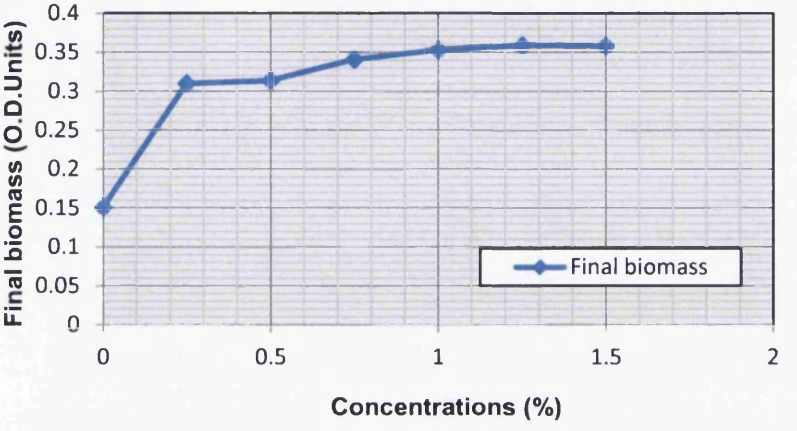

Figure B-6: Final biomass of bacterial growth of the sodium acetate medium with different sodium acetate concentrations after 9 h incubation.

B.2.2. Sodium Nitrate

Concentration (%)	0	0.25	0.5	0.75	1	1.25	1.5
Final biomass (O.D.Units)	0.276	0.305	0.314	0.348	0.378	0.387	0.383

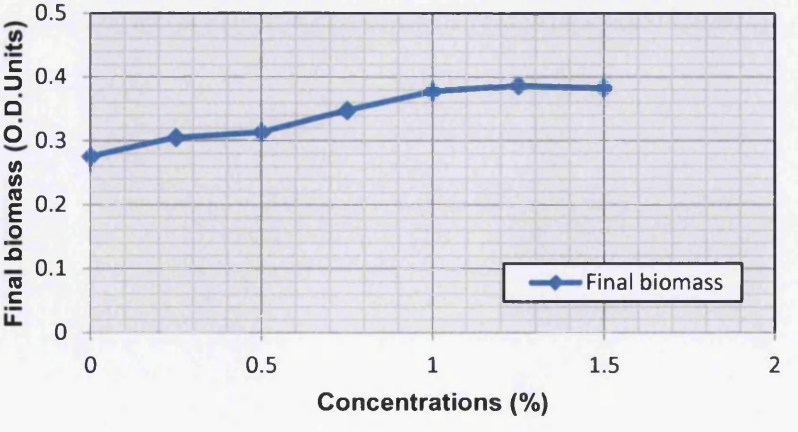

Figure B-7: Final biomass of bacterial growth of the sodium acetate medium with different sodium nitrate concentrations after 9 h incubation.

B.2.3. Potassium Dihydrogen Orthophosphate

Concentration (%)	0	0.25	0.5	0.75	1	1.25	1.5
Final biomass (O.D.Units)	0.289	0.314	0.335	0.341	0.367	0.323	0.301

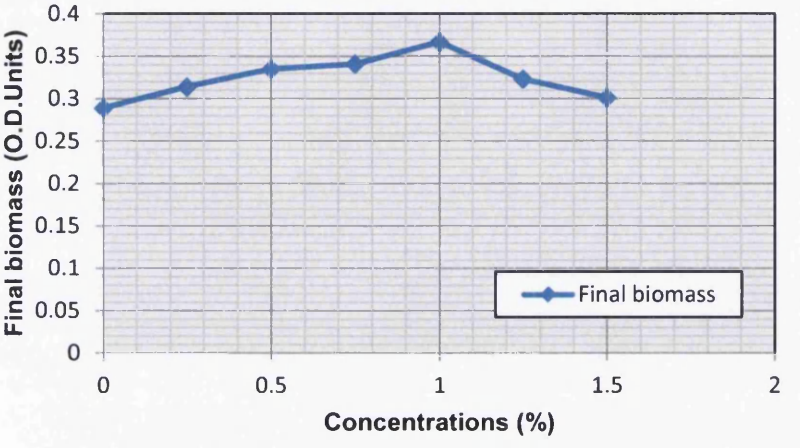

Figure B-8: Final biomass of bacterial growth of the sodium acetate medium with different potassium dihydrogen orthophosphate concentrations after 9 h incubation.

B.2.4. Ammonium Sulphate

Concentration (%)	0	0.1	0.2	0.3	0.4	0.5
Final biomass (O.D.Units)	0.298	0.314	0.333	0.345	0.354	0.358

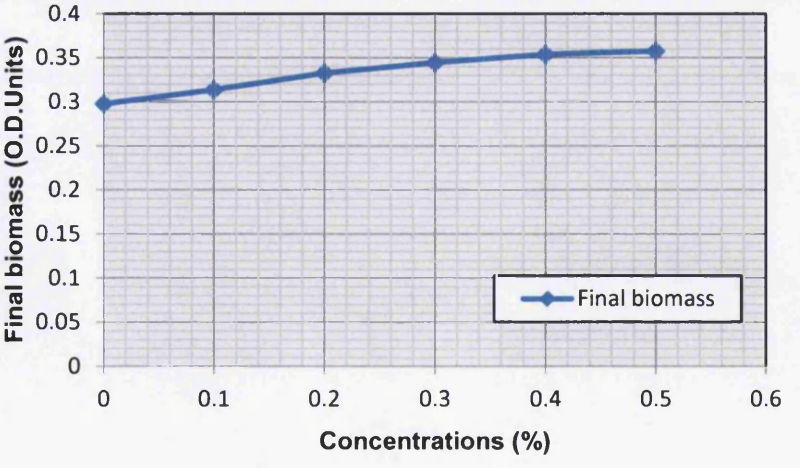

Figure B-9: Final biomass of bacterial growth of the sodium acetate medium with different ammonium sulphate concentrations after 9 h incubation.

B.2.5. Yeast Extract

Concentration (%)	0	0.05	0.1	0.15	0.2	0.25	0.5	0.75
Final biomass (O.D.Units)	0.248	0.314	0.555	0.645	0.826	0.939	1.139	1.345

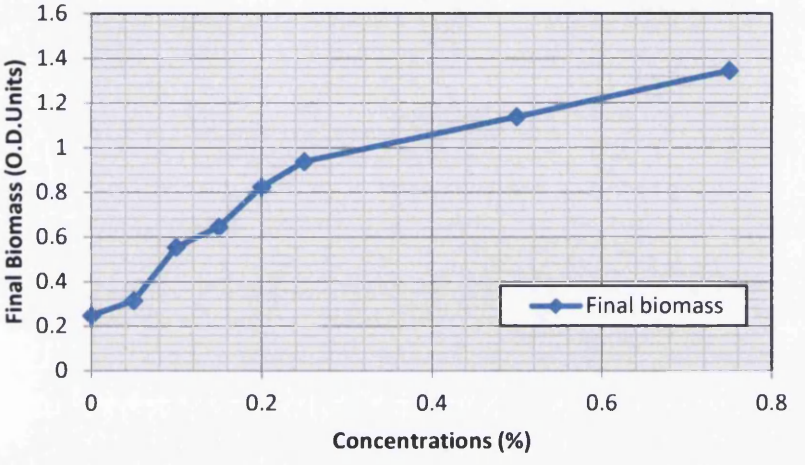

Figure B-10: Final biomass of bacterial growth of the sodium acetate medium with different yeast extract concentrations after 9 h incubation.